



Technische Universität München

Lehrstuhl für Analytische Lebensmittelchemie

Design and Development of a Heart-Cut Two-Dimensional Capillary Electrophoresis System with Mass Spectrometric Detection using a Mechanical Valve as Interface

Felix Jonas Kohl

Vollständiger Ausdruck der von der Fakultät Wissenschaftszentrum
Weihenstephan für Ernährung, Landnutzung und Umwelt der Technischen
Universität München zur Erlangung des akademischen Grades eines

Doktors der Naturwissenschaften

genehmigten Dissertation.

Vorsitzender: Prof. Dr. E. Grill

Prüfer der Dissertation: 1. apl. Prof. Dr. Ph. Schmitt-Kopplin
2. Prof. Dr. M. Rychlik
3. Prof. Dr. C. Neusüß (HAW Aalen)

Die Dissertation wurde am 18.01.2017 bei der Technischen Universität
eingereicht und durch die Fakultät Wissenschaftszentrum Weihenstephan für
Ernährung, Landnutzung und Umwelt am 29.05.2017 angenommen.

Die wahren Zweifel des Forschers beginnen manchmal erst mit der Gewissheit.

– Niels Bohr –

Acknowledgement

I would like to express my very great appreciation to my supervisor Christian Neusüß who gave me the opportunity to participate in his research group on this challenging and exciting topic. I have received all the support necessary to accomplish this work. Furthermore, my special thanks go to Philippe Schmitt-Kopplin who was willing to be my doctoral supervisor and, therefore, made it possible for me to do my PhD. Thank you for all your support and the fruitful discussions in Munich.

I thank the Federal Ministry of Education and Research (BMBF) for the financial support of the project within the framework of the funding line "IngenieurNachwuchs" of the funding round 2010 (FKZ 17N1110).

I thank the IMM in Mainz and the department of surface engineering at the HAW Aalen, especially Günter Tilk, for their support in processing the damaged valve parts and taking all the fantastic microscopic pictures. Further, I gratefully thank Carolin Krüger for the meticulous proofreading of this work.

I thank all my colleagues from the research group, Angelina Rafai, Svenja-Catharina Maute, Markus Pioch, Sabine Neuberger, Nora Tromsdorf, and Laura Sánchez-Hernández for the great teamwork. Also, I thank all the Bachelor and Master students who were working in the group during my time there, especially Johannes Sommer, Carsten Lotter, and Patrick Kiefer who were doing experimental work for the project. Very special thanks go to my colleague Cristina Montealegre who was accompanying me in the last time of my work. Thank you very much for the great time in the laboratory.

Finally, I thank my family. My parents who supported me and made it possible for me to even study chemistry, my two big sisters, and of course, my beloved wife Eugenia who has been with me for all these years, who is supporting me at all times, and who gave me my little son Moritz.

List of Abbreviations

μ_e	Electrophoretic Mobility
3D-IT	Three-Dimensional Ion-Trap
BSA	Bovine Serum Albumin
<i>c.</i>	Concentration
CCD	Calcite Compensation Depth
CD	Cyclodextrin
CEC	Capillary Electrochromatography
CGE	Capillary Gel Electrophoresis
CIEF	Capillary Isoelectric Focusing
CITP	Capillary Isotachopheresis
CSE	Capillary Sieving Electrophoresis
CZE	Capillary Zone Electrophoresis
<i>d.</i>	Diameter
DAD	Diode Array Detector
<i>E.</i>	Electric Field Strength
EIE	Extracted Ion Electropherogram
EKC	Electrokinetic Chromatography
EOF	Electroosmotic Flow
ESI	Electrospray Ionization
FAc	Formic Acid
FWHM	Full Width at Half Maximum
GC	Gas Chromatography
Glu-Fib	[Glu1]-Fibrinopeptide B
HAc	Acetic Acid
HCl	Hydrochloric Acid
HPC	Hydroxypropyl Cellulose
HPLC	High Performance Liquid Chromatography
HPMC	Hydroxypropyl Methyl Cellulose

HV	High Voltage
i.d.	Inner Diameter
ICC	Ion Charge Control
IMM	Institut für Mikrotechnik Mainz
IPA	Isopropyl Alcohol
LC	Liquid Chromatography
l_{eff}	Effective Capillary Length
Leu-Enk	Leucine-Enkephalin
LIF	Laser Induced Fluorescence
LIT	Linear Ion-Trap
LN	Low Normal Coating
LOD	Limit of Detection
l_p	Signal Length
l_r	Remaining Capillary Length
l_{tot}	Total Capillary Length
m/z	Mass to Charge Ratio
MEKC	Micellar Electrokinetic Chromatography
MeOH	Methanol
MS	Mass Spectrometry
MSD	Mass Selective Detector
n	Peak Capacity
N	Number of Theoretical Plates
NIR	Near Infrared
o.d.	Outer Diameter
PAEK	Polyaryletherketone
PEEK	Polyetheretherketone
PEG	Polyethylene Glycol
PTFE	Polytetrafluoroethylene
PVA	Polyvinyl Alcohol
q	Total Charge
Q	Quadrupole, Quantity
QqQ	Triple Quadrupole
RF	Radio Frequency
R_s	Resolution
S/N	Signal-to-Noise Ratio
SDS	Sodium Dodecylsulfate

SEC	<i>Size Exclusion Chromatography</i>
SL.....	<i>Sheath Liquid</i>
SPE.....	<i>Solid Phase Extraction</i>
t_{inj}	<i>Injection Time</i>
tITP	<i>Transient Isotachopheresis</i>
TLC.....	<i>Thin Layer Chromatography</i>
t_m	<i>Migration Time</i>
TOF.....	<i>Time of Flight</i>
t_s	<i>Switching Time</i>
V	<i>Volume</i>
v_e	<i>Electrophoretic Velocity</i>
V_s	<i>Acceleration Potential</i>
V_{tot}	<i>Total Velocity</i>
w_b	<i>Baseline Width</i>
Δp	<i>Pressure Difference</i>
η	<i>Dynamic Viscosity</i>
σ^2	<i>Peak Dispersion</i>

Zusammenfassung

Die Kapillarelektrophorese findet immer weiter Verbreitung in der Industrie und Forschung. Sie bietet, als eine Alternative zu den üblicheren Trenntechniken wie beispielsweise Flüssigkeitschromatographie, eine spezielle Selektivität, eine sehr hohe Trenneffizienz und verschiedene anwendbare Detektionstechniken. Die Elektrosprayionisierung-Massenspektrometrie ist hier besonders hervorzuheben. Sie lässt sich prinzipiell sehr gut mit der Kapillarelektrophorese koppeln, ermöglicht sehr empfindliche und selektive Detektion und gibt Informationen über die Struktur und die Zusammensetzung der Analyte. In vielen etablierten kapillarelektrophoretischen Methoden enthält jedoch der Hintergrundelektrolyt für die Trennung notwendige Additive, welche nicht flüchtig sind. Diese Additive können die Ionisierung und damit die Detektion stören. Solche Methoden lassen sich deshalb nicht direkt mit der Elektrosprayionisierung-Massenspektrometrie koppeln.

Ziel dieser Arbeit war die Konzipierung und Entwicklung eines Ansatzes, der die massenspektrometrische Detektion in solchen Anwendungen prinzipiell ermöglicht. Dieses Ziel sollte durch den Einsatz eines zweidimensionalen heart-cut Trennsystems erreicht werden, in welchem Analyte von einer nicht mit der Massenspektrometrie kompatiblen Trennung (erste Dimension) ausgeschnitten und über eine kurze zusätzliche Trennstrecke (zweite Dimension) in das Massenspektrometer überführt werden können. Die zweite Dimension sollte dazu genutzt werden, die störenden Additive vor der Detektion von den Analyten abzutrennen. Die grundlegende Idee war dabei die Einbindung eines mechanischen Ventils als Interface.

Es wurden die speziellen Anforderungen evaluiert, die an das Ventil gestellt werden. Diese sind: komplette elektrische Isolierung, ein Probenschleifenvolumen von wenigen zehn Nanolitern und eine vollständige räumliche Trennung der beiden Dimensionen. Ein spezielles Zwei-Wege Ventil, welches diese Anforderungen erfüllt, wurde gewählt und charakterisiert. Grundlegende Untersuchungen anhand eines vereinfachten eindimensionalen Systems zeigten, dass es prinzipiell möglich ist, das Ventil in den elektrischen Hochspannungsstromkreis der Kapillarelektrophorese einzubinden. In den ersten erfolgreichen Trennungen durch das Ventil konnten nur relativ leichte Signalverbreiterungen um den Faktor ≤ 2 beobachtet werden.

Im Verlauf dieser Arbeit wird der schrittweise Aufbau eines kompletten zweidimensionalen Systems mit massenspektrometrischer Detektion in der zweiten Dimension gezeigt. Um ein präzises Ausschneiden der Analyte zu ermöglichen, wurde ein zusätzlicher Detektor in der ersten Dimension direkt vor dem Ventil installiert. Dadurch konnten wiederholbar und selektiv Signale, mit einer Abweichung von unter 20 % bezüglich der Signalfläche, geschnitten werden. Weiterhin wurde ein Leitfähigkeitsdetektor für die Detektion von organischen Lösungsmitteln eingesetzt. Experimente, in welchen Lösungsmittelpfropfen mit dem Ventil ausgeschnitten wurden zeigen, dass solche Pfropfen sehr präzise innerhalb der Trennstrecken positioniert werden können. Dies ermöglicht beispielsweise das Erzeugen von effektiven Aufkonzentrierungsschritten in der zweiten Dimension.

Leider traten während der Experimente regelmäßig Probleme mit dem Ventilmaterial auf. Durch elektrische Überschlüge im Inneren des Ventils bildeten sich Partikel, welche während des Schaltvorgangs zu Kratzern und damit zu Undichtigkeiten führten. Ein Limitieren der Hochspannung, beziehungsweise der Stromstärke, während der Analyse konnte die Entstehung der Partikel jedoch minimieren.

Schließlich wurden zweidimensionale Analysen mit einem nicht flüchtigen, Phosphat-basierten Hintergrundelektrolyten in der ersten Dimension durchgeführt. Hierbei konnte das störende Phosphat erfolgreich in der zweiten Dimension abgetrennt und dadurch die Analyten mit Elektrosprayionisierung-Massenspektrometrie detektiert werden.

Das neuartige zweidimensionale heart-cut Kapillarelektrophoresesystem mit massenspektrometrischer Detektion unter Verwendung eines mechanischen Ventils als Interface eröffnet zahlreiche neue Möglichkeiten bei der Kopplung verschiedener kapillarelektrophoretischer Modi und Methoden mit der Massenspektrometrie. Weiterhin kann das System auch eingesetzt werden, um verschiedene kapillarelektrophoretische Modi, oder auch andere Techniken wie beispielsweise die Flüssigkeitschromatographie, für die Analyse komplexer Gemische in einem klassischen zweidimensionalen Ansatz zu koppeln.

Summary

Capillary electrophoresis is widespread in industry and research. As alternative to more common separation techniques like liquid chromatography, it provides special selectivity, very high separation efficiency, and various applicable detection techniques. Especially, electrospray ionization-mass spectrometry is ideally suited for its hyphenation to capillary electrophoresis. It provides very high selectivity and sensitivity as well as informations about the structure and the composition of the analytes. Unfortunately, many established capillary electrophoretic methods cannot be used directly with electrospray ionization-mass spectrometry because the background electrolyte contains additives that are required for the separation but are not volatile. These compounds interfere with the ionization process and contaminate the interface and the detector.

The aim of this work was to design and develop a system that enables mass spectrometric detection in these kinds of applications in principle. This was to be achieved by a heart-cut two-dimensional capillary electrophoresis approach where analytes are transferred from a first, non-mass spectrometry compatible separation (first dimension) over a short additional separation (second dimension) to the mass spectrometric detection. Here, the second dimension should be used to separate the analytes of interest from the interfering compounds previous to the detection. The basic idea, thereby, was the implementation of a fully electric insulated mechanical valve as the interface.

The specific requirements related to the valve were discovered. These are: fully electric insulation, a sample loop volume in the range of several tens of nanoliters, and a complete spatial separation of the two separation dimensions. A special 4-port valve which fulfilled these requirements was selected and characterized.

Fundamental experiments, which were carried out using a simplified one-dimensional system, showed that it is possible to integrate the valve into the high voltage electric circuit of the capillary electrophoresis. Furthermore, only a slight peak broadening of a factor of ≤ 2 was observed in the first successful separations through the valve.

This work shows the stepwise development of a complete heart-cut two-dimensional system with mass spectrometric detection in the second dimension. To enable precise cutting of the analytes by the valve, an additional detection was introduced to the first dimension directly in front of the valve. Repeatable selective cutting with a deviation of $< 20\%$ regarding the peak area from multiple injections was found to be possible. In addition, a conductivity detector was used for the detection of organic solvent plugs within the separation capillaries. The ability to very precisely position solvent plugs in the separation system was further confirmed. Such plugs can be used e.g. to introduce effective re-concentration steps in the second dimension.

Unfortunately, problems with the valve material arose periodically during the experimental work. Particles were formed inside the valve due to electric flashovers. During the switching steps, these particles created scratches on the valve material and, therefore, to leakages. However, the application of a limited voltage or electric current respectively minimized the formation of those particles.

Finally, two-dimensional separations were performed using a non-volatile, phosphate based background electrolyte in the first dimension. Here, the interfering phosphate was separated from the analytes in the second dimension and, therefore, the analytes could be successfully detected by electrospray ionization-mass spectrometry.

The innovative heart-cut two-dimensional capillary electrophoresis system with mass spectrometric detection using a fully electric insulated mechanical valve as interface introduces many possible applications in coupling capillary electrophoretic methods, modes, and techniques to mass spectrometric detection. This enables selective and sensitive detection as well as analyte identification.

In addition, the system can be applied for the hyphenation of two different capillary electrophoretic modes, or even different techniques like liquid chromatography, for the separation of complex mixtures in a classical two-dimensional approach.

List of Publications / Award

CZE-CZE ESI-MS Coupling with a Fully Isolated Mechanical Valve

Felix J. Kohl, Christian Neusüß

Methods in Molecular Biology – Capillary Electrophoresis,
Schmitt-Kopplin, P. (Ed.), Humana Press 2016, 155-166.

On-line two-dimensional capillary electrophoresis with mass spectrometric detection using a fully electric isolated mechanical valve

Felix J. Kohl, Cristina Montealegre, Christian Neusüß

Electrophoresis 2016, 37, 954-958.

Capillary electrophoresis in two-dimensional separation systems – techniques and applications

Felix J. Kohl, Laura Sánchez-Hernández, Christian Neusüß

Electrophoresis 2015, 36, 144-158.

Oral presentation:

Anwendung der Komplexbildung zur Bestimmung von EDTA und DTPA mittels Kapillarelektrophorese-Massenspektrometrie

Felix J. Kohl

CE-Forum 2011, Regensburg, Germany

Poster presentations:

Design and Development of a Heart-Cut Two Dimensional Capillary Electrophoresis System with Mass Spectrometric Detection

Felix J. Kohl, Laura Sánchez-Hernández, Christian Neusüß

CE-Forum 2013, Jena, Germany

Capillary Electrophoresis-Mass Spectrometry for the Determination of EDTA and Similar Complexing Agents

Felix J. Kohl, Johannes Sommer, Angelina Taichrib, Christian Neusüß

ANAKON 2011, Zurich, Switzerland

Award:

Award of the "Fachgruppe Analytische Chemie" of the Gesellschaft deutscher Chemiker (GDCh) e.V. for the best degree in analytical chemistry in the year 2009

ANAKON 2011, Zurich, Switzerland

Table of Content

Acknowledgement.....	5
List of Abbreviations.....	7
Zusammenfassung.....	11
Summary	15
List of Publications / Award	19
Table of Content.....	21
Part I Introduction	25
1 Objective	27
1.1 Dissertation Organization.....	28
2 Two-Dimensional Capillary Electrophoresis	33
2.1 Two-Dimensional Separations	33
2.2 Techniques in Two-Dimensional Capillary Electrophoresis	34
2.2.1 Offline Two-Dimensional Capillary Electrophoresis	35
2.2.2 Two-Dimensional Separation in a Single Capillary	36
2.2.3 Hyphenated Two-Dimensional Capillary Electrophoresis	38
3 Capillary Electrophoresis	47
3.1 Principles of Electrophoresis.....	47
3.2 Modes of Capillary Electrophoresis	48
3.3 Instrumentation in Capillary Electrophoresis	50
3.4 Detection Options in Capillary Electrophoresis	53
4 Capillary Electrophoresis - Mass Spectrometry	57
4.1 Electrospray Ionization	57

4.2	Coupling Techniques.....	59
4.3	Mass Spectrometry.....	60
4.4	Specific Characteristics and Limitations in CE-MS	65
4.4.1	Limitations in CE-MS	65
4.4.2	The Role of the BGE in CE and CE-MS	65
4.4.3	Strategies for CE-MS Coupling of non-ESI Compatible CE Techniques and Modes	66
Part II Methods.....		71
5	Instrumentation, Materials, and Methods	73
5.1	Instrumentation	73
5.1.1	Capillary Electrophoresis Instrumentation	73
5.1.2	Mass Spectrometry Instrumentation.....	74
5.1.3	Additional Detection Options	74
5.2	Materials and Chemicals.....	75
5.2.1	Materials	75
5.2.2	Chemicals.....	75
5.3	Methods.....	76
5.3.1	Capillary Electrophoresis.....	76
5.3.2	Detection.....	78
5.3.3	1D and 2D System.....	81
Part III Results and Discussion.....		83
6	Valve: Selection and Integration.....	85
6.1	Valve Requirements.....	85
6.2	Actual Valve Design.....	87
7	Applicability of Spectroscopic Detection and Conductivity Detection.....	93
8	One-Dimensional Experiments.....	99
8.1	1D System with UV Detection	100
8.2	1D System with MS Detection	101

8.3	Cutting and Reintroducing of Specific Signals	104
8.4	Integration of Additional UV Detection in Front of the Valve	107
8.5	Evaluation of the Cutting Precision with C ⁴ D and MS Detection	110
9	Experimental Setup of the Two-Dimensional System	115
9.1	Instrumental Setup of the 2D System	115
9.2	Capillary Lengths in the 2D System.....	119
10	Two-Dimensional Experiments	121
10.1	Peptide Analysis by 2D CZE-CZE MS	122
10.2	Application of Coated Capillaries for the 2D CZE-CZE Analysis of Proteins	126
10.3	Application of a non-ESI-MS Compatible BGE in the First Dimension	127
11	Pitfalls and Technical Issues	131
11.1	Automation of the 2D System	131
11.2	Capillary Clogging.....	133
11.3	Valve Damages	133
12	Concluding Remarks	137
	Appendix	139
	List of Figures	141
	List of Tables.....	149
	Bibliography.....	151
	Curriculum Vitae.....	161

Part I

Introduction

1 Objective

Separation and identification of components in complex samples is a challenging task in analytical chemistry. Besides the most common separation techniques liquid chromatography (LC) and gas chromatography (GC), capillary electrophoresis (CE) appears to be a very powerful tool and is increasingly used in a broad range of applications in industry and research. Due to its different selectivity and high separation efficiency CE is an interesting alternative. Especially in the analysis of large bio-molecules (e.g. intact proteins) capillary zone electrophoresis (CZE) and related CE modes, like capillary sieving electrophoresis (CSE) and capillary gel electrophoresis (CGE), or different electromigrative techniques, like capillary isoelectric focusing (CIEF), are of high relevance.

In most commercial CE instruments, detection is commonly carried out by an integrated optical detector. This appears to be suitable since these detectors are robust, easy to use, and universal. However, mass spectrometry (MS) is an excellent alternative because it provides high sensitivity, high selectivity, and information on the composition and the structure of the analytes. Since in most CE modes already charged molecules are needed to even enable separation, electrospray ionization (ESI) is ideally suited for coupling of CE and MS.

However, in many CE applications or CE modes, established in industry and research, background electrolytes (BGE) are applied which contain salts like e.g. borate or phosphate or different substances which are charged or can be easily ionized by ESI. Such substances interfere in the ESI process which leads to signal quenching and pollution of the ESI interface and the MS instrument. Therefore, direct coupling is impractical.

Unfortunately, many of these validated applications cannot be changed easily to a volatile BGE. Further, in different techniques like CGE, CSE, micellar electrokinetic chromatography (MEKC) etc. ESI interfering compounds in the BGE are essential for the separation. Hence, some strategy is needed to remove these compounds previous to MS detection.

The goal of the project was to establish an analytical approach enabling the hyphenation of non-ESI compatible CE methods and modes to MS detection. In the presented concept, the basic idea was the development of a fully electric insulated valve for its integration to a CE separation system. The function of the valve should be the transfer of analytes from a first, non-ESI compatible separation (first dimension) to a second, short separation (second dimension). In this case, the second dimension appeared as a short cleanup step for the separation of the interfering compounds from the analytes prior to ESI-MS detection.

Such a system is described as a heart-cut two-dimensional (2D) separation system. Besides the use as a cleanup step in order to eliminate matrix influences before MS detection, the second dimension can play further roles like a second separation dimension in principle. Such multidimensional separation systems offer a very high separation power and peak capacity and can be applied for the separation of very complex samples.

Besides CE-CE coupling, the technical principle can be used for various combinations of analytical techniques like LC and CE for two-dimensional separation. Therefore, the presented system introduces various possible applications in many fields of analytical chemistry.

1.1 Dissertation Organization

The work presented here is divided into the three parts: "Introduction", "Methods", and "Results and Discussion".

The first part "Introduction" comprises four main chapters, "Objective", "Two-Dimensional Capillary Electrophoresis", "Capillary Electrophoresis", and "Capillary Electrophoresis-Mass Spectrometry".

In the first chapter "Objective", a short overview of the dissertation objective, the motivation, as well as the organization of the work is given. In "Two-Dimensional Capillary Electrophoresis" 2D separations in principle and state of the art 2D CE techniques are discussed. This chapter is followed by the third chapter "Capillary Electrophoresis" where theoretical and technical fundamentals of capillary electrophoresis are given. The fourth chapter "Capillary Electrophoresis-Mass Spectrometry" comprises the hyphenation of capillary electrophoresis and mass spectrometry, as well as the used mass spectrometric techniques. The differences and pitfalls in using an open CE-MS system in comparison to a closed CE system equipped with a non-destructive (optical-) on-capillary detection are discussed. Further, limitations in CE-MS are described with the focus on applicable BGEs and CE modes followed by a discussion on the role of the BGE in CE and CE-MS. At least, some strategies are shown which can be applied to diminish the limitations described before. Here, emphasis is taken on the partial filling technology.

In part two: "Methods", the instruments, materials, and chemicals which were used to perform the various experiments during the project work, as well as the main method parameters are summarized. Detailed experimental conditions are always given in the specific sections.

The setup and characterization of the 2D system is described and discussed in several steps in part three: "Results and Discussion". It is divided into seven main chapters: "Valve: Selection and Integration", "Applicability of Spectroscopic Detection and Conductivity Detection", "One-Dimensional Experiments", "Experimental Setup of the 2D System", "Two-Dimensional Experiments", and "Pitfalls and Technical Issues" while the work closes with the last chapter "Concluding Remarks".

The small structures and volumes as well as the strong electric fields which are used in CE require special instrumentation. By nature, the same applies to a valve which should be used as a 2D interface. For this reason, the selection of the interface was of major importance. A fully insulated mechanical valve was found to be able to fulfill the requirements for its application in a 2D CE system. A detailed description of the actually used valve and the integration into the 2D system are discussed in "Valve: Selection and Integration".

Detection of the analytes before they migrate into the valve is of high importance to ensure precise and selective cutting. For this reason, external detectors are required which can be installed directly in front of the valve. The suitability for the integration of the optical detectors, ultra violet/visible (UV/Vis) and laser induced fluorescence (LIF), as well as the capacitively coupled contactless conductivity detector (C⁴D) was tested. The sensitivity of the different external detectors was compared to the sensitivity of an integrated detector of a CE instrument to evaluate the usefulness for their application in the 2D system. The results are shown in the chapter "Applicability of Spectroscopic Detection and Conductivity Detection".

The valve was integrated into a CE separation system with UV as well as with MS detection. Different concepts were tested using a simplified one-dimensional approach. The analytical power of the system containing the valve was compared to a system equipped with a continuous capillary. Further, the ability to cut single signals was studied by the analysis of peptides. Moreover, the external detectors were introduced to increase cutting precision. Further possibilities using the C⁴D were evaluated. The integration of the valve and the external detectors is described in the section "One-Dimensional Experiments".

The setup of a 2D system shows different technical and instrumental conditions than a 1D system because additional parts and considerations are required. The different possibilities to enable 2D separations, as the necessary instrumentation, the spatial arrangement of the instruments, as well as the different possibilities for capillary lengths, are discussed in the section "Experimental Setup of the 2D System".

Subsequently, the complete 2D system is studied in detail in the chapter "Two-Dimensional Experiments". First, sample transfer from the first to the second dimension was studied in a CZE-CZE MS approach on the examples of the analysis of peptides as well as proteins. Further, the feasibility of the system is shown by direct coupling of a non-ESI compatible phosphate-based CZE system with MS detection. Here, interfering phosphate was successfully separated before the analytes were detected by ESI-MS.

Unfortunately, some technical problems arose during the experimental work, especially regarding the valve material. These problems as well as possible solution approaches are comprised by the chapter "Pitfalls and Technical Issues". The last chapter "Concluding Remarks" summarizes the results of this work and provides an outlook for future application opportunities of the presented innovative 2D CE System.

2 Two-Dimensional Capillary Electrophoresis

In 2D separation systems two separation techniques or modes are combined. Therefore, the sample is first separated by a first separation technique (first dimensions) and subsequently by a second (second dimension).

A two-dimensional system where the second dimension is used to separate interfering compounds previous to MS detection appears to be very promising. However, all of the described 2D approaches were applied in order to achieve a higher peak capacity for the separation of complex samples in such cases, where the conventional separation techniques are no more able to achieve sufficient separation power. In the following, different concepts to carry out 2D CE, as well as their applicability to enable CE-MS hyphenation, are discussed.

Parts of the following chapter are published in [1]:

Kohl, F. J., Sánchez-Hernández, L., Neusüß, C., *Capillary electrophoresis in two-dimensional separation systems: Techniques and applications, Electrophoresis* 2015, 36, 144-158.

2.1 Two-Dimensional Separations

Two-dimensional separation techniques, especially the combination of chromatographic techniques like e.g. LC-LC [2, 3], GC-GC [4], or thin layer chromatography-thin layer chromatography (TLC-TLC) [5] are increasingly applied for the separation of complex samples. In such systems mostly two separation techniques or methods with different selectivity are combined to achieve an improved peak capacity in comparison to a 1D system.

In an ideal 2D approach, the selectivities of the two separation mechanisms show the possibly lowest degree of correlation which means they are orthogonal. When orthogonality is given, the peak capacity of the 2D system ($n_{c,2D}$) is the product of the peak capacities of the single dimensions (1n_c , 2n_c) [6] and the maximum peak capacity is reached (equation 1).

$$n_{c,2D} = {}^1n_c \times {}^2n_c \quad (1)$$

Besides the enhancement in peak capacity, the second dimension can have further functions and can act as a pre-concentration or cleanup stage in order to remove e.g. interfering matrix compounds.

In 2D systems it can be distinguished between heart-cut and comprehensive approaches [3]. In heart-cut 2D separation, the portion of interest is cut from the first separation dimension and transferred to the second while in comprehensive approaches the whole entirety of the first dimension effluent is subjected to the separation in the second dimension. Hence, in comprehensive 2D analysis, the separation time of the second dimension must be low enough to not decrease resolution [6]. Further on, all (disturbing) matrix components from the first dimension will enter the second dimension in the comprehensive concept.

From a technical aspect, it needs to be distinguished between offline and online systems. In offline approaches, in contrast to online systems, the two separation dimensions are not directly hyphenated. The online approaches, in turn, can be divided into systems using a single capillary, an interface, or a valve. Further on, microfluidic devices for 2D separations became important [7-10]. However, because this work deals with 2D separation using classical capillary electrophoresis, microfluidic approaches are not further discussed in the following.

2.2 Techniques in Two-Dimensional Capillary Electrophoresis

Besides 2D LC and GC coupling also some 2D approaches were developed, including at least one CE dimension. CE techniques and modes mostly show a different selectivity in comparison to LC.

Thus, 2D systems with at least one electrophoretic dimension appear to be an interesting option in order to reach orthogonality.

Due to the relative short analysis time, CE is mostly applied as the second dimension although it has also been used as first dimension. In addition, electrophoretic techniques can be used in both dimensions. However, due to the small sample amounts or injection volumes respectively and the application of separation high voltage (HV), special coupling techniques and interfaces are required, especially in online approaches. Different strategies are summarized recently for 2D separations in general including 2D CE [11-13] and for 2D CE in particular [1, 14-16]. In the following, 2D-CE systems are discussed with the focus on interfaced heart-cut approaches.

2.2.1 Offline Two-Dimensional Capillary Electrophoresis

In offline 2D separation, fractions are collected after a first separation of the sample compounds (first dimension). Subsequently, the fractions are manually transferred to the second dimension and are subjected to a second separation step. This concept has some advantages compared to direct online coupling. The selection of the two separation techniques is nearly unrestricted regarding chemical (e.g. solvent composition, additives, pH) and physical conditions (e.g. sample volume, flow rate, pressure, temperature). Hence, it is comparable easy to reach orthogonality. Nearly any commercially available instrument can be applied with any detection technique, including mass spectrometry.

Further on, treatment of the first dimension fractions like e.g. matrix separation, digestion, or derivatization is easily possible before separation in the second dimension. Using a comprehensive approach, analysis time in the second dimension is uncritical since the fractions can be stored until the separation in the second dimension is completed. Nevertheless, offline 2D separations are often time consuming and, in many cases, automation is not possible. In addition, unwanted sample modifications like e.g. dilution or degradation can be caused by fraction collection, storage, and transfer to the second dimension.

The comparable large number of applications where CE is applied as the second dimension and high performance liquid chromatography (HPLC) [17-31], capillary LC [32-36], and size exclusion chromatography (SEC) [37] as the first, shows the technical possibilities to combine a chromatographic technique with CE.

At this, the chromatographic technique was predominantly used as the first dimension. The main reasons for this may be the, compared to the most CE techniques, high bulk flow and the high injection volume which simplify the fraction collection process. However, the high volumes in LC can also dilute the samples or fractions respectively. Therefore, the analyte concentration could be too low for CE analysis where often only very small volumes can be injected. Hence, additional sample pre-concentration would be required (e.g. large volume sample stacking or solid phase extraction (SPE) [18, 25, 26]) previous to the separation in the second CE dimension.

Although CE was successfully applied as the first dimension of a 2D system with HPLC [38-40] or a second CE mode [41] in the second dimension, it suffers from several drawbacks. The first dimension CE mode is limited to approaches that show an electroosmotic flow (EOF) in outlet direction to enable fraction collection in principle. Otherwise, pressure needs to be applied during the analysis or sample zones need to be hydrodynamically mobilized after separation. Both leads to additional diffusion and, therefore, lowers the separation efficiency. But, even though pressure is applied or a strong EOF is used, fraction collection is still more challenging compared to LC because of the low bulk flow and the small injection volumes in CE. Further, the electric circuit must be closed at the outlet of the CE separation capillary by e.g. a liquid which leads to dilution of the effluent or the collected fractions respectively. Treatment of the collected samples is difficult as well because of the small fraction volumes.

2.2.2 Two-Dimensional Separation in a Single Capillary

Besides the offline and hyphenated 2D strategies, 2D CE can be carried out in a single capillary. Here, the sample is separated by an initial CE mode. Subsequently, the BGE is exchanged and the sample is subjected to a second separation with different selectivity.

Because the same capillary is used in both dimensions no particular interface is needed and the system setup is comparably simple. In addition, no fraction collection step is applied. Therefore, it can be classified as an intermediate between offline and interfaced approaches.

2D CE in a single capillary is, by nature, used with different CE techniques in both dimensions and was already applied for applications with CZE in the first and CSE [42, 43], MEKC [44, 45], electrokinetic chromatography (EKC) [46, 47], and CZE [48-51] in the second dimension.

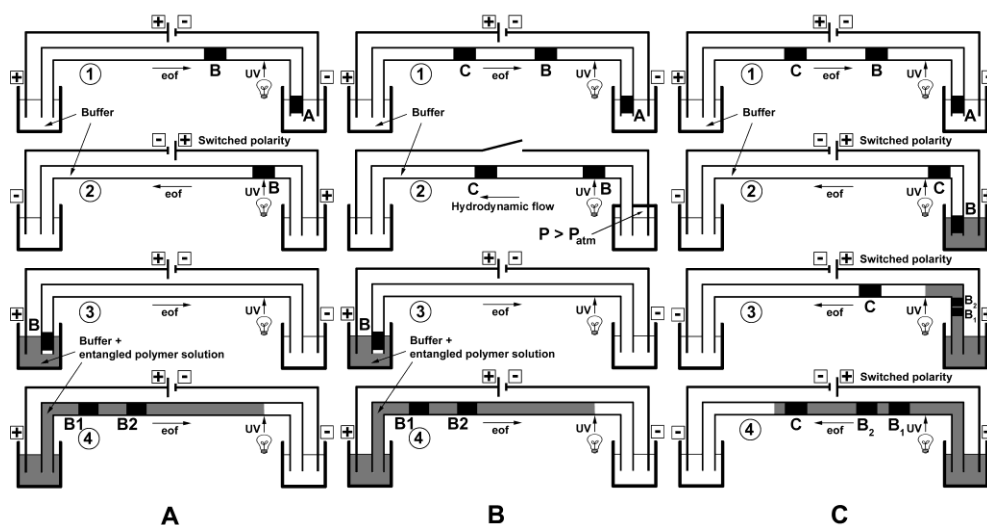


Figure 1: Schematic Illustration of the Three Different Strategies (A-C) in 2D CE in a Single Capillary [42].

Three different strategies are used in 2D CE in a single capillary: In the first strategy (Figure 1 A), the anionic compounds are separated from the anodic inlet to the cathodic outlet supported by a strong EOF. Afterwards, the analytes are mobilized back to the inlet by polarity switching. The inlet buffer vial is exchanged by a CSE buffer and the analytes are subsequently separated again towards the cathodic outlet with the help of the EOF. Since the analytes are slowed down due to their migration towards the anode, they are swapped by the CSE buffer enabling a second separation step in CSE mode. The second strategy (Figure 1 B) is similar to the first but the analytes are transported back to the inlet after the first separation step by hydrodynamic mobilization. In the third strategy (Figure 1 C), the outlet buffer vial is exchanged by a CSE buffer after the CZE separation.

Subsequently, the polarity is interchanged and the analytes are separated in CSE mode towards the cathodic inlet. Equally to the first strategy, the analytes are swapped by the CSE buffer in the second separation step. In addition, matrix compounds as well as early and late migrating substances can be removed during the mobilization steps. Hence, these strategies can be applied to perform heart-cut 2D separations.

2D CE in a single capillary is technically simple and easy to set up using commercial instruments. However, there are several limitations. 2D CE in a single capillary is restricted to CZE and related techniques. It is not possible to combine CZE with a pressure driven technique like LC. This makes it very difficult to reach orthogonality.

Capillary treatment, like e.g. coating of the capillary inner wall or packing of the capillaries, is limited since it needs to be suitable for both dimensions. Control of EOF velocity and direction is very important which further reduces the application range. Moreover, MS detection is hardly possible since a (pressurized) outlet vial is needed.

Besides 2D separation in a single capillary, in-line SPE-CE, which is actually used as a pre-concentration technique [52-54], can be considered as 2D separation when multistep elution is applied. It can be classified as 2D LC-CE in a single capillary since no fraction collection process is applied and no specific interface is needed. In contrast to 2D CE in a single capillary, only comprehensive separation is possible. But here, MS detection can be applied because no outlet vial is necessary [50, 51].

2.2.3 Hyphenated Two-Dimensional Capillary Electrophoresis

Different types of interfaces are applied in order to enable 2D separation with at least one CE dimension. All of them show particular abilities as well as specific advantages and disadvantages.

However, in contrast to 2D CE in a single capillary, most of the interfaced approaches are less limited in the application of different separation techniques and modes (e.g. LC, CE) and detection options. Table 1 summarizes the common interfaces. At this, gating interfaces are most frequently used.

Table 1: Different Interfaces, Advantages and Disadvantages.

Interface	Advantages	Disadvantages
Dialysis [55-59]	Technical comparably easy to set up	Only comprehensive coupling possible
Porous Junction [60, 61]	No mechanical device needed Only one capillary	Only comprehensive coupling possible
Tee-Union [62-64]	Technical comparably easy to set up	Direct hyphenation of the two capillaries
Hydrodynamic [65]	Valve free	Difficult to couple two electromigrative techniques
Gating [65-86]	Heart-cut possible Various combinations of techniques possible	High technical effort
Valve [87-96]	Complete spatial separation of the two dimensions Almost all combinations of different techniques possible	High technical effort

Dialysis Interface

Dialysis interfaces are used to hyphenate two electromigrative techniques like e.g. CIEF and CGE [57] or CIEF and CSE [59]. The setups differ slightly, but all of them create an electro conductive gap between two capillaries. This gap separates the two electric circuits of the two dimensions. Hence, the analytes are first separated towards the dialysis interface. Subsequently, they are transferred (e.g. by hydrodynamic mobilization) to the second dimension and are subjected to another separation with a different selectivity. Figure 2 shows the exemplary setup of a 2D CIEF-CSE approach using a dialysis interface.

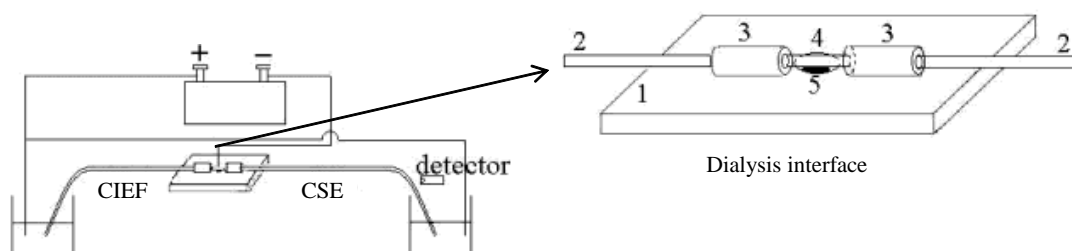


Figure 2: Setup of a 2D CIEF-CGE Approach using a Dialysis Interface which is Constructed of: 1) Methacrylate Plate, 2) Separation Capillaries, 3) Teflon Tubes, 4) Hollow Fiber, and 5) Buffer Reservoir [59].

In comparison to 2D CE in a single capillary the application of a dialysis interface shows some advantages. The mobilization steps are needles which reduces diffusion and increases separation efficiency. Further, different capillaries with regard to e.g. coatings or packing can be applied in the two dimensions and MS detection is possible in principle since no outlet vial is needed. However, these systems are limited to CE modes and techniques as well. In addition, control of EOF direction and velocity is of highest importance to prevent mixing of the different BGEs at the transition between the capillaries. Further, only comprehensive analysis is possible.

Porous Junction Interface

The porous junction interface can be considered as a further development of the dialysis interface. The separation of the electric circuits of the two dimensions is no more carried out by a gap between the two capillaries but by a porous junction. This junction is created by etching a small part of the separation capillary with hydrofluoric acid to achieve an electric conductive membrane.

The porous junction interface is technically more simply constructed compared to the dialysis interface but the main disadvantages (e.g. limited to CE techniques and modes, EOF control, only comprehensive separation) are similar. In addition, different treatment of the capillaries (e.g. coating) in the two dimensions is even more challenging since the capillaries cannot be treated separately. Problems with the robustness, which arose due to the fragile etched capillary part, could be solved by etching only a part of the capillary and not the whole circumference [61].

Tee-union Interface

A further option to hyphenate two CE modes for 2D analysis is the application of a tee-union as interface. Similar to the dialysis and the porous junction interface, the third connection of the tee-union serves as an electric connection which enables the separation of the electric circuits of the two separation dimensions.

Even though the tee-union allows separate flushing of the particular dimensions, these approaches are still very limited with regard to applicable separation modes and techniques since the dimensions are directly connected.

Anyhow, good results could be achieved in hyphenation of CZE and MEKC [62] as well as CITP and CE [64] but it was also shown, that a microfluidic device shows much better transfer characteristics compared to a tee-union due to distortion of the electric and fluid flow fields [63].

Gating Interfaces

The most frequently applied interface techniques to enable 2D CE separation are the flow gating interfaces. Here, the two separation capillaries are installed in a special device towards each other with a small gap in between. This small gap allows the application of a liquid flow in orthogonal direction to the separation capillaries. This flow draws upcoming effluent from the first dimension to waste.

The transfer of a sample from the first to the second dimension is carried out by either hydrodynamic or electrokinetic injection after stopping the transverse flow. Only the portion of interest is injected. Influencing (matrix) compounds are drawn to waste before or after the injection by the transverse flow. Therefore, this system is a real heart-cut approach.

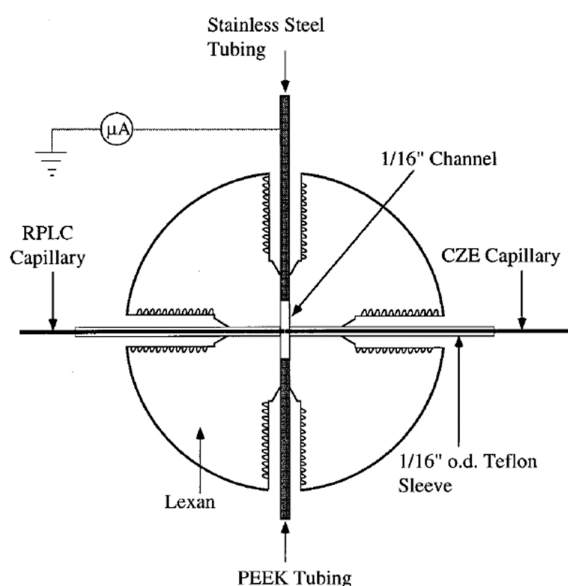


Figure 3: Schematic Setup of the Clear Flow Gating Interface [68].

Besides the first transverse flow gating interface [66], an improved transparent flow gating interface is described (Figure 3) [68]. This interface is constructed of a transparent polycarbonate disc which allows direct observation of the gating and injection process (Figure 4).

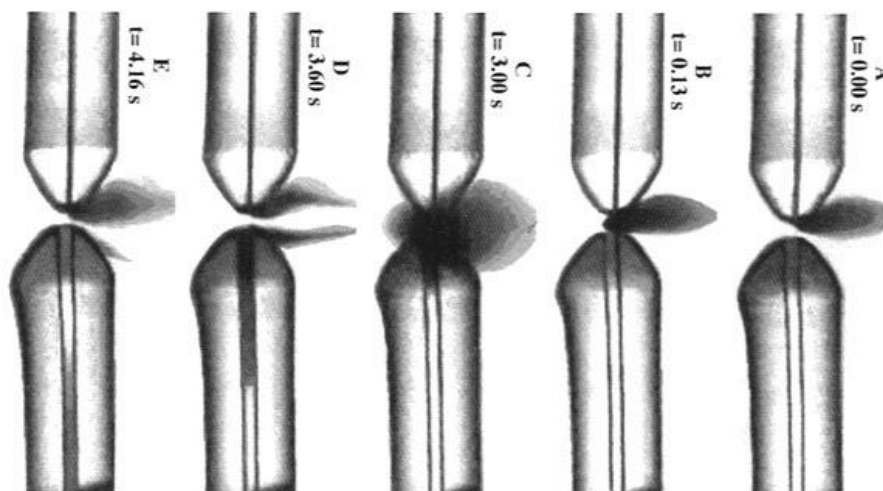


Figure 4: Frame-Grabbed Video Images of the Injection Process using the Transparent Flow Gating Interface [68].

The application of a special coupling device or an interface respectively increases the number of possible combinations of separation techniques in contrast to 2D CE in a single capillary. Gating interfaces were used for the hyphenation of two electromigrative techniques like CSE and MEKC [72, 74, 75] or CIEF and CZE [81] as well as for the hyphenation of a pressure driven separation technique and CE like LC and CZE [67, 83].

However, EOF control is still essential in this open interfaced system in order to prevent the liquid from the transverse flow from entering one of the separation capillaries. This further diminishes possible capillary treatments. In addition, it appears to be difficult to transfer a defined volume without dilution by the liquid of the gating flow. Although MS detection is applied in flow gating approaches [82, 83], it seems to be challenging because a (pressurized) outlet vial is needed to perform hydrodynamic injection in the second dimension.

2D Systems using a Mechanical Valve

For complete spatial separation of the two separation dimensions, a mechanical valve can be applied as the interface. This separation of the dimensions enables nearly unlimited selection of separation conditions like e.g. migration of the compounds, EOF velocity and direction, volumes and flow rates, additives, and capillary treatments.

Combinations of CE and pressure driven techniques are easily possible. In addition, all method actions like flushing, injecting, or applying separation HV can be carried out independently or even simultaneously in both dimensions.

In spite of this, integration of a mechanical valve into a HV driven CE system is rather challenging. Most commercial valves are designed for their use in HPLC systems. The requirements here differ from those in CE applications. Various valves are produced from conductive material like stainless steel which is complicated to integrate in the HV electric circuit of CE. Furthermore, dimensions of the valve structures, the dead volumes, and the sample loop volumes are mainly matched with LC flow rates. For CE applications, dead volumes need to be minimized and a sample loop with a volume of typical CE peak or injection volumes respectively (mid nL range) must be available for the complete transfer to the second dimension.

Nevertheless, the use of a stainless steel valve in a 2D setup for the hyphenation of HPLC in the first and CZE in the second dimension could be shown [87]. Here, the second HV driven separation dimension is grounded at the connection between the separation capillary and the valve and HV is applied at the capillary outlet vial. Hence, the valve is excluded from the CZE electric circuit. Since the first dimension is pressure driven, no further grounding is necessary.

Anyway, the implementation of a HV driven first dimension is also possible by grounding at the connection between the outlet of the first dimension separation capillary and the valve as shown by the setup in Figure 5 [92]. Here, electrokinetic injection is carried out in the second dimension. Therefore, a comparable high sample loop volume of 10 μL can be used.

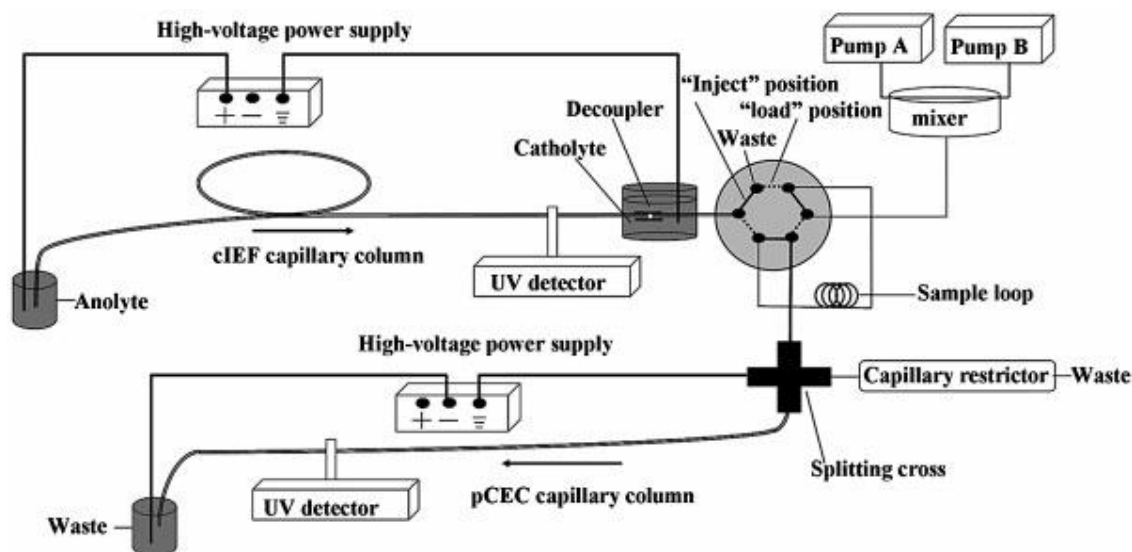


Figure 5: Schematic Diagram of a CIEF-pCEC 2D System using a Six-Port Valve as the Interface. The Two HV Driven Separation Dimension are Grounded in Front of the Valve or Behind the Valve Respectively [92].

Although this strategy has overcome the issues of the conductive valve material and the large valve structures, MS detection is not possible because an outlet vial is needed in the second dimension in order to apply separation HV and to enable flushing.

Alternatively, a nanoinjector 6-way valve with a port-to-port volume of 25 nL made from ceramic material is used [93]. Because of the non-conductive material, the hyphenation of CIEF in the first and CEC in the second dimension could be established with two separated and independent electric circuits without additional grounding.

In this setup, using the 6-way valve, the CIEF capillary of the first dimension needs to be connected to the capillary of the second dimension by switching the valve in order to carry out injections. Subsequently, the sample is transferred from the first to the second dimension by hydrodynamic mobilization. After the valve is switched back, the separation in the second dimension can be started. Therefore, there is no transfer of a defined sample loop volume from the first to the second dimension but a hydrodynamic injection while the two dimensions are directly connected.

Although UV detection is applied, implementation of MS detection would be unproblematic since the flushing and injection processes in the second dimension could be carried out by the pressurized inlet vial.

Anyhow, in the described 2D systems with a valve as interface mainly a chromatographic technique like CEC is used as the second dimension. This may be due to the opportunity to use higher injection volumes and to re-focus the analytes at the column head. Re-focusing is more simple using a chromatographic technique and more effective in comparison to the re-focusing techniques in CE like e.g. large volume sample stacking.

In conclusion, using a mechanical valve as the interface is probably the technically most challenging alternative. However, only the usage of a valve leads to complete spatial separation of the two dimensions enabling nearly unlimited selection of separation techniques, modes, and methods as well as unrestricted MS compatibility. However, no hyphenation of two CZE modes using a mechanical valve as the interface for the complete transfer of a defined sample loop volume was performed so far.

3 Capillary Electrophoresis

Capillary electrophoresis is based on the separation of charged species in an electric field [97]. CE shows high analytical power and generates very high efficiencies. Separation is usually completed in minutes. Because of the small structures and the low volumes, CE shows very low sample and solvent consumption. These characteristics and capabilities of CE have promoted it as a powerful technique in research and industry. Several instrumental improvements and the increasing request for alternative high performance separation techniques have led to a continuously expanding of routine CE applications.

3.1 Principles of Electrophoresis

Electrophoresis is the migration of charged particles under the influence of an electric field [98]. The velocity (v_e) of this migration depends on the strength of the electric field (E) and on the size/shape and the charge state of the particle. The charge state and the size/shape are summarized in the electrophoretic mobility (μ_e) which is naturally constant for a single kind of particle. The electrophoretic velocity can be described by equation 2.

$$v_e = \mu_e \cdot E \quad (2)$$

Besides the migration of the ions in the electric field, the EOF appears principally in CE. The EOF is a bulk flow and is pH dependent, formed by deprotonation of the hydroxyl groups on the surface of fused silica capillaries [98]. By nature, the EOF also transports uncharged particles and molecules.

The separation power of a CE system is described by the separation efficiency or the number of theoretical plates respectively. The number of theoretical plates illustrates the baseline width of a peak (w_b) at the corresponding migration time.

A system, providing a high number of theoretical plates will always generate more narrow peaks than a system with a lower number of theoretical plates and, therefore, provides a higher peak capacity. The number of theoretical plates (N) can be calculated by:

$$N = \left(\frac{4 \cdot l_{eff}}{w_b} \right)^2 = \frac{l_{eff}^2}{\sigma^2} \quad (3)$$

Here, l_{eff} is the effective capillary length while σ^2 is the peak dispersion which is caused by diffusion during migration. The migration time is indirect proportional to the electric field strength. Hence, while the peak dispersion is direct proportional to the migration time, an increased separation HV leads to less peak dispersion and, therefore, to a higher separation efficiency or number of theoretical plates respectively. Besides the separation efficiency, the resolution (R_s) describes the feasibility to separate two adjacent peaks:

$$R_s = \frac{1}{4} \cdot \frac{\Delta\mu_e}{\bar{\mu}_e} \cdot \sqrt{N} \quad (4)$$

Equation 4 illustrates, that the differences in electrophoretic mobility are influencing the resolution much more than the number of theoretical plates or the separation HV respectively. In order to increase the resolution by a factor of two, the HV must be increased by a factor of four. Anyway, in CZE a difference of only < 0.05 % in electrophoretic mobility can be sufficient for baseline separation of two compounds.

3.2 Modes of Capillary Electrophoresis

The term "capillary electrophoresis" comprises a variety of different modes of operation which provide completely different separation selectivities. Although, CE is often considered as a synonym for CZE it stands for all electrophoretic separation techniques where ions are separated in a capillary by the differences in their charge to size ratio under the influence of an electric field [99].

Besides CE, there are further related electromigrative analytical separation techniques carried out in a capillary like e.g. capillary isotachopheresis (CITP), capillary electrochromatography (CEC), MEKC, and CIEF.

CZE is the most basic CE mode and is also called “free solution capillary electrophoresis” or “free zone electrophoresis”. Under the influence of a HV field analytes migrate with different velocities according to their electrophoretic mobility and are separated in discrete zones. Therefore, separation in CZE occurs according to the differences in the charge-to-size ratio of the ions.

In addition to the electro migration, the analytes are transported by the EOF in CZE. In standard systems without any capillary coating, the EOF moves in cathodic direction. Hence, the total velocity (v_{tot}) of the cations is increased by the EOF while the velocity of the anions is decreased by the EOF in a system with cathodic detection.

If the EOF velocity exceeds the electrophoretic velocity of an anion, the anion will be swapped to the cathodic end of the capillary. Therefore, analysis of anodic and cathodic compounds can be performed simultaneously in a single run by CZE with normal EOF and cathodic detection. Neutral compounds are transported by the EOF only and are not separated since their charge is zero. Anions with an electrophoretic velocity higher than the EOF velocity can be analyzed either by increasing the EOF velocity or by using anodic detection.

In order to influence the selectivity in CZE, several additives in the BGE like e.g. inorganic salts, organic solvents, or acids and bases can be applied. Among others, the electrophoretic mobility can be changed by these additives which may help solving two substances of similar or same electrophoretic mobility.

Further, special selectivities can be achieved by special BGE additives. For example, separation of isomers can be obtained by the addition of a chiral selector. Cyclodextrins (CD) permit chiral separation by stereoselective interaction with the analyte [100, 101]. Both, charged as well as neutral enantiomers can be separated by this application by using charged CDs for neutral compounds or neutral CDs for charged compounds respectively. The application of a chiral selector can be classified as a hybrid of CZE and MEKC.

Besides, separation by size can be achieved by CSE [102]. At this, the influence of the molecule size on the separation is increased by the addition of a sieving matrix.

In contrast to CGE, where cross-linked gels are polymerized inside the capillary, linear polymers like e.g. linear polyacrylamide, hydroxyl-ethyl cellulose, galactomannan, dextran, polyvinylalcohol, polymethylacrylamide, polydimethylacrylamide, polyethylene oxid, agarose, or polyacryloylaminopropanol [103-106] are applied in CSE. These polymers are able to form an entangled network. This network exhibits sieving properties similar or even identical to those of a cross-linked gel [107], but with the opportunity to replace the sieving matrix in the capillary by flushing.

Therefore, CSE can be used according to conventional slab gel electrophoresis e.g. for the separation of proteins as sodium dodecylsulfate (SDS) complexes. In those approaches, the charge of the proteins is masked by the SDS resulting in separation of the anionic complexes only after their differences in size. In contrast to slab gel electrophoresis, CSE provides the benefits of the automated CE system and various online detection possibilities.

3.3 Instrumentation in Capillary Electrophoresis

Figure 6 shows the schematic setup of a standard CE instrument with optical detection. It includes an inlet and an outlet vial which are connected by the separation capillary, a pump, a HV power supply connected to the inlet electrode, a grounded connection at the outlet electrode, and a detector in front of or at the capillary outlet. Commercial instruments are equipped with an auto sampler for automated changing of the inlet and outlet vials. Both, inlet and outlet can further be pressurized or vacuum can be applied respectively.

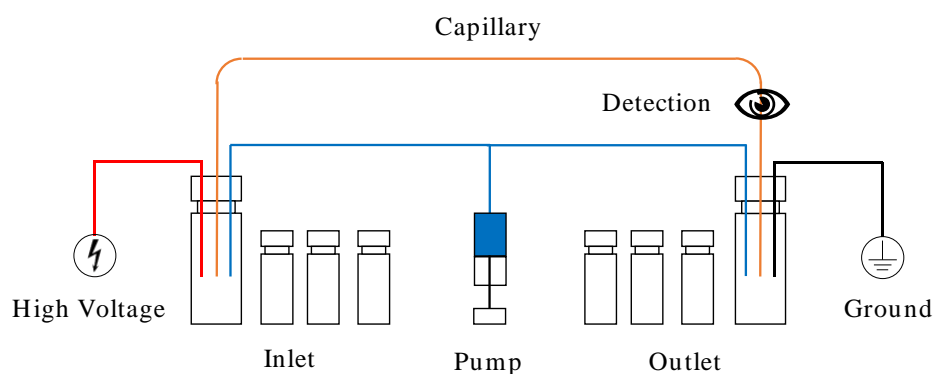


Figure 6: Schematic Setup of a CE Instrument.

Fused silica capillaries are used in most CE applications with a typical inner diameter (i.d.) of 10 to 250 μm and an outer diameter (o.d.) of 150 to 520 μm . The length of the capillary depends on the application and reaches from several centimeters to one meter and more. Fused silica capillaries are mostly coated outside by a plastic material to prevent fracturing, to get it flexible and robust.

Besides fused silica, for some special applications, also capillaries made from glass or polymer material, e.g. polyether ether ketone (PEEK) or polytetrafluoroethylene (PTFE), are used.

Inlet and outlet of the CE instrument are both equipped with an electrode, commonly produced from a platinum or platinum/iridium alloy which provides a high hydrogen over-potential. The separation HV source is connected to the inlet electrode and is typically working in a range of -30 to +30 kV. The outlet electrode is grounded in order to close the electric circuit.

Usually, the CE instrument operates with a defined separation HV. But, most instruments also provide the possibility to use a defined current for separation. This option can be useful if problems with joule heating are expected in defined current regions. While working with a fixed voltage, the behavior of the current is always a quality characteristic for the electrophoretic run. Current fluctuations or break-downs respectively indicate basic problems like e.g. gas-bubble formation inside the capillary or capillary fracture.

Sample injection in CE can be carried out by either hydrodynamic injection or electrokinetic injection. In hydrodynamic injection, pressure is applied to the sample vial at the capillary inlet or vacuum is applied to the outlet vial. Hence, the sample solution is pressed or sucked respectively into the capillary. The injected volume (V) depends on three factors: I) the pressure difference between the inlet and the outlet (Δp), II) the counter pressure provided by the BGE filled capillary, comprising the inner diameter of the capillary (d), the dynamic viscosity of the BGE (η), and the total capillary length (l_{tot}), and III) the injection time (t_{inj}). These factors are summarized by equation 5.

$$V = \frac{\Delta p \cdot d^4 \cdot \pi \cdot t_{inj}}{128 \cdot \eta \cdot l_{tot}} \quad (5)$$

Injection volumes in CE are typically in the range of several nanoliters which corresponds to some percent of the total capillary volume. Too high injection volumes lead to system overloading and peak broadening caused by high zone widths due to diffusion and field inhomogeneity in the sample zone. The limited injection volume is one of the main sensitivity limitations in CE, although, there are several pre-concentration strategies like e.g. stacking, transient isotachopheresis (tITP), and others [108].

In some cases it is not possible to conduct hydrodynamic injection. This may be due to e.g. a very high counter pressure of the capillary, caused by a very high viscosity of the sample solution or the BGE, or to avoid entrance of matrix into the capillary. In that case, electrokinetic injection can be used as an alternative.

Electrokinetic injection is carried out by the application of HV. Therefore, analytes migrate into the capillary and are additionally transported by the EOF. Different to hydrodynamic injection, not a volume but a quantity (Q) is injected.

This quantity depends on the electrophoretic mobility of the particular solute and the EOF velocity, on the field strength indicated by the applied HV and the total capillary length, on the capillary cross section, as well as on the solute concentration (c), and the injection time (t) (equation 6):

$$Q = (\mu_e + \mu_{EOF}) \cdot E \cdot \pi \cdot r^2 \cdot c \cdot t \quad (6)$$

Besides the transportation by the EOF, which is identical for all compounds of the sample solution, the injection quantity mainly depends on the electrophoretic mobility. Since the electrophoretic mobility differs between the different kinds of analytes, also the injected quantity differs.

Further on, variations in the sample composition (caused by e.g. matrix effects or depletion of the sample solution by multiple injections) can lead to differences in the electrical resistance of the sample solution and thus, differences in the injection quantity. Therefore, electrokinetic injection is less reproducibility in comparison to hydrodynamic injection.

3.4 Detection Options in Capillary Electrophoresis

Various detection techniques can be applied in CE. Besides mass spectrometry and C^4D , mostly optical detection techniques are used. Table 2 gives an overview of different detectors which are used in CE, including the limit of detection (LOD) as well as specific advantages and disadvantages.

Table 2: Detection Techniques in CE.

Technique	LOD (mol/L)	Advantages/ Disadvantages
UV-absorption	$10^{-5} - 10^{-7}$	+ Universal + Spectral information
Fluorescence	$10^{-7} - 10^{-9}$	+ Sensitive - Usually requires sample derivatization
Laser induced fluorescence	$10^{-9} - 10^{-12}$	+ Extremely sensitive - Usually requires sample derivatization - Expensive
Amperometry	$10^{-10} - 10^{-11}$	+ Sensitive +/- Selective but useful only for electroactive analytes - Comparatively low robustness
Conductivity	$10^{-6} - 10^{-7}$	+ Universal
Mass spectrometry	$10^{-8} - 10^{-9}$	+ Sensitive + Structural information - Complex interface

Detection by UV absorption is most common in CE as it is easy to use and universal. UV detection is generally non-destructive and not influencing the separation. Following the principles of UV spectroscopy, a monochromatic light beam is sent through the capillary.

The optical transmission of the solution inside the capillary is determined. Upcoming analytes attenuate the light intensity and the light transmission is lowered. From this change in transmission an electric signal is generated.

Besides UV detectors with a fixed or variable detection wavelength, diode array detectors (DAD) are used where an optical spectrum is registered simultaneously by an array of several single detectors (Figure 7).

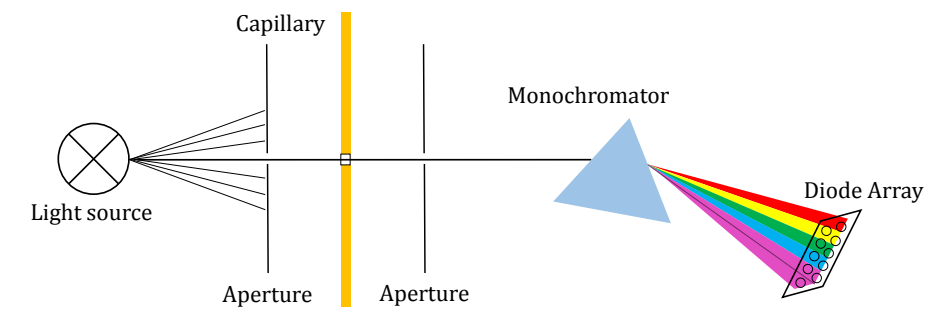


Figure 7: Typical Setup of a DAD.

A DAD enables the registration of a defined spectral range for every data point. Therefore, a further spectral detection dimension is introduced. This spectral data provides several additional application possibilities like e.g. the determination of the absorption maximum and the peak purity, analyte identification, and, however very limited, information about the chemical structure. Figure 8 A-B compare the two-dimensional data achieved by using a fixed wavelength (Figure 8 A) and the three-dimensional data of the identical electrophoretic run achieved by a DAD (Figure 8 B).

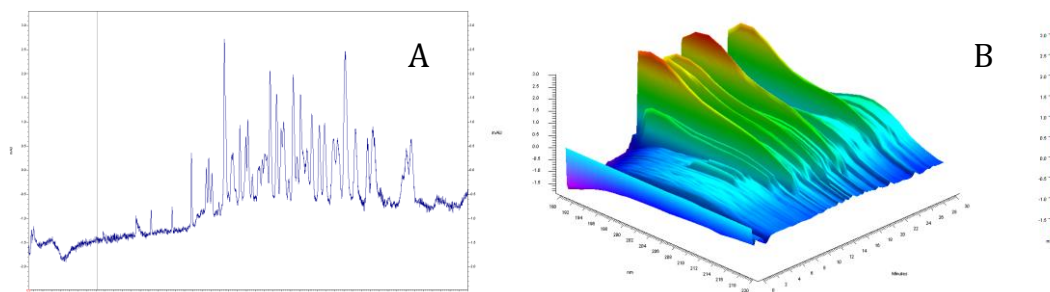


Figure 8 A-B: Comparison of Two-Dimensional Data achieved by an UV Detector with Variable Wavelength at 190 nm (A) and Three-Dimensional Spectral Data achieved by a DAD (B).

Besides UV detection, LIF is another optical detection technique which takes part in many CE approaches. Fluorescence is a spontaneous emission of light shortly after excitation by a light beam, whereby the emitted light is shifted to a higher wavelength.

In contrast to UV detection, where the excited molecules lose their energy by collision and, therefore, by emission of heat, in fluorescence detection, the excitation energy is partly emitted as light.

Unfortunately, natural fluorescence is a quite rare phenomenon and, therefore, LIF detection is by nature limited to just a few compounds. However, due to this, LIF shows a very high selectivity and sensitivity. Furthermore, compounds showing no natural fluorescence can be derivatized with a fluorogenic label, enabling the usage of the highly selective LIF detection.

Conductivity detection or C^4D respectively is another option for non-destructive, on-capillary detection in CE. The C^4D consists of two tube electrodes around the capillary, actuator and pick-up electrode, with a defined distance in-between (Figure 9). An oscillating frequency is applied to the actuator electrode causing a capacitive transition between the actuator electrode and the solution inside the capillary.

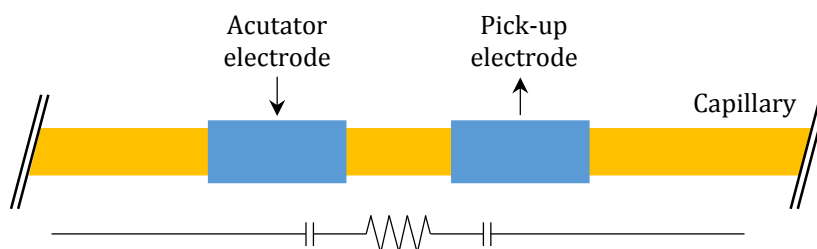


Figure 9: Schematic Setup of a C^4D .

This transition also takes part between the second, pick-up electrode and the solution after the solutes passed the distance between the two electrodes. The gap in between the electrodes acts as an electrical resistor. Therefore, the electrical resistance or the conductivity respectively changes while solutes pass the gap. This conductivity variation between the electrodes is then effectively detected [109, 110].

Conductivity detection is a very universal on-capillary detection possibility and well suited for many compounds which are difficult or impossible to detect by optical detection such as several inorganic ions or organic solvents. Also, photo sensitive compounds can be detected without photo-degradation.

A transparent capillary material is not necessary which enables detection using capillaries made from non-transparent plastic material or packed capillaries. Further on, removal of the outside capillary coating in order to create an optical window is needless when using fused silica capillaries.

Sensitivity in C^4D depends on the differences in the conductivity of the BGE and the solutes. This is a main disadvantage since high BGE conductivity leads to a high noise level and, therefore, increases detection limits. Variations in the BGE composition or the temperature during the analysis lead to further noise. Nevertheless, detection limits in the ppm and ppb region can be reached. Further, C^4D is ideal for the detection of organic solvents like e.g. methanol (MeOH) which usually lowers the conductivity and generates very high conductivity variations in comparison to the BGE.

4 Capillary Electrophoresis - Mass Spectrometry

Besides optical detection, MS detection is increasingly applied in CE and emerged to the most important technique especially in the characterization of bio-molecules [111, 112]. The main reasons are the option for very sensitive and selective detection as well as the possibility to acquire information on the elemental composition of the analytes by high-resolution MS and the structure of the analytes by MS/MS fragmentation experiments. However, MS detection requires a comparable complex interface which is a further source of error. Since MS detection is located at the end of the separation capillary and not, as e.g. optical detection, in front of the end of the capillary, selection of possibly applicable methods is limited with regard to e.g. EOF velocity and direction. In addition, MS interfacing itself influences the separation in CE e.g. by suction effects.

4.1 Electrospray Ionization

In order to enable mass spectrometric detection, the analytes must be available as ions in the gas phase. To hyphenate separation techniques which work in the liquid phase (e.g. CE, LC) to mass spectrometry, the analytes need to be ionized and transferred to the gas phase. Besides other techniques like e.g. atmospheric pressure chemical and photo ionization, electrospray ionization (ESI) is the most common technique used.

In many capillary electrophoretic separation techniques like CZE and related techniques, analytes need to be already charged to even enable separation in the electric field.

Hence, ESI appears to be an ideal coupling technique since analytes only need to be transferred from the liquid phase to the gas phase.

In ESI, upcoming effluent is fed through a conductive spray capillary. With the help of a nebulizer gas, the liquid is sprayed as fine droplets into a strong electric field between the conductive capillary and the MS inlet. The potential of typically some kV is applied either at the spray capillary or the MS inlet.

By the balance between the force of the electric field and the surface tension of the solution the TAYLOR cone is formed at the spray capillary tip. Additionally, charge separation occurs. Therefore, the generated liquid droplets have a charge excess and are attracted to the MS inlet.

Due to solvent evaporation, the initially formed droplets with a radius of about 1-3 μm shrink until the repelling force between the even charged molecules reaches the surface tension of the droplet. This is described by the REYLIGH limit. If the REYLIGH limit is exceeded, the droplets burst into several smaller droplets by a COULOMB explosion. This process is repeated until micro droplets are formed.

Solvent evaporation is thereby supported by a heated dry gas flow coming from the MS inlet which furthermore prevents ambient air and neutral molecules from entering the MS instrument. Figure 10 illustrates the ESI process.

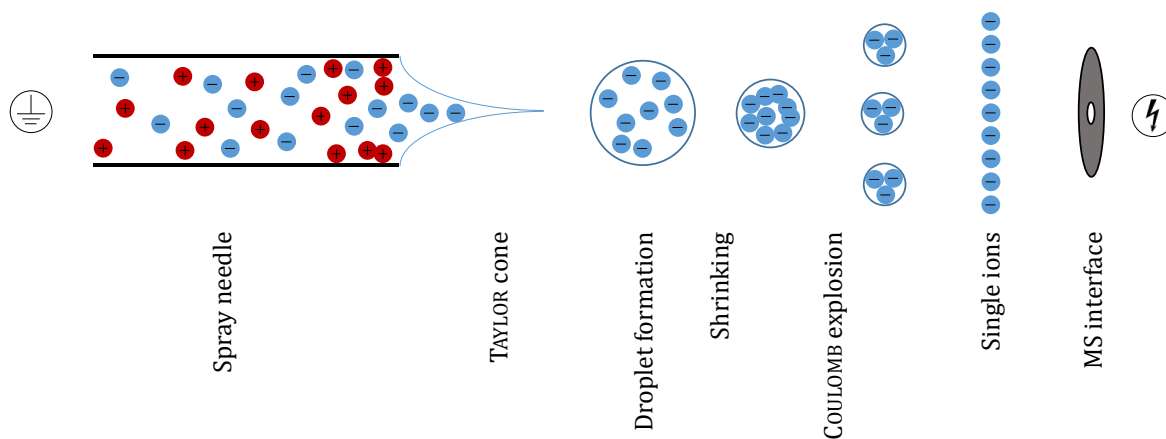


Figure 10: Schematic Illustration of the ESI Process.

For the generation of single ions from the micro droplets two theories exist. The ion evaporation model assumes that the droplets shrink by evaporation until the field strength at their surface is sufficiently large that solvated ions can be expelled from the droplet [113, 114]. The charge residue model assumes that the process of shrinking and exploding keeps going on until droplets are left containing only a single ion. The ion is set free by evaporation of the remaining solvent [113]. These two theories are contrary since the charge density would be lowered by expelling single ions and, therefore, inhibits or slows down the process leading to further COULOMB explosions.

ESI is a comparable soft ionization technique which hardly leads to any fragmentations inside the source. Therefore, ESI is very well suited for the analysis of large intact bio-molecules [115].

4.2 Coupling Techniques

In contrast to LC, in most CE techniques there is no or just a very low real bulk flow generated only by the EOF and the suction effect of the electro-spray and the nebulizer gas. The solvent amount is often too low to form a stable spray and varies strongly. In addition to the absence of a bulk flow, another challenge is the closure of the electric circuit of the CE at the capillary outlet tip without a grounded vial. Hence, special coupling techniques, different to those used for LC-MS coupling, need to be applied.

Besides nano and sheath less ESI techniques [116, 117] sheath liquid (SL) spray systems are mostly applied [118-120]. In those approaches, a supporting liquid flow surrounds the CE separation capillary tip. This additional flow enables a stable spray and establishes electrical contact between the separation capillary tip and the spray needle. A standard system is the coaxial triple tube design which also enables the use of a nebulizer gas (Figure 11).

The triple tube sprayer consists of an inner and an outer steel tube. The separation capillary is inserted into the inner steel tube protruding the tube tip some μm .

The inner tube has an i.d. of 400 μm which is well suited for the use of standard separation capillaries with an o.d. of 375 μm . The gap between separation capillary and inner tube is used for sheath liquid delivery. The two inner tubes (steel tube and separation capillary) are surrounded by the outer steel tube. The gap between inner and outer steel tube is used to deliver the nebulizer gas.

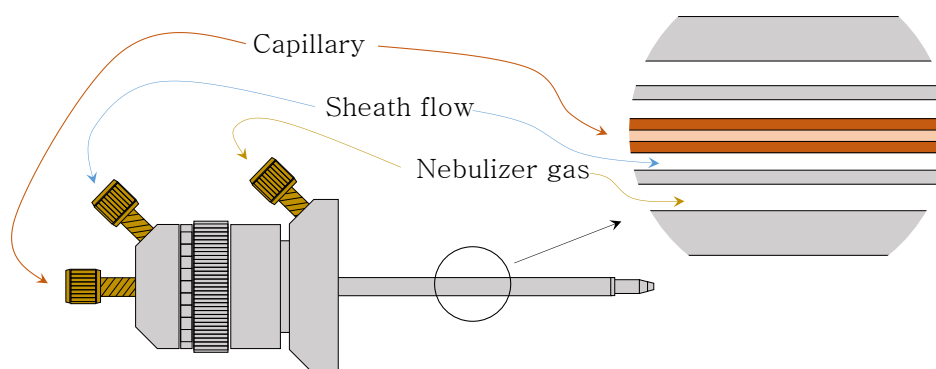


Figure 11: Illustration of the Agilent Coaxial Triple Tube CE-MS Sheath Liquid Sprayer.

The sheath liquid, which is delivered by a syringe or LC pump, is mostly ultrapure water with a volatile acid or base, e.g. formic acid (FAc), acetic acid (HAc), or ammonia, to support the ionization process and an organic solvent content of 50-100 % for improved vaporization during the ESI process. Flow rates are typically in the range of 1-10 $\mu\text{L}/\text{min}$. Thereby, the flow rate should be as low as possible to minimize sample dilution, but high enough to create a stable spray.

4.3 Mass Spectrometry

The terms mass spectrometer or mass selective detector (MSD) comprise the techniques where ions are separated after differences in their mass to charge ratio (m/z). The terms cover different techniques and instruments like e.g. quadrupole and triple quadrupole MS (Q, QqQ), linear and three-dimensional ion-traps (LIT, 3D-IT), time of flight MS (TOF), fourier transform ion cyclotron resonance MS, and others.

Mass spectrometry is widely used in industry and research since it provides high selectivity, sensitivity with LODs down to the ppt range, and the possibility to determine informations on the elemental composition as well as on the structure of the analytes [121, 122]. In routine analysis, predominantly QqQ, 3D-IT, and Q-TOF instruments are applied [123].

All of these different techniques show specific advantages and disadvantages as differences in selectivity, sensitivity, sampling speed, and mass resolution. In this work, Q-TOF and 3D-IT mass spectrometers were used. Hence, these two techniques are described in more detail in the following.

Ion-Trap Mass Spectrometer

The 3D-IT mass spectrometer uses a quadrupolar electric field for the storage of ions. A typical 3D-IT is constructed of a ring electrode and two end caps (Figure 12 A).

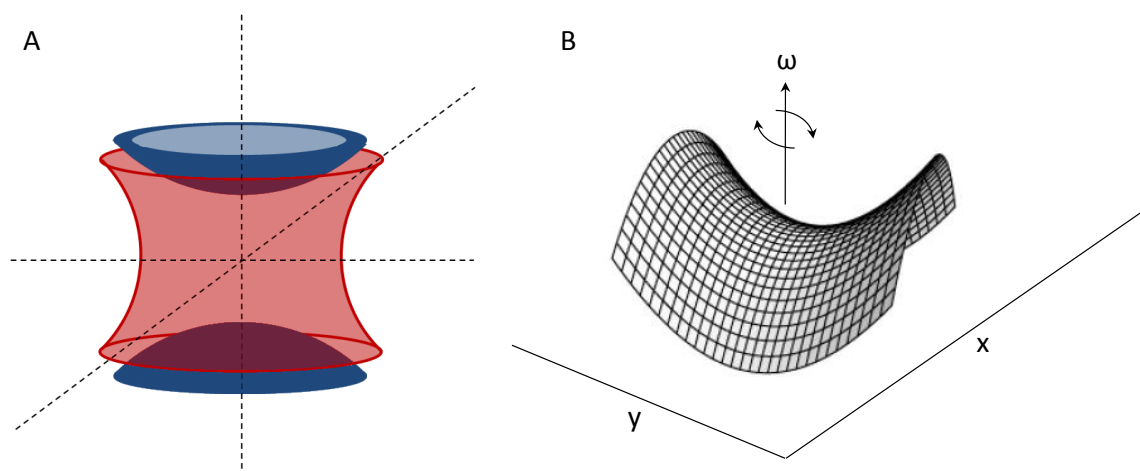


Figure 12 A-B: A: Schematic Setup of a 3D-IT consisting of Two Endcaps (blue) and the Ring Electrode (red); B: Saddle Field of a PAUL Trap.

Applying a constant radio frequency (RF) of 781 kHz to the ring electrode enables the trapping of different ions within a relative wide m/z range. The generated electric field has the shape of a saddle (Figure 12 B) and rotates around the ω -axis.

Due to the rotation, the ions which are located in the middle of the field will not fall down the shoulders. Trapped ions perform oscillating trajectories inside the trap with specific frequencies which, at fixed field parameters, are determined by the m/z ratio of the ion. This enables a mass selective detection of the stored ions [124].

In contrast to quadrupole MS which use MS in space, an IT uses MS in time [125]. The filling of the trap is controlled by an electrostatic lens. After filling of the trap, the incoming ion beam is blocked by this lens.

For m/z determination, the ions are successively ejected by raising the ring electrode RF amplitude continuously which destabilizes the trajectories of the ions in order of their m/z ratio. Subsequently, ions leaving the trap are detected by a secondary electron multiplier.

Besides m/z ratio scanning, a 3D-IT offers the option to perform MS^n experiments. Due to the MS in time technique, multiple fragmentation steps are possible. To conduct MS/MS experiments, a single sort of ion is isolated inside the IT.

Subsequently, the isolated ions are accelerated by a RF near their natural resonance frequency without destabilizing the trajectories. Due to collisions of the excited ions with helium atoms, fragmentation of the ions is generated and fragments are accumulated in the saddle field. Because the natural resonance of the fragments is different to the natural resonance of the initial ions, the fragments do not get excited. Therefore, in contrast to MS/MS in space, there are almost no multiple fragmentations. The isolation and fragmentation cycle can be repeated with one of the fragments leading to multiple MS/MS experiments. In contrast to e.g. QqQ of Q-TOF instruments, where only one MS/MS experiment is possible, this is a main advantage of 3D-IT instruments.

Time of Flight Mass Spectrometer

In TOF instruments the ions are separated according to their velocities after their initial acceleration by an electric pulse, when they drift in a low pressure flight tube [125, 126].

Upcoming ions, which are generated by the ion source (e.g. ESI), are focused by an ion optic and transferred to the pulser. Here, the ions are accelerated by a potential into the flight tube. Since all ions are accelerated by the same kinetic energy they pass the flight tube with different velocities according to their m/z ratios, and strike the detector after different flight times. Measuring these times enables m/z determination.

The velocity v of the ions depends on the total charge $q = z \cdot e$, the mass of the ion, and the acceleration potential V_s and can be expressed by equation 7:

$$v = \left(\frac{2ezV_s}{m} \right)^{1/2} \quad (7)$$

After the initial acceleration, the ions pass the flight tube with a constant velocity. The time the ions need to reach the detector (t) is depending on the flight path length L and the ion velocity.

$$t = \frac{L}{v} \quad (8)$$

When the term for v from equation 7 is inserted into equation 8 it shows, that m/z is indirect proportional to the square root of t (equation 9):

$$\frac{m}{z} = \left(\frac{2eV_s}{L^2} \right) t^2 \quad (9)$$

Besides linear TOF systems, actual instruments are usually constructed as reflectron TOF mass spectrometers. The reflectron is installed at the end of the free flight path, usually at the end of the flight tube. It consists of electrostatic lenses which are creating a retarded field and act as an ion mirror. Incoming ions enter the field and are accelerated in the opposite direction towards the detector. Thereby, ions with a higher kinetic energy penetrate the reflectron more deeply than ions with a lower kinetic energy. Consequently, the faster ions will spend more time in the reflectron and will reach the detector at the same time as slower ions with the same m/z ratio [125]. Here, the reflectron compensates small differences in the kinetic energy and, therefore, increases the mass accuracy and also the mass resolution due to the doubled flow path length.

Modern TOF instruments provide a mass accuracy of a few ppm with a mass resolution of about 10.000 – 20.000 [127]. Hence, TOF instruments can be categorized as medium resolution systems in contrast to the 3D-IT which delivers only low mass resolution.

Besides single TOF instruments hybrid instruments are used containing an additional analytical quadrupole and a second quadrupole acting as a collision cell to enable MS/MS fragmentation experiments.

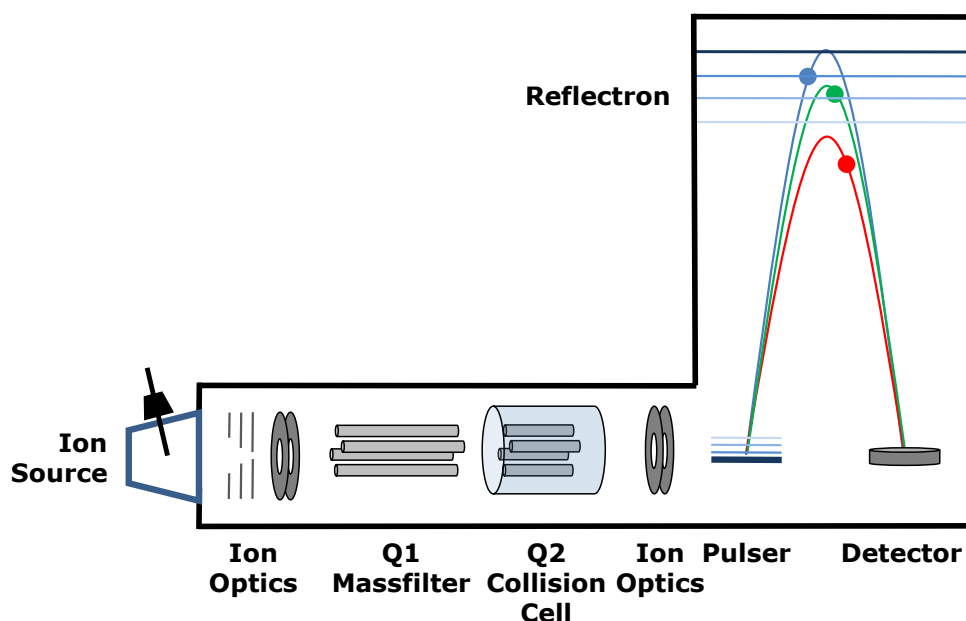


Figure 13: Typical Setup of a Reflectron Q-TOF Instrument.

Figure 13 shows the setup of such a Q-TOF instrument. Ions in the gas phase are generated by the ion source. Subsequently, they enter the MS instrument and are focused by ion optics towards the analytical quadrupole (Q1). With the help of Q1, the ions can be filtered by their m/z ratio. The second quadrupole (collision cell, Q2) is filled with gas, typically nitrogen or helium. Due to acceleration in the Q2, the ions collide with the gas atoms and are fragmented. The fragments are again focused by ion optics and guided to the pulser. Here, the ions are accelerated into the flight tube. The ions describe a parabolic flight path and, after passing the reflectron, reach the detector where t , and, therefore, m/z , is determined.

4.4 Specific Characteristics and Limitations in CE-MS

4.4.1 Limitations in CE-MS

In CE-MS coupling via a sheath liquid ESI interface, there are some pitfalls and limitations. First of all, in contrast to LC coupling, there are two electric circuits, one for CE separation and another for ESI. The easiest way to separate the two electric circuits is the use of MS instruments where the ESI high voltage is applied to the MS interface.

In this setup, the ESI needle is grounded and separates the two electric circuits. This setup is used in e.g. instruments from Agilent Technologies and Bruker Daltonik. In most other MS instruments the ESI high voltage is applied to the spray needle. In this case, coupling is also possible but more challenging since resistors are required to limit the currents [128].

Only CE techniques and methods with an EOF in MS direction or a suppressed EOF can be hyphenated to MS detection. Otherwise, if the EOF is in inlet direction, sheath liquid would be sucked into the separation capillary which leads to current variations or breakdowns in CE separation. Therefore, also the application of special CE capillary treatments, like e.g. coatings, is limited to those who do not cause an EOF in inlet direction.

Furthermore, though the application of a supporting SL flow increases the robustness of the CE-MS system, the additional liquid lowers the analyte concentration at the CE capillary tip. Due to this, the detection sensitivity, which in ESI-MS is predominantly concentration sensitive, is reduced [129]. Therefore, the SL flow rate should be as low as possible. This issue can be overcome by the use of a miniaturized sheathless nano spray. However, these nano spray systems show other difficulties and limitations as well as a lower robustness.

4.4.2 The Role of the BGE in CE and CE-MS

Many established CZE applications use BGEs which are containing non-volatile compounds and are, therefore, not compatible to direct ESI-MS detection. Different to HPLC, where selectivity mainly depends on the stationary phase, selectivity in CZE depends on the BGE composition.

In CZE mostly inorganic acids, bases, and salts like e.g. phosphate or borate are used. Different selectivity can be obtained by changing ionic strength and pH of the BGE by varying concentration and composition of the used salts. Further, also the type of anion and cation of the BGE compounds influences the selectivity. Unfortunately, BGEs which contain non-volatile inorganic salts are incompatible with MS detection since these compounds are ionized during the ESI process and, therefore, soil the MS interface and lead to massive signal quenching [130, 131].

In principle, non-volatile BGE compounds can be replaced by volatile compounds in CZE like e.g. HAc, FAc, and NH₃. Anyhow, slight changes in selectivity are likely to be accepted. Further, in industry and research many methods are established and validated for CE with UV or different optical detection. It would be desirable to enable direct hyphenation of these methods to MS detection without the need of repeating the validation process for the changed BGE composition.

In contrast to CZE, in many other techniques and modes individual selectivity is reached by special BGE additives. Such additives could be e.g. micelle forming agents in MEKC, crown ethers or CDs for chiral separation in CZE, sieving matrix in CSE, or ampholytes in CIEF. These methods and techniques are not compatible to MS detection using standard direct ESI coupling. Further, the BGE additives are indispensable to achieve the required selectivity and it is impossible to replace them by a volatile alternative. In order to apply MS detection to those methods and techniques a special strategy is needed to prevent the interfering compounds from reaching the detector.

4.4.3 Strategies for CE-MS Coupling of non-ESI Compatible CE Techniques and Modes

Since one of the future areas of application of the 2D system should be the coupling of CGE and CSE with MS detection, the influence on MS detection and possible separation of gel matrix compounds in a standard 1D system was evaluated, as an example, in the beginning of the experimental work.

The influence on mass spectrometric detection of the four different gel matrix compounds dextran MW 100 000, hydroxypropyl cellulose MW 100 000 (HPC), hydroxypropyl methyl cellulose (HPMC), and polyethylene glycol MW 35 000 (PEG) was tested.

The effect of using a capillary filled with CSE buffer in a CE-MS system should be simulated. Therefore, the capillary of a standard CE-MS system was flushed with the particular CSE buffer solution at 5 bar. Subsequently, separation HV was applied to the CE inlet and MS data was recorded for about 1 min.

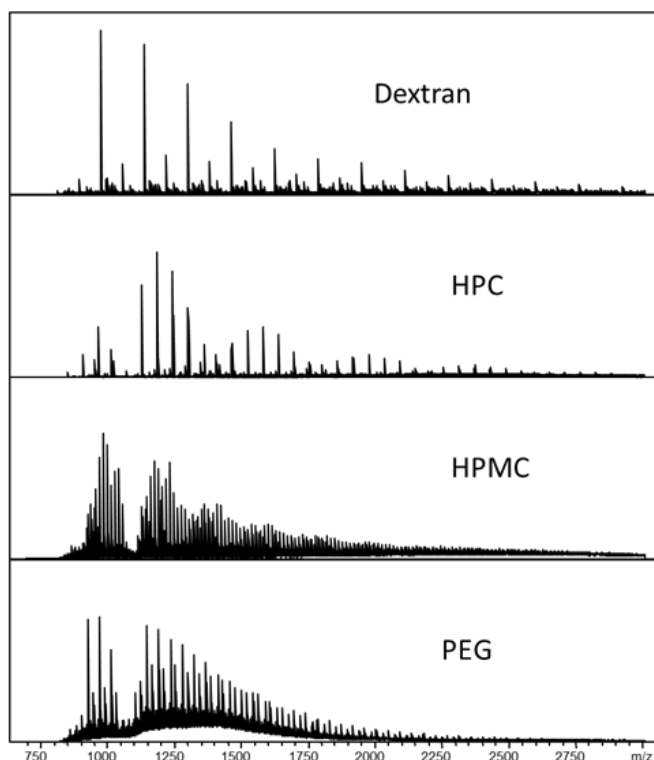


Figure 14: Mass Spectra Obtained by the Usage of Capillaries Filled with four Different CSE Matrix Compounds Dextran, HPC, HPMC, and PEG, each 1 wt % dissolved in 1.5 M FAc. Capillary length: 60 cm; Separation HV: +20 kV; CE Instrument: Agilent 7100; MS Instrument: Bruker micro TOF-Q; Mass Spectra averaged over 1 min.

Figure 14 shows the obtained mass spectra for all four compounds. It is obvious, that all compounds are ionized during the ESI process and are, therefore, accessible for MS detection. Hence, direct hyphenation of CSE to ESI-MS using one of these additives leads to massive entry of CSE matrix compounds to the MS and causes severe contamination of the MS instrument and quenching of the analyte signal.

Partial Filling Technology

As an alternative, to avoid the entry of influencing matrix compounds to the MS instrument, the partial filling technology can be applied [132-134]. In these approaches, the capillary is first filled with a volatile, MS compatible BGE. Subsequently, the capillary is filled partly with the BGE containing the non-MS compatible compounds. Thus, the outlet of the capillary, which is installed in the MS interface, is not containing disturbing substances. Experiments to evaluate the feasibility of the partial filling technology were performed.

For evaluation of the filling time for partial filling, the capillary was first flushed with a solution of 1 mg/mL caffeine in MeOH which could be detected by the used UV detector. Afterwards, the capillary was filled with CSE buffer solution using a pressure of 2 bar. Break down of the signal in the UV detection, conducted by the caffeine, indicated complete filling of the capillary with CSE buffer.

Effective length filling was measured at 50 s leading to a filling time of the capillary total length of 59 s. To carry out partial filling experiments, the capillary was first flushed with a volatile buffer followed by flushing with CSE buffer half of the time to achieve filling of about 50 % (29 s at 2 bar).

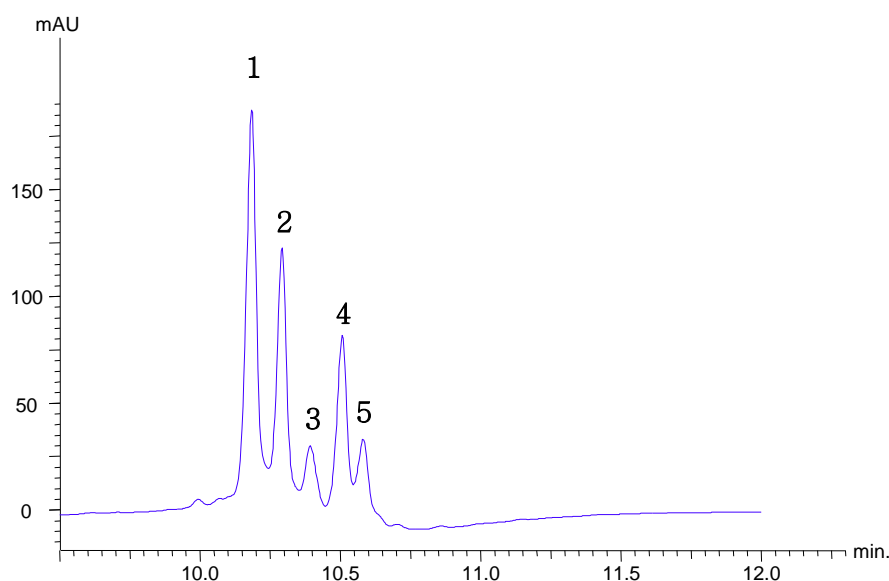


Figure 15: Separation of a RNase B Sample using a 50 % CSE BGE Filled Capillary, UV Detection at 200 nm, CSE BGE: 1.5 % w/w HPC MW 100,000 in 1.5 M FAc, Volatile BGE: 1.5 M FAc; Sample: 1 µg/L RNase B; CE Instrument: Agilent G7100A; Capillary Length: 60 cm Total Length, 52 cm Effective Length.

Figure 15 shows the electropherogram achieved by the separation of a RNase B sample using the 50 % CSE BGE filled capillary in a CE system with UV detection. For comparison of the resolution achieved by the use of the partially filled capillary and the resolution achieved by the use of a capillary completely filled with CSE BGE, the sample was further separated by the same system but with a capillary completely filled with HPC matrix solution.

The resolution was determined between the adjacent peaks marked in Figure 15. Table 3 shows the comparison of the achieved resolutions with completely and partially filled capillaries.

Table 3: Comparison of the Electrophoretic Resolution Achieved by the Separation of a RNase B Sample with a System using a Completely and a Partially Filled Capillary. BGE: 1.5% w/w HPC MW 100.000 in 1.5 M FAc, Sample: 1 µg/µL RNase B; CE Instrument: Agilent 7100; Capillary Length: 60 cm Total Length, 52 cm Effective Length.

Peak number	1/2	2/3	3/4	4/5
Complete filling	2,48	2,54	2,80	2,08
Partial filling	1,69	1,25	1,43	0,97

As expected, the use of a partially filled capillary leads to a loss of electrophoretic resolution by a factor of 0.8-0.5 in comparison to the use of the completely filled capillary. Nevertheless, nearly baseline separation is still achieved with a 50 % filled capillary.

In contrast to the experiment with the completely filled capillary, the entry of matrix compounds in the MS is negligible when the 50 % CSE BGE filled capillary is applied. Therefore, partial filled capillaries possibly can be used for direct hyphenation of CE techniques with MS influencing compounds and MS detection like shown in [135] and [136].

Nevertheless, besides the loss in electrophoretic resolution, application of the partial filling technology is restricted to techniques and methods where the matrix compounds do not or only very slightly migrate by electrophoresis or are transported by the EOF in MS direction. Further on, before flushing, the capillary should be disconnected from the ESI spray needle to not contaminate the interface.

Heart-Cut 2D Capillary Electrophoresis

Also during the cutting and reintroduction process in a 2D system using a mechanical valve with a sample loop a small portion of the first dimension CSE buffer is entering the second separation dimension. In order to finally apply the 2D system for the hyphenation of non-MS compatible CE modes, like e.g. CSE, to MS detection it needed to be ensured that the second dimension is in general capable to separate the influencing compounds from the analyte molecules to prevent them from reaching the detector.

In order to simulate this transfer process of a sample in gel matrix from a first CSE separation dimension to a second non-gel dimension a RNase B sample was dissolved in the commercially available Beckman Proteom Lab™ SDS-MW buffer to a concentration of 1 µg/µL and injected to a one-dimensional CE-MS system with a volatile BGE (hydrodynamic injection, 30 s at 50 mbar).

In this case, the one-dimensional system simulated the second dimension of a 2D system. The second dimension should prevent the matrix compounds from reaching the detector. Furthermore, it could be tested if it is possible to separate the complexing SDS from the peptides.

As expected, the SDS could not be detected by the MS. Due to the negative charge, the SDS molecules migrate in outlet direction in the used system with cathodic detection. Also, further components of the buffer could not be observed in the MS. Therefore, an influence on MS detection is not probable and a two-dimensional approach should be able to effectively separate the MS influencing SDS from the analyte molecules.

Part II

Methods

5 Instrumentation, Materials, and Methods

This chapter covers a description of all instruments, materials, and chemicals used during the project work. Detailed method data is not described in this chapter and is given in the particular sections.

5.1 Instrumentation

5.1.1 Capillary Electrophoresis Instrumentation

One-dimensional experiments were carried out using an Agilent 7100 CE instrument (Agilent Technologies, Waldbronn, GER) with an internal DAD. For two-dimensional experiments, a combination of a Beckman PA 800 *plus* (Beckman Coulter, Brea, CA, USA) and an Agilent G1600AX 3D CE instrument (Agilent Technologies, Waldbronn, GER) was used. Further on, in some experiments a special external HV source and an external grounding vial was used for second dimension HV delivery instead of the Agilent G1600AX 3D. The external HV source was constructed by CalvaSens GmbH (Aalen, GER) and was used in combination with the PA 800 *plus* CE instrument. The HV source was able to deliver a predefined potential of 0 to +30 kV with a predefined ramping time. Switching of the HV source could be carried out either manually or by one of the relays of the PA 800 *plus* CE instrument. Therefore, external HV could be controlled by the Beckman CE control software. The external HV source could only deliver a positive potential. In experiments were in both dimensions a negative potential was needed, the HV source of a P/ACE MDQ CE instrument was used (Beckman Coulter, Brea, CA, USA).

Three different versions of the C4N-4354-.02D 4-port-valve were purchased from VICI AG International (Schenkon, CH). The valves are discussed in detail in chapter 6.

5.1.2 Mass Spectrometry Instrumentation

In MS experiments, three different mass spectrometers were used, an Esquire 6000 3D ion trap and two Q-TOF instruments, micro TOF-Q and Compact. All MS instruments were from Bruker (Bruker Daltonics, Bremen, GER).

Only scan mode was used in the experiments. CE-MS coupling was carried out by a triple tube sheath liquid ESI interface (Agilent Technologies, Waldbronn, GER).

Sheath liquid was delivered by a KD 78-9100K syringe pump (KD Scientific, Holliston, MA, USA) equipped with a 5 mL SGE 5MDR-GT gastight syringe (SGE analytical science, Melbourne, AUS).

5.1.3 Additional Detection Options

In 1D experiments, the internal DAD of the Agilent 7100 CE instrument was used (Agilent Technologies, Waldbronn, D). Additional UV detection in the first dimension for 2D experiments was carried out by a TIDAS calcite compensation depth (CCD) UV/near infrared (NIR) detector and an appropriate detection cell (J&M Analytik AG, Essingen, GER). For LIF detection two lasers were available. A FQSS266-Q2 laser with an excitation wavelength of 266 nm (CryLaS GmbH, Berlin, GER) and a P/ACE laser module with an excitation wavelength of 488 nm (Beckman Coulter, Brea, USA).

Both, the detection cell for LIF and the detection cell for UV detection were constructed by J&M Analytik AG (Essingen, GER). Both cells were equipped with in-house constructed detection cell housings. With these housings, the detection cells could be installed at the valve by an in-house constructed detection cell mount (Figure 16). The cell housing was attached to two guiding rods and could be moved up and down and further fixed to reach an ideal alignment of detection cell and optical window of the capillary. The detection cell was positioned in the first capillary of the first separation dimension about 4 cm in front of the valve and was connected to the light source and the detector by two fiber optics.

Conductivity detection was carried out by a TraceDec C4D (Innovative Sensor Technologies GmbH, Strasshof, A).



Figure 16: Valve, Equipped with Detection Cell, Cell Housing, and Cell Mount.

5.2 Materials and Chemicals

5.2.1 Materials

In all experiments fused silica capillaries were used with an o.d. of 375 μm and an i.d. of 50 μm purchased from Polymicro (Polymicro Technologies, Phoenix, AZ, USA). Before use, capillaries were conditioned.

Further on, coated capillaries were used. Permanent polyvinyl alcohol (PVA) and low normal (LN) coating was applied to the capillaries previous to connecting them to the valve. Divergent capillary treatments as well as detailed coating procedures are given in the specific sections.

5.2.2 Chemicals

Ultrapure water (18 $\text{M}\Omega/\text{cm}$ at 25 $^{\circ}\text{C}$) was produced by a SG Ultra Clear UV ultra pure water system (SG Wasseraufbereitung und Regenerierstation GmbH, Hamburg, GER). Isopropyl alcohol (IPA) and methanol (Rotisolv, LC-MS), and acetic acid and formic acid (Rotipuran) were purchased by Roth (Carl Roth GmbH & Co. KG, Karlsruhe, GER). Sodium hydroxide, phosphoric acid, and hydrochloric acid (HCl) (p.a.) were purchased by Merck KGaA (Darmstadt, GER). ES Tuning mix solution was obtained from Agilent (Agilent Technologies, Waldbronn, GER). Proteom LabTM SDS gel buffer was obtained from Beckman (Beckman Coulter, Brea, CA, USA).

SDS (10 % in water), Lysozyme (from chicken egg white, purity not specified), β -lactoglobulin (from bovine milk, $\geq 90\%$), myoglobin (from horse skeletal muscle, 95 – 100%), RNase A and B (from bovine pancreas, $\geq 80\%$), Dextran (MW 100.000), hydroxypropyl cellulose (HPC, MW 100.000), hydroxylpropyl methyl cellulose (HPMC), polyethylene glycol (PEG, MW 35.000), glutaraldehyde (50 % in water), and polyvinyl alcohol (MW 89,000 – 98,000) were purchased from Sigma-Aldrich (St. Louis, MO, USA). UltraTrol™ low normal coating solution was purchased from Target Discovery (Palo Alto, CA, USA). [Glu1]-fibrinopeptide B (Glu-Fib), leucine-enkephalin (Leu-Enk), and bovine serum albumin (BSA) tryptic digest samples were supplied by Bruker (Bruker Daltonics, Bremen, GER).

5.3 Methods

In the following, the methods and instrumental parameters, which were used in the experiments, are given. Detailed and respective method data can be found in the specific sections.

5.3.1 Capillary Electrophoresis

Three capillary electrophoresis instruments were used, the Beckman PA 800 *plus* and the Agilent 7100 and G1600AX 3D.

In addition to the CE instruments, the external power supply was used in the 2D experiments for the delivery of separation HV in the second dimension, mostly in combination with an external grounding vial.

Injection was carried out either by hydrodynamic or electrokinetic injection. Electrokinetic injection was performed at 7 kV for 10 s. Hydrodynamic injection was typically 10 s at 100 mbar but varied from 6-10 s at 100-200 mbar.

Capillaries were always conditioned before experiments and, in case of experiments applying the valve, before connecting to the valve. Conditioning was performed by flushing 10 min at 1000 mbar MeOH, 5 min at 1000 mbar H₂O, 15 min 1000 mbar 1M NaOH, and 5 min 1000 mbar H₂O. Subsequently, the capillaries were filled with BGE.

Coated capillaries were applied in some experiments. Here, LN as well as PVA coating was used. The coating procedures, given in the following, took place after conditioning:

LN coating: The coating procedure was performed by flushing the capillary 5 min with ultrapure water, 15 min with the LN coating solution, another 5 min with water, and 10 min with BGE always at a pressure of 1 bar.

Since LN is a semi permanent coating, the coating needed to be refreshed every five to ten runs. This was carried out by flushing the capillary 15 min with 3 M HCl followed by the above mentioned procedure.

PVA Coating: Coating procedure was carried out according to [137]: The coating was based on treating the capillary surface with a solution of glutaraldehyde as cross-linking agent (3.25 µg/mL in 1.21 M HCl) followed by a solution of PVA (45 mg/mL in 0.6 M HCl), which resulted in an immobilization of the polymer on the capillary surface.

The procedure was organized as follows: (I) the capillary was dried with air during 15 min at 5 bar after the first conditioning, (II) the capillary was 35 % filled with the glutaraldehyde solution at 5 bar, (III) immediately afterwards an acidified PVA solution was pressed at 5 bar into the column (70% of the capillary), (IV) the capillary was then emptied and pre-dried under a nitrogen flow for 15 min, (V) thereafter, the capillary was incorporated in a gas chromatography oven and while the capillary was flushed in a nitrogen flow, the oven was heated from 40 to 160 °C with 6 °C/min. After cooling down the capillary to room temperature, 5 cm of both ends were cut.

Separation was carried out at a separation HV of 20-30 kV in both dimensions. In most experiments, the separation current was limited to 7 µA to prevent damage of the valve material. This was achieved by either using a preset separation current instead of a separation HV by the CE instrument or software respectively or by adjusting the separation HV to a corresponding current of 7 µA previous to the experiments.

Using the external HV source, the current always needed to be adjusted by varying the separation HV since it was not possible to preset a separation current.

The CE instrument could be used with a preset current. However, it turned out that the instrument was not able to deliver a preset current as constant as a voltage. Therefore, in most cases the current was also adjusted by the suitable separation HV, conducting the experiments with a preset HV.

The BGEs used during the experiments are listed in Table 4.

Table 4: Different BGEs which were used During the Experiments.

BGE No.	BGE composition
1	1 M HAc with 2 % HPC
2	0.5 M HAc
3	0.2 M FAc
4	10 % v/v aqueous HAc
5	10 mM phosphoric acid at pH 2.5

5.3.2 Detection

Three different UV detectors were used during the experiments, the internal detectors of the Agilent G1600AX 3D and 7100 CE instruments and the external J&M CCD detector, all three at a detection wavelength of 190, 200, and 210 nm. The external CCD detector was operating at an integration time of 80-100 ms at a frequency of 1 Hz.

In the LIF experiments detection was carried out by the FQSS266-Q2 laser with an excitation wavelength of 266 nm in combination with the appropriate detection cell.

The detection cells of the additional UV and LIF detector and the sensor of the C⁴D were positioned 2.6-4.0 cm in front of the valve.

Three MS instruments were used, the Bruker micro TOF-Q, the Compact Q-TOF, and the Esquire 6000 3D-IT. All three were hyphenated to the CE instrument via the Agilent triple tube SL interface.

The Q-TOF instruments were used in positive ionization mode at an ionization HV of - 4500 V and with a mass range of 50-1500 m/z for peptide and 700-3000 m/z for protein analysis.

Dry gas was set to 4.0 L/min with a temperature of 170 °C. Nebulizer gas operated at a pressure of 0.2 bar. SL was 1:1 ultrapure water : IPA with 0.2 % v/v FAc and was delivered by the syringe pump at a flow rate of 4 µL/min. Before conducting the experiments, the Q-TOF instruments were daily tuned using the Agilent tune mix.

The Esquire 600 3D-IT was as well used in positive ionization mode at a HV of -4000 V and a mass range of 100-2500 m/z. The IT was tuned to a target m/z of 2000. Filling of the trap was controlled by the ion charge control (ICC) with an ICC target of 20000. Dry gas was set to 5.0 L/min at a temperature of 300 °C. Nebulizer gas operated at a pressure of 10 psi. SL was 1:1 ultrapure water : IPA and was delivered by the syringe pump at a flow rate of 4 µL/min.

For the creation of extracted ion electropherograms (EIE) in the experiments with BSA tryptic digest as analyte, the m/z ratios in Table 5 were used while Table 6 lists the m/z ratios used for creation of EIEs in the peptide analysis experiments.

Table 5: *m/z* Ratios used for the Creation of EIEs in the Peptide Analysis Experiments.

<i>m/z</i>	<i>z</i>	Peptide Sequence	<i>m/z</i>	<i>z</i>	Peptide Sequence
333.19	2	KFWGK	488.52	3	TCVADESHAGCEK
356.68	2	SEIAHR	507.80	2	QTALVELLK
379.71	2	GACLLPK	511.58	3	LKECCDKPLLEK
383.93	4	LKECCDKPLLEK	517.77	2	NECFLSHK
395.23	2	LVTDLTK	526.25	3	ECCHGDLLECADDR
409.71	2	ATEEQLK	536.75	2	SHCIAEVEK
417.20	3	FKDLGEEHFK	547.32	3	KVPQVSTPTLVEVSR
424.25	2	LSQKFPK	569.78	2	CASIQKFGER
435.90	3	HLVDEPQNLIK	571.84	2	KQTALVELLK
449.74	2	LCVLHEK	582.30	2	LVNELTEFAK
461.73	2	AEFVEVTK	593.60	3	CCAADDKEACFAVEGPK
464.23	2	YLYEIAR	627.97	3	RPCFSALTPDETYVPK
467.55	3	TVMENFVAFVDK	634.95	3	NECFLSHKDDSPDLPK
473.88	3	LKECCDKPLLEK	653.36	2	HLVDEPQNLIK
476.22	4	NECFLSHKDDSPDLPK	673.99	3	LKPDPNTLCDEFKADEK
480.60	3	RHPEYAVSVLLR	682.38	3	RHPYFYAPELLYYANK
487.72	2	DLGEEHFK	722.31	2	YICDNQDTISSK

Table 6: *m/z* Ratios used for the Creation of EIEs in the Protein Analysis Experiments.

<i>m/z</i>	<i>z</i>	Protein	<i>m/z</i>	<i>z</i>	Protein
942.7	18	Myoglobin	1244.8	11	RNase A
1148.6	16	β -Lactoglobulin	1431.4	10	Lysozyme
1242.5	12	RNase B			

5.3.3 1D and 2D System

In the first 1D experiments, only two capillaries were connected to the valve. The valve was not switched during the experiments and always in position A. Therefore, separation was through the sample loop and not through the short-cut. In further 1D experiments, the valve was switched without installing the capillaries of the second dimension.

In experiments without additional detection in front of the valve, the migration velocities (v_m) of single compounds could be calculated by the migration times (t_m) which were determined by a reference experiment:

$$v_m = \frac{l_{eff}}{t_m} \quad (10)$$

Switching time (t_s) was determined by dividing the length of the first capillary (l_{1A}), (the distance the solute needed to reach the sample loop), by the migration velocity:

$$t_s = \frac{l_{1A}}{v_m} \quad (11)$$

Peak volume (V_p) of specific signals in a 50 μm i.d. capillary was calculated by:

$$V_p = \pi \cdot r^2 \cdot l_p \quad (12)$$

Thereby, the signal length (l_p) was calculated by:

$$l_p = FWHM \cdot v_m \quad (13)$$

Using the external detector in front of the valve, switching time was t_m plus the time the compound needed to cover the remaining capillary length (l_r) which was the distance between the external detection and the sample loop:

$$t_s = \frac{l_r}{v_m} + t_m \quad (14)$$

In plug positioning experiments by C⁴D, migration velocity of the plug with respect to the C⁴D was determined at a pressure of 500 mbar and 50 mbar. Therefore, the sample was injected by hydrodynamic injection 5 s at 50 mbar and flushed with 500 mbar or 50 mbar respectively in detector direction.

Migration velocity (v_m) at 500 mbar and 50 mbar was calculated to:

$$v_{m,500} = \frac{l_{eff}}{t_{m,500}} = \frac{43 \text{ cm}}{89.6 \text{ s}} = 0.48 \frac{\text{cm}}{\text{s}} \quad (15)$$

$$v_{m,50} = \frac{l_{eff}}{t_{m,50}} = \frac{43 \text{ cm}}{860 \text{ s}} = 0.05 \frac{\text{cm}}{\text{s}} \quad (16)$$

In 1D separation, HV was always stopped at the switching time in both dimensions and the valve was switched from position A to position B. Subsequently, separation HV was switched on again.

In 2D experiments, all four capillaries were connected to the valve. The outlet of the CE instrument was used as first dimension inlet. Therefore, the electrode of the instrument outlet was connected to the external HV source. Further, the system was equipped with an external grounded outlet vial to close the electric circuit of the first dimension.

Again, the separation HV was stopped in both dimensions during the switching step, except in the multiple switching experiments. The HV in the first dimension was stopped before switching. After switching, separation HV was applied in the second dimension.

Part III

Results and Discussion

Parts of this chapter were published in [138] and [139]:

Kohl, F. J., Montealegre, C., Neusüß, C., *On-line two-dimensional capillary electrophoresis with mass spectrometric detection using a fully electric isolated mechanical valve*, *Electrophoresis* 2016, 37, 954-958.

Kohl, F. J., Neusüß, C., *CZE-CZE ESI-MS Coupling with a Fully Isolated Mechanical Valve*, *Methods in Molecular Biology – Capillary Electrophoresis*, Schmitt-Kopplin, P. (Ed.), Humana Press 2016, 155-166.

6 Valve: Selection and Integration

6.1 Valve Requirements

The basic idea to the set up of the 2D system was the implementation of a mechanical valve as the interface. The valve should contain a sample loop which can be switched between the dimensions. The valve should not connect the capillaries of the two dimensions among each other, as in [93], in order to create fully spatial separation of the two dimensions. This is essential to enable nearly unlimited selection of CE mode, BGE composition, and EOF speed and direction in the first dimension.

Further on, the structure dimensions of the valve needed to be in the same region as the used CE capillaries to avoid peak broadening and carry-over due to turbulences or strong variations in the electric field strength by abrupt changes of the cross section. The connections and through-holes of the valve needed to be in the range of 100 μm or smaller. Otherwise, dead volumes are created which would lead to a lack of analytical power and further field inhomogeneities. In addition, precise cutting of specific analytes turns out to be more challenging due to high dead volumes. Hence, most commercial 6-way valves are not applicable since the port-to-port dead volumes, even in nano valves, are already in the range of some tens of nanoliters.

Moreover, the sample loop volume needed to be in the range of typical hydrodynamic injection volumes or volumes which correspond to the signal width in the first dimension respectively (several nanoliters). It needed to be ensured that the volume is low enough to allow the transfer of the complete volume, but as well, high enough to enable complete cutting of the signals. The possibility to change the sample loop volume appeared to be important. This allows the adjustment of the system to a wide range of applications.

Again, commercial 6-port valves seemed to be ideal because of the possibility to insert capillary parts of different lengths between two connections as sample loop. Anyhow, even the shortest possible capillary which can be used to connect two ports would be several centimeters long. This would lead to a high sample loop volume, probably too high to carry out complete transfer in many applications. The use of capillaries as the loop with a lower i.d. than the separation capillaries appeared to be unpractical. Increased diffusion was expected due to turbulences in the changes in the cross sections and the differences in the electric field strength.

Most commercial analytical valves are intended for their application in LC approaches. Therefore, they, or at least parts of them, are mostly produced from stainless steel which shows very good pressure resistive properties but is impractical for its use in HV driven CE. In most CE approaches, pressure resistive properties play a secondary role since only pressure of a few bars is applied for flushing. But, in order to implement the valve into the CE HV circuit without additional grounding, it is required that all parts which may be in contact with the BGE are made of a non-conductive material. Particular attention should be paid on the breakdown voltage of the specific material. The structures of the valve, as explained, need to be very small and the applied voltage is very high. It must be ensured that the current cannot leak outside the valve so not to cause safety issues.

Fused silica or glass seemed to be ideal since it is the same material as the one used for the capillaries. Surface chemistry and behavior during the separation and influence on the separation is well studied. Further on, processing technologies from microchip machining enable the creation of very fine structures in these materials. However, it is very difficult to generate sufficient pressure resistance applying fused silica as valve material even for CE applications. In addition, movement between two fused silica parts would cause further durability issues. Ceramic material is expected to show advantages comparable to fused silica but without the knowledge of the behavior of the surface during the separation. Especially in the case of the analysis of proteins, which tend to adsorb on fused silica surfaces, a lack of resolution and carry-over problems were suspected.

Obviously, different plastic materials are a further alternative. There are several materials which are also used as material for CE capillaries like PTFE and PEEK. The chemical resistance is well known and most are non-conductive. Plastic is comparably easy to process and the material is available with variable density which enables the selection of the most suitable material for ideal pressure resistance of the valve.

6.2 Actual Valve Design

A C4N-4354-.02D microinjector 4-port-valve with an internal 20 nL sample loop was chosen and purchased from VICI which should fulfill all the requirements. It is designed and assembled of three individual parts (Figure 17): I) the valve body which contains the mechanics of the valve. The valve body is made from stainless steel and is grounded. II) The rotor, which is the moving part and driven by the mechanics of the valve body. It contains the sample loop which is milled into its surface. III) The stator, which is the fixed part and contains the connections for the capillaries.

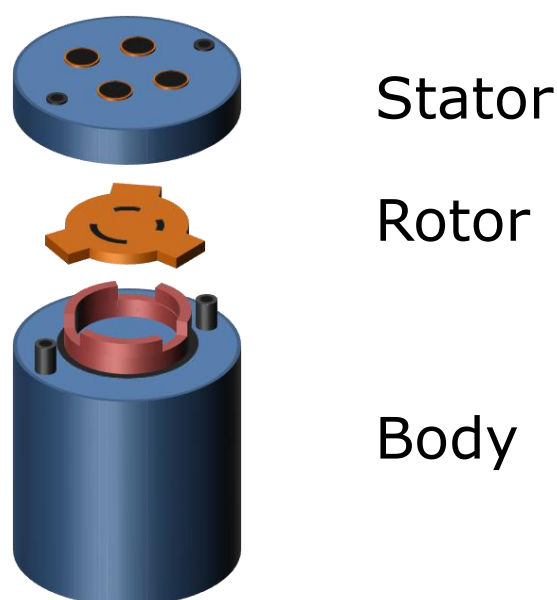


Figure 17: Individual Parts of the used 4-Port Microinjector Valve.

The rotor is already produced from non-conductive plastic material. The stator is normally made from stainless steel. For the implementation of the valve into the CE HV circuit, a special isolation shim, made from (black) plastic material, was purchased from VICI. The shim was installed between a customized stainless steel stator and the rotor and body (Figure 18 A).

However, in first experiments only a very low electrical potential could be applied to the valve. Although only non-metal surfaces were used, high potentials led to current fluctuations probably induced by electric breakdowns.

Because the rotor was made from a comparable thin platelet, it was assumed that the electric breakdowns occur between the rotor and the grounded stainless steel valve body.

Therefore, the valve was further equipped with an additional insulating layer of several millimeters between rotor and valve body. However, further experiments showed that this modification led to no improvement. Measurements revealed a very low electrical resistance of the black plastic material of the stator shim. Because of the black color, it was assumed that the material contains graphite which would explain the high conductivity.

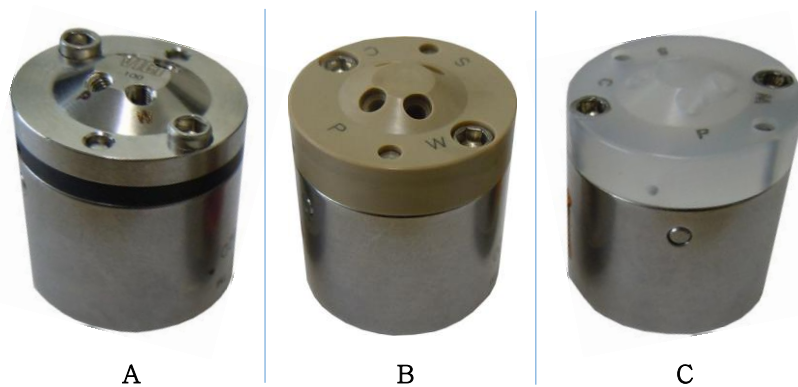


Figure 18 A-C: Different Valves which were used During the Experiments.

In order to have a fully insulated valve available, VICI provided an alternative stator made from Valcon E[®] which is a polytetrafluoroethylene/polyaryletherketone (PTFE/PAEK) composition (Figure 18 B). By using the stator produced from this material, it was possible to integrate the valve into the CE HV circuit applying voltages up to 30 kV.

Because of issues with the mechanic stability of the plastic material, which are discussed in detail in chapter 11.3, a further stator made from a third alternative clear plastic material was tested (Figure 18 C). Unfortunately, only a few experiments revealed insufficient mechanical characteristics even worse than that of the previously used material. Therefore, no further studies of the valve using the clear material were conducted.

The stator has four connections labeled as S, W, P, and C, (Figure 19 A) designed for the use of 1/32" micro finger tight fittings (Figure 19 B). In combination with the appropriate micro tight sleeves, the fittings allow the connection of capillaries with an o.d. of 375 μm . The through hole of the connection outlet has a diameter of about 100 μm (Figure 19 C).

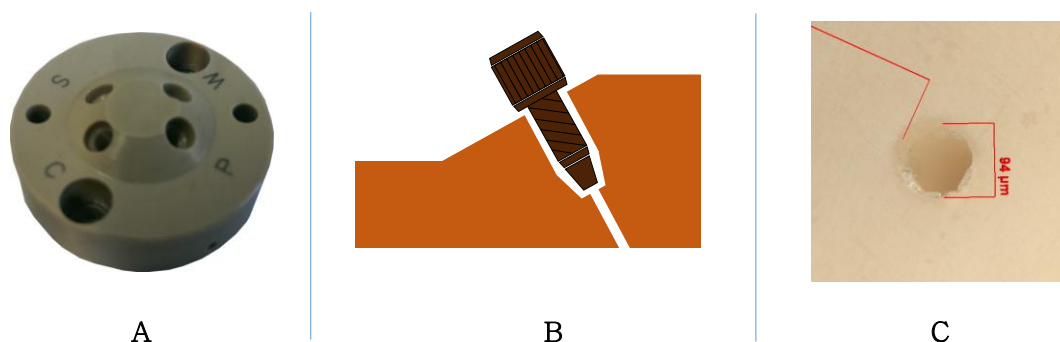


Figure 19 A-C: Connections of the Stator; A: Photography of the Stator Connections; B: Schematic Cross Section of the Stator Connection Geometry; C: Microscopic Picture of the Stator Connection Through Hole.

The rotor is made from a platelet, about 1.3 mm thick, and has three channels. One 20 nL channel which is the sample loop and two additional short-cut channels with a volume estimated to about 1/3 of the loop volume (roughly 7 nL) (Figure 20). The channels are milled into the surface of the rotor and have a trapezoid cross section with a depth of 80-180 μm and a broadness of about 100 μm (Figure 21). Although only the standard rotor was used during the project, there are rotors available with 4, 10, and 20 nL sample loop volume. In principle, further rotors with different shaped channels can be produced. The rotor platelets can be exchanged in the valve very easy and fast. Therefore, the sample loop volume is variable in this valve design.

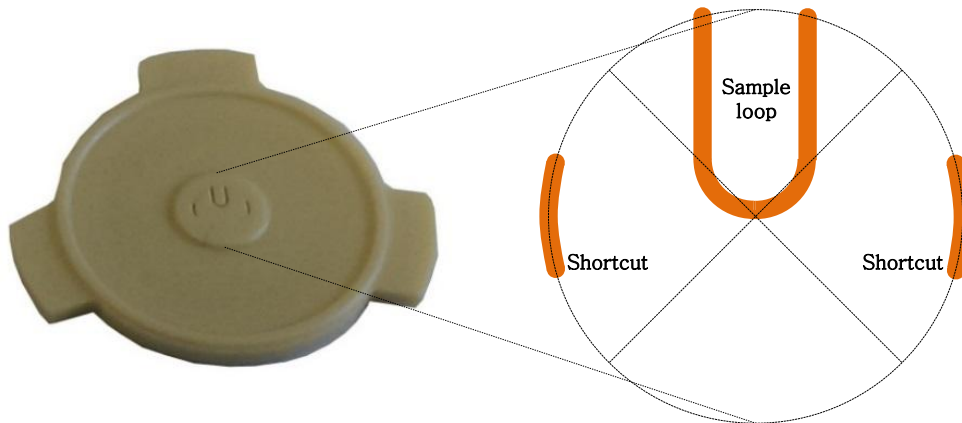


Figure 20: Rotor; Left: Photographic Picture of the Rotor; Right: Schematic Geometrys of the Sample Loop and the Two Short-Cuts.

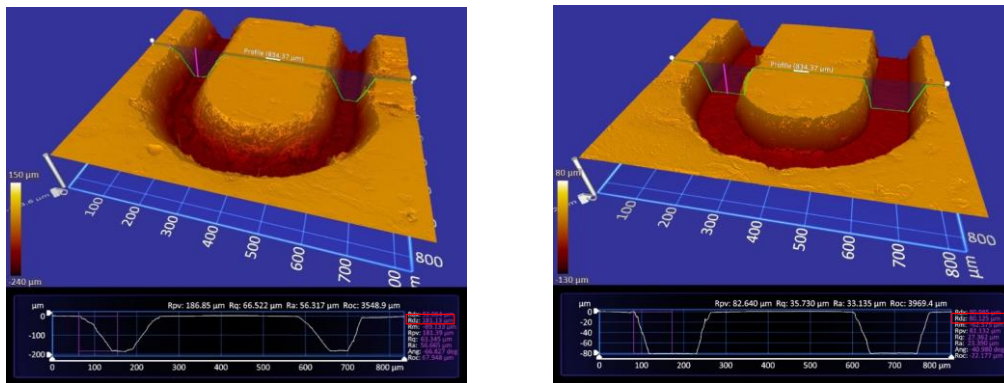


Figure 21: Profile of the Sample Loop Channel; Depth: Left: 180 μm , Right: 80 μm .

The rotor is installed in the intended notches in the valve body. The stator is placed on the top, guided by two rods ensuring ideal alignment of stator connections and rotor channels. The three parts are fixed by two bolt screws. Further on, the valve is equipped with an electric valve actuator.

The valve can be switched in two positions by the valve actuator: position A (load position) and position B (inject position) (Figure 22). In position A, the ports S and W are connected by the sample loop while the ports P and C are connected by one of the two short-cuts. In position B, the ports S and W are connected by the other short-cut while P and C are connected by the sample loop.

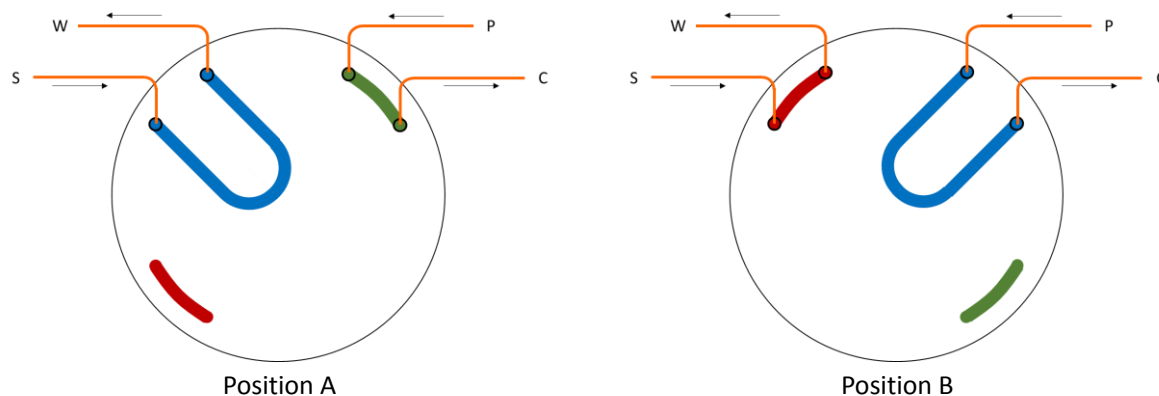


Figure 22: Switching Scheme of the Valve; Position A: Load Position; Position B: Inject Position [139].

Four capillaries can be connected to the four ports of the valve, capillary 1A and 1B for the first and capillary 2A and 2B for the second dimension. The two capillaries of the first separation dimension connect the inlet of the first dimension to port S (capillary 1A) and port W to the outlet (capillary 1B). Capillary 2A connects the second dimension inlet to port P of the valve and capillary 2B connects port C to the second dimension outlet.

Having the valve integrated into the 2D system, the sample should be separated from the inlet of capillary 1A to the outlet of capillary 1B through the valve. When the portion of interest is located inside the sample loop, the valve is switched to position B. Subsequently, the analytes should be separated through the second capillary of the second dimension (capillary 2B) from port C of the valve to the second dimension outlet.

In this valve design, there is never a connection between the two dimensions. Hence, it is possible to apply all actions like e.g. flushing or applying voltage in both dimensions independently or even simultaneously.

7 Applicability of Spectroscopic Detection and Conductivity Detection

One of the main topics of the work was the integration of different external detectors to the 2D system in the first dimension in order to determine valve switching times run-by-run. This is one of the main requirements to enable precise and reproducible cutting of specific signals. Detection directly at the inlet of the sample loop seemed to be ideal. Unfortunately, detection inside the valve was not possible in the actual used valve design. Hence, the additional detection option in the first dimension should be installed as near as possible in front of the valve in capillary 1A.

Due to the design of both, the valve and the used commercial CE instruments, the valve could not be installed directly behind the internal detector of the CE instrument. Therefore, additional external detectors were tested on their suitability for their application in the 2D system. By nature, only non-destructive and on-capillary detectors were suitable.

A LIF detector, a CCD UV detector, and a C⁴D detector were available for their use in the 2D system. Both optical detectors were working with an external detection cell which was connected to the particular light source and the detector by two fiber optics. Therefore, positioning of the cell directly in front of the valve could be carried out by an in-house designed cell mount. The C⁴D anyhow was equipped with a detection cell which could be positioned freely at the capillaries. All three available detectors were tested and compared to the internal detector of the available Agilent CE instrument in order to evaluate their usefulness for the 2D system. This evaluation of the external detection options was carried out in a standard CE system with a single capillary and without the valve.

In the first step, the detection capability of the J&M CCD detector was compared to the integrated DAD of the Agilent 7100 CE instrument. Therefore, the two model analytes lysozyme and myoglobin were analyzed at three different concentration levels. Table 7 shows the signal heights and signal-to-noise ratios (S/N) achieved with both detectors.

Table 7: Comparison Signal Height [mAU] and S/N Achieved by the Internal DAD of the Agilent 7100 CE Instrument and the J&M CCD Detector; Detection at 200 nm; Samples: Lysozyme and Myoglobin at Three Different Concentration Levels (0.03, 0.06, and 0.03 $\mu\text{g}/\mu\text{L}$ Each); CE Instrument: Agilent 7100; Capillary Total Length: 60.0 cm, Effective Length with Respect to the External Detector: 24.0 cm; Effective Length with Respect to the Internal Detector: 51.5 cm.

	Conc. [$\mu\text{g}/\text{L}$]	DAD		CCD	
		Height [mAU]	S/N	Height [mAU]	S/N
Lysozyme	0.30	139	278	57	11.4
	0.06	76	152	32	6.4
	0.03	7.2	14.4	6.7	1.3
Myoglobin	0.30	77	154	32	6.4
	0.06	29.6	59.2	19	3.8
	0.03	0	0	0	0

The results show, that the internal DAD of the Agilent 7100 is able to detect lysozyme at comparable high S/N ratios at the two lower concentration levels of 0.06 and 0.03 $\mu\text{g}/\mu\text{L}$. At these concentration levels the LOD of the CCD detector is nearly reached (S/N = 3) with achieved S/N ratios of 6.4 and 1.3. Both devices are not capable to detect myoglobin at the lowest concentration level of 0.03 $\mu\text{g}/\mu\text{L}$. However, the DAD achieved a S/N ratio of 59.2 for myoglobin at a concentration of 0.06 $\mu\text{g}/\mu\text{L}$. In contrast, the CCD detector again nearly reaches its LOD with an achieved S/N of 3.8.

The comparable low detection capability of the CCD detector was not due to the additional detection cell but due to the high noise level with an amplitude of about 5 mAU at the used detection wavelength of 200 nm (Figure 23). However, the detection capability of the CCD detector is acceptable for most applications.

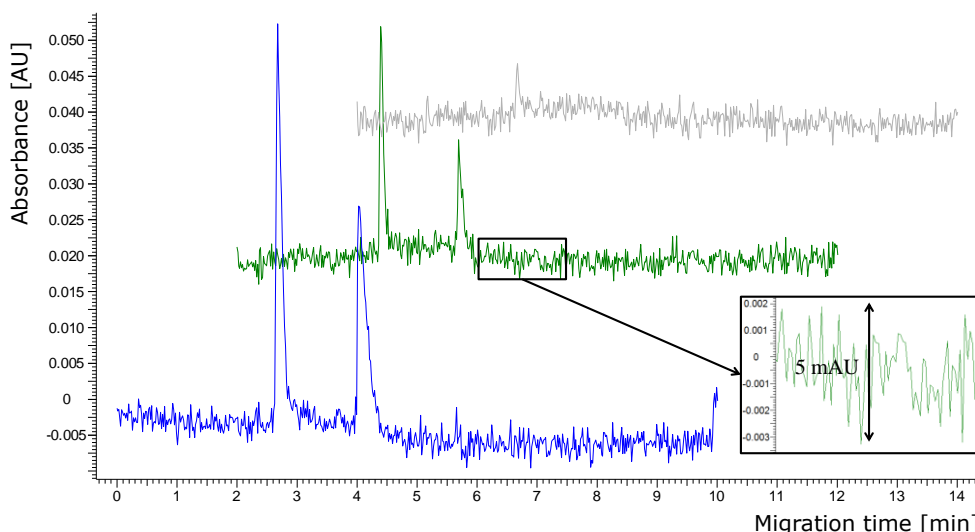


Figure 23: Electropherograms and Illustration of the Noise Level of Three Separations of Lysozyme and Myoglobin at a Concentration of $0.30 \mu\text{g}/\mu\text{L}$ (Blue), $0.06 \mu\text{g}/\mu\text{L}$ (Green), and $0.03 \mu\text{g}/\mu\text{L}$ (Gray) Detected with the CCD Detector at 200 nm. CE Instrument: Agilent 7100; Capillary Total Length: 60.0 cm, Effective Length with Respect to the External Detector: 24.0 cm.

As a further optical non-destructive detection option, LIF was tested with the focus on non-derivatized substances which show natural fluorescence. For this reason, a mixture of the three aromatic amino acids phenylalanine, tryptophan, and tyrosine with a concentration of $0.5 \mu\text{g}/\mu\text{L}$ each was analyzed and detected by LIF at an excitation wavelength of 266 nm.

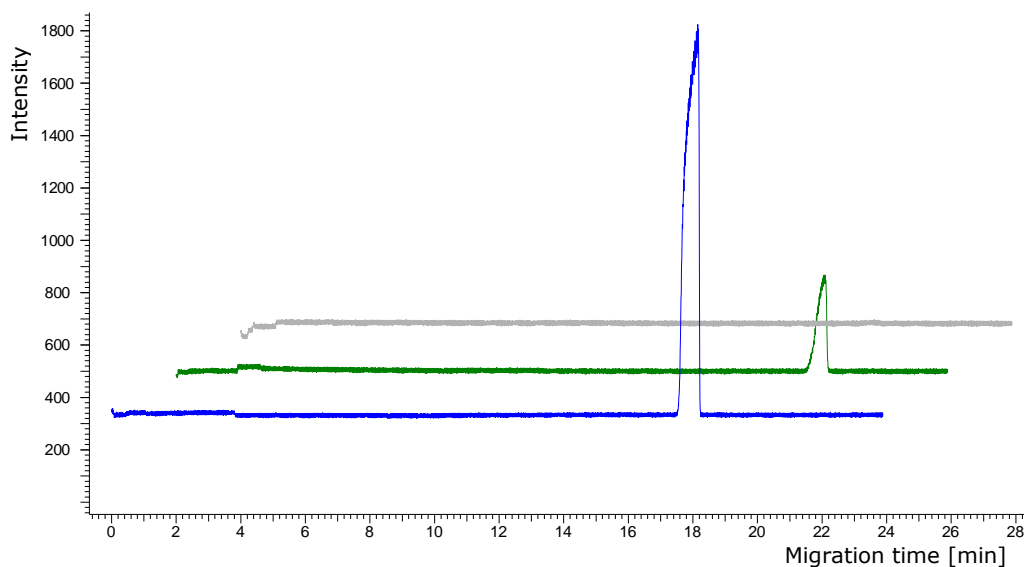


Figure 24: CE-LIF Electropherograms of Analysis of Phenylalanine (Grey), Tyrosine (Green), and Tryptophan (Blue) at a Concentration of $0.5 \mu\text{g}/\mu\text{L}$ Each; Excitation Wavelength: 266 nm; CE Instrument: Agilent 7100; Capillary Total Length: 60.0 cm, Effective Length with Respect to the External Detector: 24.0 cm.

Figure 24 shows that, at the given concentration level, phenylalanine could not be detected in contrast to tyrosine and tryptophan.

Further experiments with cytochrome c and myoglobin as model analyte, which both have a high number of aromatic amino acids, showed that the detection capability of the external LIF detector is not sufficient for the analysis of non-derivatized proteins (Figure 25). Therefore, applicability is limited to derivatized analytes.

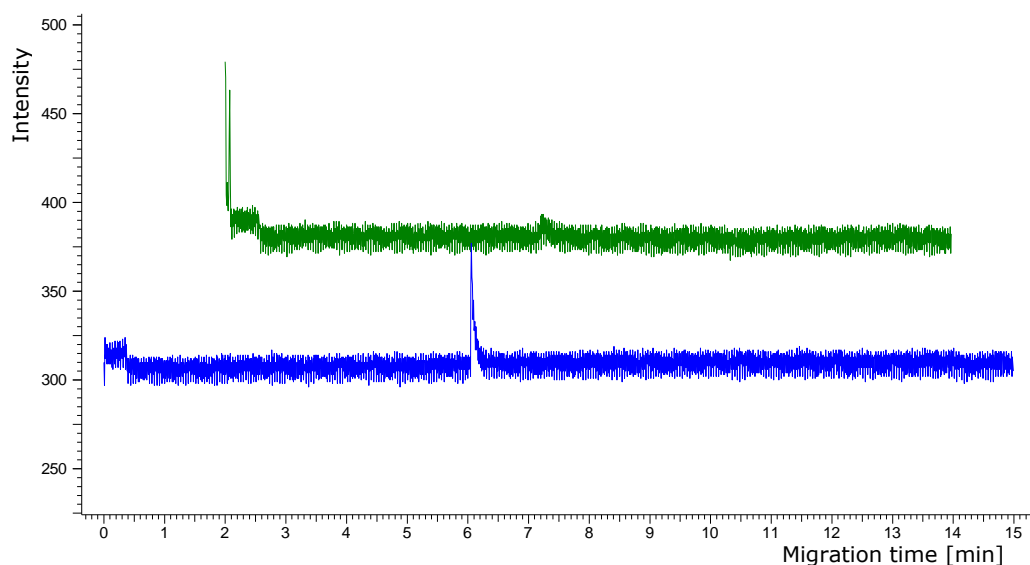


Figure 25: CE-LIF Electropherograms of Analysis of Cytochrome C (Green), and Myoglobin (Blue) at a Concentration of 0.5 $\mu\text{g}/\mu\text{L}$ Each; Excitation Wavelength: 266 nm; CE Instrument: Agilent 7100; LN Coated Capillary; Capillary Total Length 80.5 cm, Effective Length 44.0 cm; Electrokinetic Injection: 10 s at 7 kV.

Further on, the applicability of the available C⁴D was tested. For this reason, the peak areas as well as the peak area-to-noise ratios obtained by the C⁴D were compared to those obtained by the internal DAD of the Agilent 7100 at a detection wavelength of 200 nm (Table 8). Because of the wide variations in the peak widths between the samples at the relatively high concentration levels, the peak area-to-noise ratio was chosen to ensure comparability between the two different detection techniques.

As Table 8 shows, the peak areas obtained by the C⁴D are 6 to 10 times lower as the peak areas obtained by the DAD.

Table 8: Comparison of the Peak Area and the Area-to-Noise Ratio Obtained by the Internal DAD and the Additional C⁴D Analyzing Cytochrome C, Myoglobin, Tryptophan, Tyrosine, and Phenylalanine at a Concentration of 0.5 µg/µL Each; CE Instrument: Agilent 7100; LN Coated Capillary; Total Length: 80.0 cm, Effective Length with Respect to the C⁴D: 70.0 cm, Effective Length with Respect to the UV Detector: 72.0 cm; Electrokinetic injection: 10 s at 7 kV; Separation HV: +30 kV.

	Area		Area-to-noise	
	DAD [mAU/s]	C ⁴ D [mV/s]	DAD	C ⁴ D
Cytochrome C	687	78.5	1374	785
Myoglobin	667	81	1334	810
Tryptophan	7614	749	15228	7490
Tyrosine	4031	432	8062	4320
Phenylalanine	4062	646.5	8124	6465

Since the noise level of the C⁴D is about 5 times lower compared to the noise level of the DAD, the area-to-noise values obtained by the two devices differ only by a factor of about 2. Although the detection capability of the C⁴D is lower than that of the DAD, the C⁴D seems to be still suitable for many experiments. Conductivity detection is more flexible than optical detection since no optical window is needed at the capillary. Therefore, the C⁴D sensor can be positioned at any point at the capillary. Further on, besides the detection of analyte molecules, the C⁴D is well suited for the detection of non-analyte substances like e.g. organic solvents which are creating very high conductivity variations and who are sometimes hardly accessible by optical detection.

With some restrictions, all three tested detectors were suitable for their integration into the 2D system. Although the CCD detector showed a much lower sensitivity than the internal DAD of the Agilent instrument, especially in the low wavelength region of 200 nm, it appeared to be adequate for most applications. The CCD detector is universal and robust. Furthermore, no quantification and, therefore, not an optimized detection sensitivity was required in the detection in front of the valve.

Unfortunately, the LIF detector is in principle only suitable for the detection of aromatic amino acids. Anyhow, installation on the capillary was possible and derivatization of the analyte of interest would enable the usage of this highly selective and sensitive detection option.

The used C⁴D showed rare advantages and lower sensitivity in comparison to the CCD detector. During the experimental work, this technique was especially used for the detection of non-analyte substances (organic solvents).

8 One-Dimensional Experiments

After the selection of the valve and the study of the available external detectors, the valve was integrated into a capillary electrophoretic system. In the initial experiments, a 1D setup was used to keep the setup simple. The options to integrate the valve into the HV circuit of the CE and the behavior and influence on the separation were studied using this setup.

At first, HV up to 30 kV was successfully applied to the system without the observation of current fluctuations or breakdowns caused by the valve. Subsequently, the influence on the electrophoretic resolution was studied using UV as well as MS detection. The results were always compared to those achieved by using a continuous capillary instead of the system with the integrated valve.

After the influence on the separation was evaluated, the possibility to cut specific signals was tested. Still using the simplified 1D system, specific signals were cut by the valve, stored inside the loop, and introduced back into the separation capillary.

In first cutting experiments, the switching times were calculated by the previous determined electrophoretic velocity of the specific analyte. In order to enhance cutting precision, the previous tested external CCD detector was integrated into the 1D system in front of the valve. Subsequently, further cutting and storage experiments were carried out.

8.1 1D System with UV Detection

The valve was first integrated into a 1D approach. Therefore, only capillary 1A and 1B were connected to the valve and the CE instrument. Capillary 1A connected the inlet of the CE instrument to port S of the valve and capillary 1B connected port W of the valve to the outlet vial of the CE instrument. The internal DAD of the applied Agilent CE instrument was used to carry out detection in capillary 1B (Figure 26). The valve was not switched during the experiments.

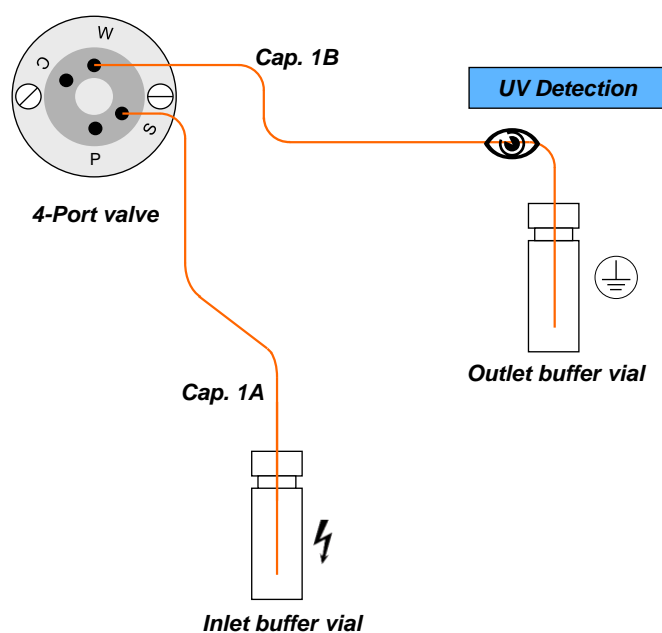


Figure 26: Schematic Setup of the 1D System with UV Detection.

In order to determine the influence of the valve on the separation, a mixture of the two peptides [Glu1]-Fibrinopeptide B (Glu-Fib) and Leucine-Enkephalin (Leu-Enk) was analyzed by the system with the valve as well as by a system equipped with a continuous capillary. Subsequently, the achieved electrophoretic resolution of the two signals was compared.

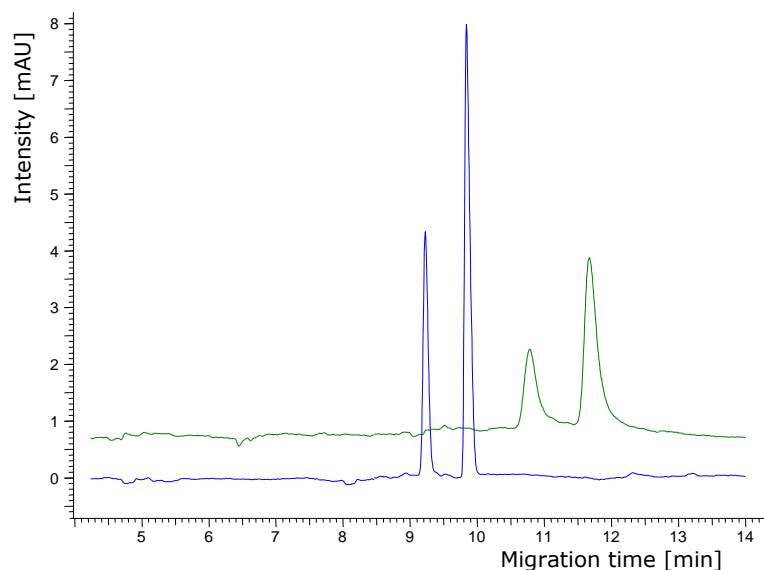


Figure 27: Comparison of the Separation of Glu-Fib and Leu-Enk at a Concentration of $0.05 \mu\text{g}/\mu\text{L}$ each, using the System with the Integrated Valve (Green Electropherogram) and a System Equipped with a Continuous Capillary (Blue Electropherogram); UV Detection at 210 nm; CE Instrument: Agilent 7100; Capillary lengths: Capillary 1A: 23.5 cm; Capillary 1B: 37.5 cm; Continuous Capillary: 61.0 cm; BGE: 0.2 M FAc; Hydrodynamic Injection 6 s at 100 mbar; Separation HV: +25 kV.

Figure 27 shows the results achieved by the valve system and the system with the continuous capillary. It shows that the integration of the valve leads to a peak-broadening (Figure 27, green electropherogram) by the factor of about 2 in comparison to the system with the continuous capillary (Figure 27, blue electropherogram) in these experiments. Due to the peak broadening also the sensitivity and the peak capacity was decreased. This was expected since the analytes need to pass several edges, transitions, and changes in the cross section during their migration through the valve. Anyhow, it shows that separation through the valve is possible in principle. Further, the separation capability seems to be sufficient for most qualitative applications.

8.2 1D System with MS Detection

In the first experiments, it was shown that the valve can be integrated into the HV circuit of the CE and separation through the valve is possible in principle. In the next step, the UV detector was exchanged by ESI-MS detection (Figure 28).

Therefore, the system was no more closed but open and the ESI interface was influencing the separation. The HV circuit of the CE was no more closed by the outlet vial but by the grounded triple tube ESI sprayer.

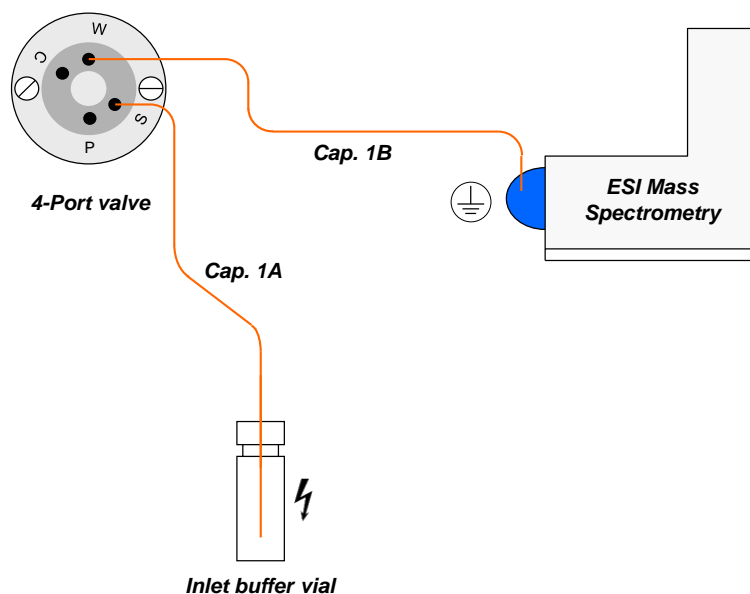


Figure 28: Schematic Setup of the 1D System with ESI-MS Detection.

Again, the electrophoretic resolution of the system with the valve was compared to that of the system with a continuous capillary. To achieve a better statistical basis, the experiments were conducted using a BSA tryptic digest as model analyte. This sample showed a higher number of signals for comparison of peak widths than the two peptide signals of the first experiments with UV detection.

The sample was first analyzed by the system with the integrated valve. The resulting EIEs are shown in Figure 29 A. Subsequently, the sample was analyzed by the system equipped with a continuous capillary (Figure 29 B). At this, the continuous capillary was 1 cm longer than the sum of the two capillaries in the valve experiment to compensate the volume of the sample loop.

Similar to the results of the experiments with UV detection, the integration of the valve led to a slight peak broadening. Full width at half maximum (FWHM) was increased significantly ($p = 0.05$) by a factor of 1.4 ± 0.13 on the average of the 34 main peaks in Figure 29 A. Migration times were almost similar with only slight differences of the factor of 0.02 ± 0.01 .

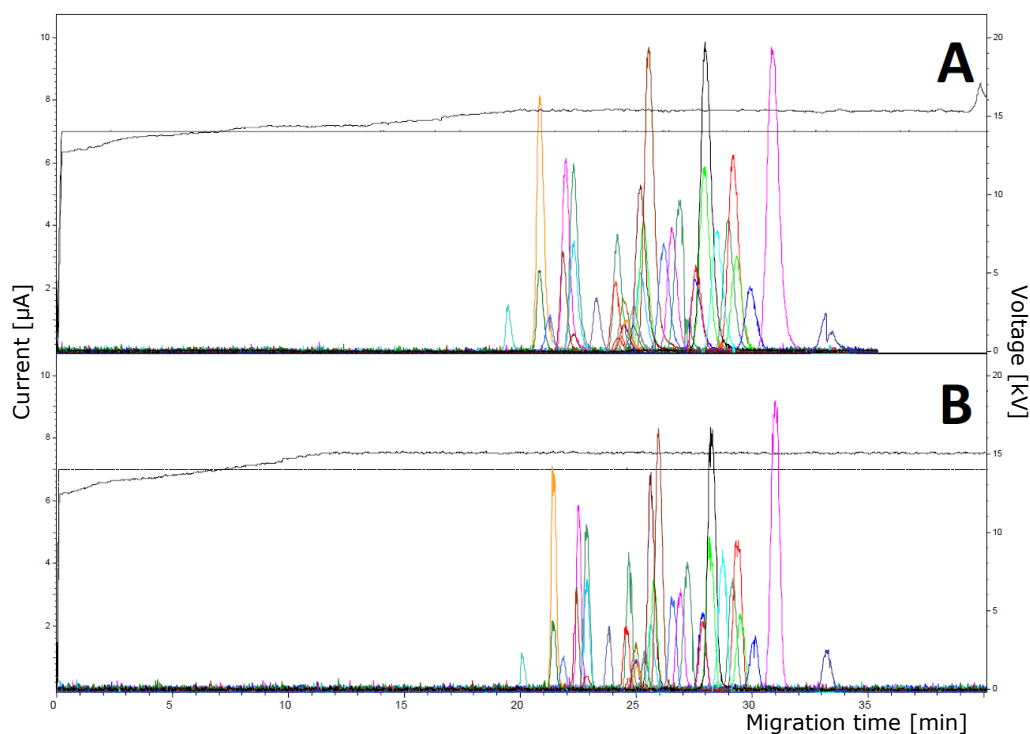


Figure 29 A-B: Comparison of the Separation of a BSA Tryptic Digest Sample ($5 \mu\text{M}$) using the System with the Integrated Valve (A) and a System Equipped with a Continuous Capillary (B) with ESI-MS Detection. EIEs of the Single Tryptic Peptides (m/z Ratios are Listed in Table 5); CE Instrument: Beckman PA 800 plus; ESI-MS Instrument: Bruker Compact Q-TOF; Capillary lengths: Capillary 1A: 23.5 cm, Capillary 1B 37.5 cm, Continuous Capillary: 62.0 cm; BGE: 10 % v/v Aqueous HAC; Hydrodynamic Injection 10 s at 100 mbar; Separation Current: $7 \mu\text{A}$; Resulting HV: $\sim 15 \text{ kV}$ [138].

Besides the EIEs of the single tryptic peptides, Figure 29 A and B show the curves for the separation HV and the current. In both experiments a fixed current of $7 \mu\text{A}$ was applied. The resulting voltage increased in the first 15 min and reached a plateau at 15 kV. Although the current was not stable, the two experiments were comparable since the curve progression as well as the reached maximum HV of 15 kV was similar.

The results shown in Figure 29 confirm the results in chapter 8.1. Separation through the valve is possible, also with MS detection, but resolution or peak capacity respectively is decreased. Additionally, it was shown that the valve has almost no influence on the separation current or HV respectively.

Although separation capacity of the system with the valve is expected to be sufficient for most applications, generally the peak capacity can be increased by re-focusing of the analyte zones in the second dimension behind the valve in a 2D system by e.g. application of a BGE with different pH or ionic strength. Improvement of the shape and surface of the sample loop may also assist with avoiding of peak broadening.

8.3 Cutting and Reintroducing of Specific Signals

Since it could be shown that separation through the valve is possible and the influence on the resolution was evaluated, the valve should be tested on its ability to cut specific signals. To keep the system simple, the 1D system with only capillary 1A and 1B connected to the valve was still used, again with the internal DAD of the CE instrument. The used setup is illustrated in Figure 30.

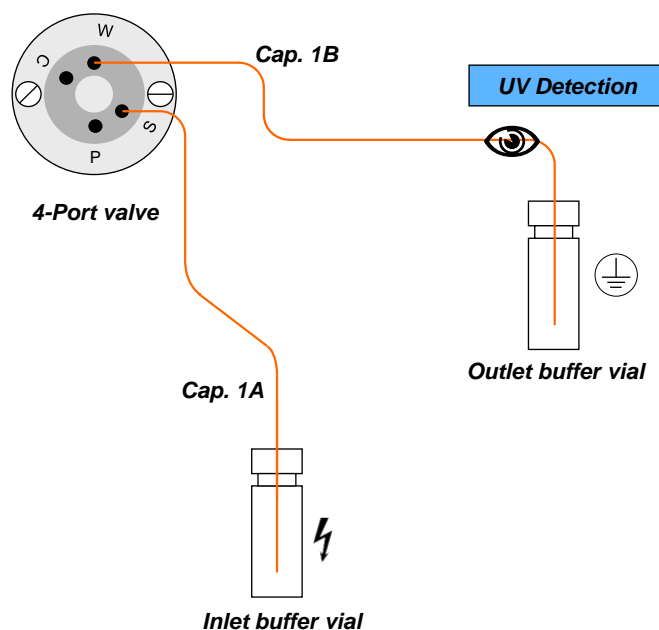


Figure 30: Schematic Setup of the 1D System with UV Detection.

To test the ability of the valve to cut and reintroduce single signals, a mixture of the two peptides Leu-Enk and Glu-Fib was analyzed. Based on a first reference experiment without switching the valve, the migration velocity was determined for each peptide in the used system.

With the migration velocities, the time the analyte needed to reach the sample loop and, therefore, the switching times could be calculated for both compounds.

In two subsequent experiments, the single signals of each, Glu-Fib and Leu-Enk, were cut by switching the valve to position B at the specific calculated switching time. Hence, the analyte was caught in the sample loop and stored outside the separation. After a delay of about 4 min, the stored compounds were reintroduced to the separation by switching the valve back to position A.

The capillaries 1A and 1B were still connected by one of the short-cuts of the valve and the separation kept running. After a delay of about 4 min, the stored compounds were reintroduced to the separation by switching the valve back to position A.

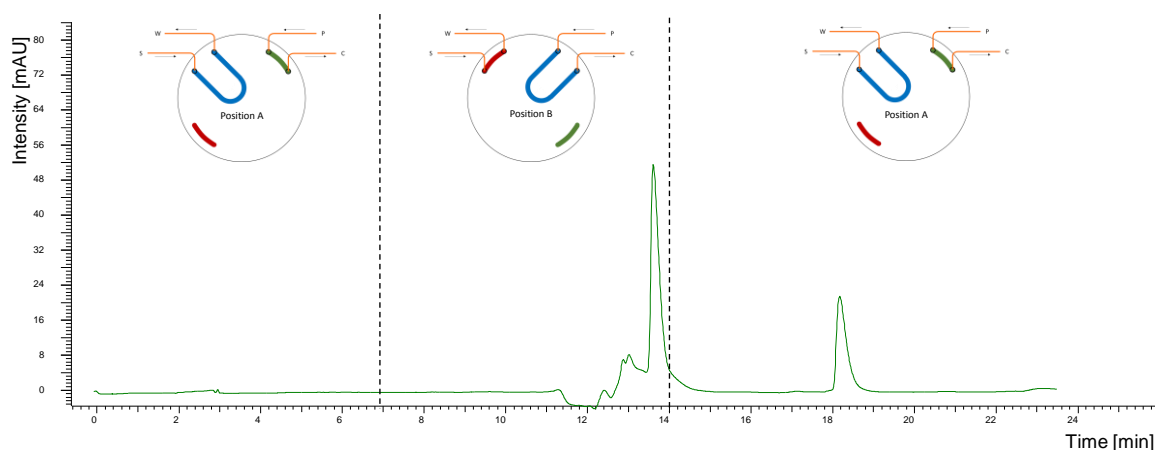


Figure 31: Switching Scheme for Cutting and Reintroducing of the Glu-Fib Signal from a Glu-Fib / Leu-Enk Sample ($0.05 \mu\text{g}/\mu\text{L}$ each); CE Instrument: Agilent 7100; UV Detection at 210 nm; Capillary Lengths: Capillary 1A: 23.5 cm, Capillary 1B: 37.5 cm; BGE: 0.2 M FAc; Hydrodynamic Injection 6 s at 100 mbar; Separation HV: +25 kV.

Figure 31 illustrates the switching procedure in the cutting and reintroducing experiments. The electropherogram shows the successful cutting and reintroducing of the first signal (Glu-Fib) leading to an interchanged migration order of the two peptides.

It was further calculated that the 20 nL sample loop of the valve should be in principal sufficient to completely capture the Glu-Fib signal. The FWHM of the Glu-Fib signal was determined to 0.127 min, leading to a peak volume of 14.2 nL.

Anyhow, the cut signal showed a lower intensity in comparison to the intensity achieved by the reference experiment without switching the valve. This lack of intensity was assumed to occur due to imprecise cutting of the peak.

Unfortunately, the calculated switching times did not perfectly match the two signals which was due to three main reasons. First: in these experiments, it was disregarded, that the volume of the sample loop is equal to the volume of a capillary with 50 μm i.d. and a length of 1 cm. Therefore, 1 cm needed to be added to the length of capillary 1A for the calculation of the migration velocity. Second: the sample was diluted in pure water and not in BGE. Therefore, the electric field strength differed between the sample zone and the BGE leading to a migration velocity which was not constant during the separation. Third: slight changes of the migration velocity in-between the runs, probably caused by e.g. changes in BGE compositions or temperature fluctuations, could not be compensated when the migration velocity was determined by a reference experiment. This further underlines the need of a detection option in the first dimension in front of the valve.

Although it is possible in principle to switch the valve while separation HV is applied, an increasing number of current fluctuations and breakdowns were observed during the cutting and reintroducing experiments, possibly caused by the formation of air bubbles inside the valve during the switching process. Hence, separation HV was stopped before switching and ramped up again after switching. Thus, current breakdowns could be minimized and even completely prevented. In contrast to pressure, like in HPLC, separation HV can be stopped immediately. Therefore, during the stop times, only diffusion can lead to further peak-broadening. Since the stop times were in the range of only several seconds, no significant peak-broadening was expected to be created by switching the separation HV off while switching the valve.

In addition, the successful stopping of the analysis progress in the first dimension enables comprehensive 2D separation in principle. Therefore, the first dimension analysis needs to be stopped until the separation in the second dimension is finished.

In a comprehensive analysis, the stopping times depend on the analysis time of the second dimension which, therefore, needs to be as short as possible. With this, peak broadening by diffusion can be avoided and the total analysis time can be minimized.

8.4 Integration of Additional UV Detection in Front of the Valve

In the previous cutting and reintroducing experiments, switching times were determined by calculating the migration velocity of the specific analytes by the reference experiment. This reference experiment was always necessary when different compounds should be analyzed or a different system, regarding BGE, capillary lengths, or separation HV, should be used. Further, slight changes in migration velocity, caused by e.g. changes in temperature or BGE composition, could not be compensated during the run.

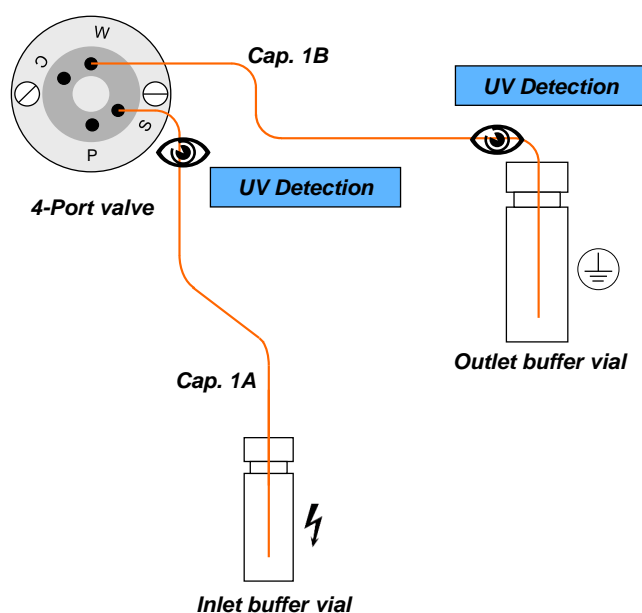


Figure 32: Schematic Setup of the 1D System with UV Detection and Additional UV Detection in Front of the Valve.

To increase the cutting precision, the switching times should be no more determined by a reference experiment but with the help of the signal of an external detector.

Therefore, the external CCD detector was introduced to the 1D system at capillary 1A directly in front of the valve. The installation of the additional detector was performed by the external detection cell which was installed on the in-house designed cell mount. Detection in the end of capillary 1B was again carried out by the internal DAD of the CE Instrument. The used system is illustrated in Figure 32. Further cutting and reintroducing experiments, as in 8.3, were performed by the system with the external detector in front of the valve.

Again, the system was integrated into the Agilent 7100 CE instrument. In order to install the now needed components, the valve, the electric valve actuator, the cell mount, the detection cell, and the two fiber optics, inside the CE instrument the cover had to be modified.

Figure 33 shows the new special in-house constructed cover. The UV detection cell thereby could be installed about 3 cm in front of the valve at capillary 1A. An optical window was integrated in the capillary and ideal alignment of the optical window and the detection cell was achieved by moving the cell at the two mounting rods until the highest transmission was reached.

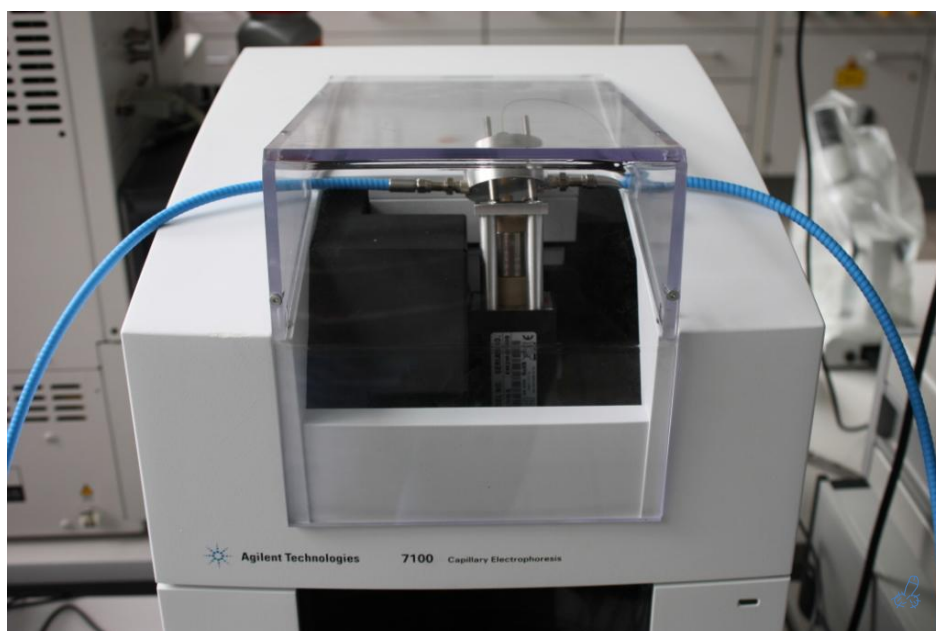


Figure 33: Agilent 7100 CE Instrument Equipped with the Modified Cover Enabling the Installation of the Valve and the Additional UV Detection Inside the CE Instrument.

In initial experiments, the Glu-Fib / Leu-Enk sample was analyzed and the two compounds were successfully detected by the additional UV detector in front of the valve (Figure 34).

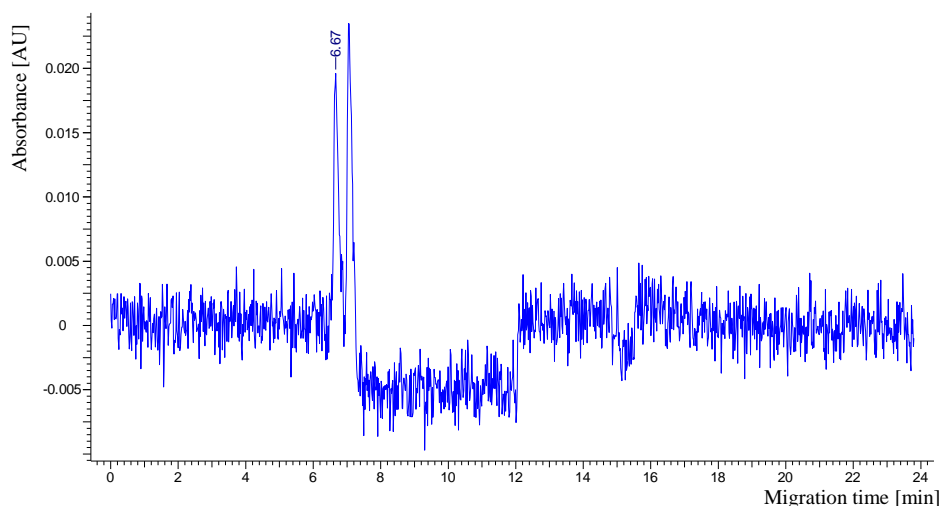


Figure 34: UV Detection in Front of the Valve; Separation of Glu-Fib and Leu-Enk ($0.05 \mu\text{g}/\mu\text{L}$ each); CE Instrument: Agilent 7100; UV Detection at 200 nm; Capillary length: Capillary 1A: 23.5 cm, Capillary 1B: 37.5 cm; Effective Length: 20.9 cm; Detection Cell 2.6 cm in Front of the Valve; BGE: 0.2 M FAc; Hydrodynamic Injection 6 s at 100 mbar; Separation HV: +25 kV.

In two experiments both signals were individually cut by switching the valve to position B at the calculated switching time. One analyte remained stored in the sample loop while the analysis kept running through the short-cut. The stored compounds were reintroduced to the electrophoretic separation after a delay of about 4 min by switching the valve back to position B. Thereby, the switching times were now calculated from the signal of the additional UV detector.

The results of these experiments, illustrated in Figure 35, show that switching times could be successfully determined by the external additional detection option without the need of an additional reference experiment. Both signals could be successfully cut and reintroduced by the valve.

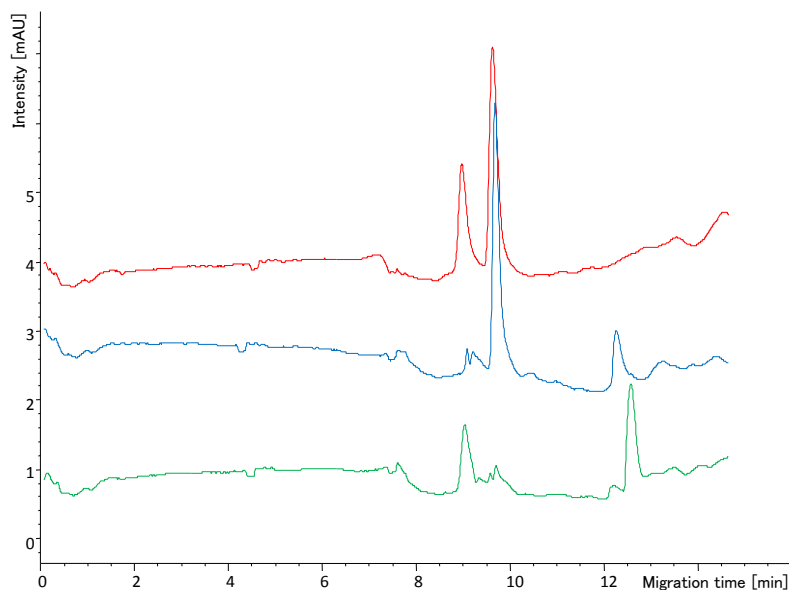


Figure 35: Cutting and Reintroducing of the Single Signals of a Glu-Fib and Leu-Enk Sample ($0.05 \mu\text{g}/\mu\text{L}$ each) after Switching Time Determination by Additional UV Detection; Red: Reference Analysis without Switching the Valve; Blue: Cutting of the Glu-Fib Signal and Reintroducing after 4 min; Green: Cutting of the Leu-Enk Signal and Reintroducing after 4 min; CE Instrument: Agilent 7100; UV Detection at 200 nm; Capillary length: Capillary 1A: 23.5 cm, Capillary 1B: 37.5cm; BGE: 0.2 M FAc; Hydrodynamic Injection 6 s at 100 mbar; Separation HV: +25 kV.

In further experiments, the repeatability of the cutting procedure was studied. For this reason, myoglobin as a single peak was cut from the first dimension and detected in the second dimension by ESI-MS. Repeatability was determined from six injections in three different days. A relative standard deviation value of 19.4 % was obtained for the peak area. This underlines the feasibility to precisely cut peaks by calculating the switching time from the on-line detection in front of the valve.

8.5 Evaluation of the Cutting Precision with C^4D and MS Detection

Besides the detection of analyte molecules, the available C^4D enables detection of non-analyte compounds like organic solvents. In several applications, it might be useful to have the option to position special plugs inside the separation system, e.g. for the creation of a re-concentration step or analyte treatment (e.g. micelle dissolving agents in MEKC) behind the valve.

To determine the possibility to position and precisely cut solvent plugs inside the separation system, a sample of caffeine dissolved in methanol was applied. A methanol plug in the BGE system is strongly lowering the conductivity and is, therefore, ideal to be detected by the C^4D . Caffeine was used to enable MS detection at the outlet of capillary 1B. A plug of the sample solution was injected to the previously used 1D system with MS detection (Figure 36). In several experiments, this plug was positioned in different positions inside the valve. Thereby, positioning was monitored by the C^4D . Further, due to the different positions, different parts of the plug were cut by the valve and stored in the sample loop as in the cutting and reintroducing experiments. The remaining part, as well as the cut part of the plug, were subsequently introduced to capillary 1B and detected by the MS. Comparison of peak area and peak shape of the different signal pairs enabled the evaluation of the correct positioning.

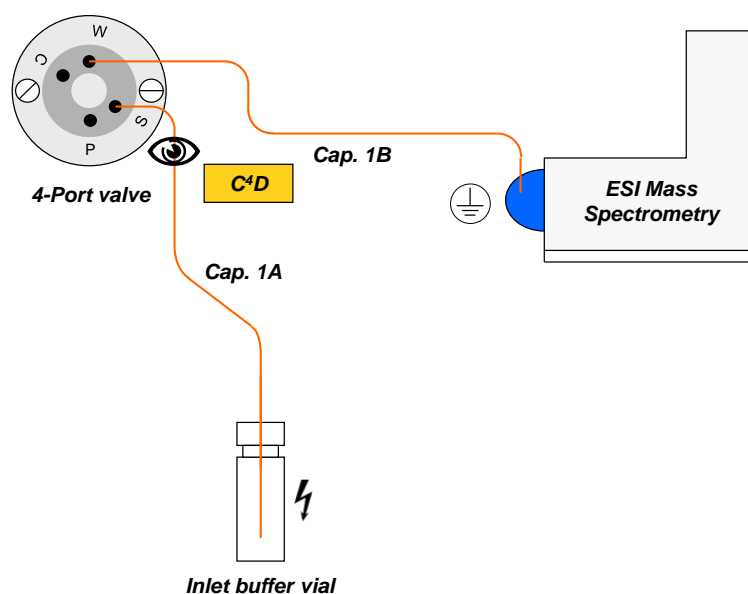


Figure 36: Schematic Setup of the 1D System with MS Detection and Additional C^4D in front of the Valve.

The sample was injected to the system and forced through the capillaries by hydrodynamic mobilization. The solvent plug was detected by C^4D and the signal was cut at 7 different calculated positions in the C^4D signal in seven experiments. Figure 37 illustrates the different calculated cutting positions spread over the signal.

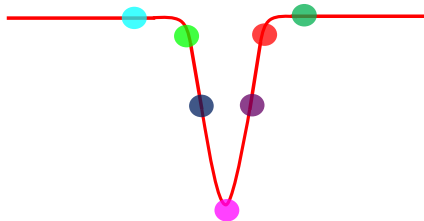


Figure 37: Calculated Cutting Positions in the Negative C^4D Signal for the 7 Positioning Experiments.

Switching times were calculated to 60 s, 66 s, 72 s, 78 s, 84 s, 90 s, and 96 s from the migration time of the peak maximum in the C^4D . The valve was switched from position A to position B at the specific switching times. The cut portion remained in the sample loop while the not cut portion of the plug was still forced in MS direction by pressure (500 mbar) through the short-cut of the valve. After a delay of about 3 min, the cut portion was reintroduced to the separation and subsequently flushed to MS detection (500 mbar). Both signals, the cut portion and the remaining portion, were detected by ESI-MS.

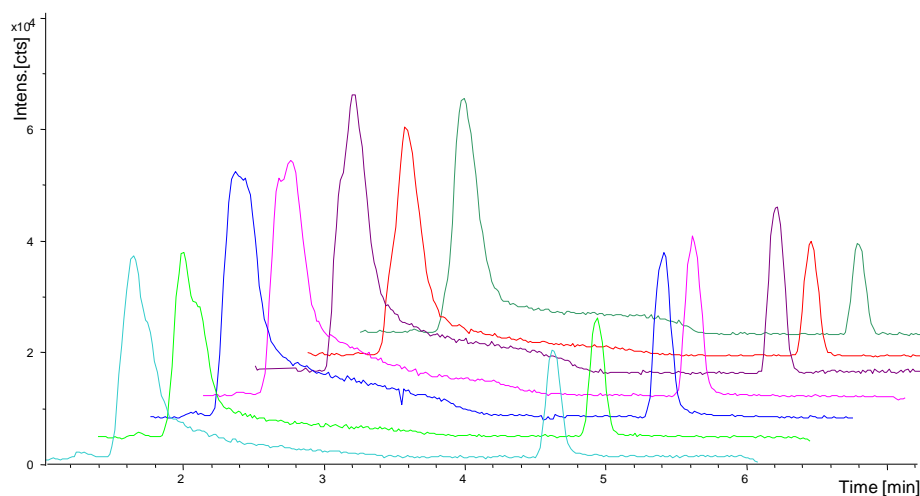


Figure 38: EIE (m/z : 159.111) of the 7 Positioning Experiments; Separation of 1000 ppm Caffeine in MeOH; CE Instrument: Beckman PA 800 plus; Capillary Lengths: Capillary 1A: 47.0 cm; Capillary 1B: 41.0 cm; Effective Length with Respect to the C^4D : 43.0; Detection in Capillary 1A, 4 cm in Front of the Valve: C^4D ; MS Detection in the End of Capillary 1B; MS Instrument: Bruker Compact Q-TOF.

Figure 38 shows the EIEs of caffeine for all 7 positioning experiments. The first peak, which is the remaining portion of the plug, of the turquoise and the green signals (first two from bottom) show a slight bend in the right flank. This indicates that cutting occurred, as calculated, in the front part of the plug (compare cutting position turquoise and green in Figure 37).

In the next three cutting positions (blue, pink, and purple), the bend is located in the middle of the peak or slightly in the front (purple) whereas in the last two cutting positions (red and green) a little bend can be seen in the front. These changes in the peak shape or the position of the bend respectively matches with the calculated cutting positions.

Figure 39 shows the ratio the of peak area of the cut portion (second signal in the EIEs in Figure 38) to the peak area of remained portion (first signal in the EIEs in Figure 38) over the different cutting positions. The ratio has its maximum at the cutting position calculated to the middle of the C⁴D signal. In this position, the maximum portion of the plug was cut by the sample loop. The ratio decreases from this maximum when the cutting position is shifted in the direction of the plug edges.

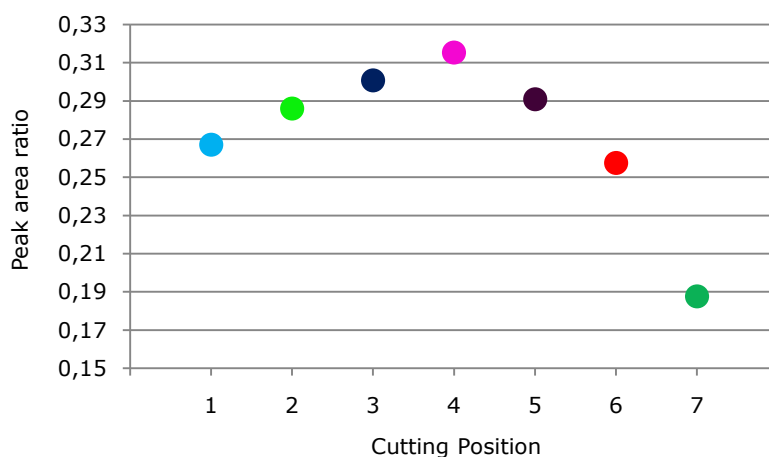


Figure 39: Positioning Experiment, Ratio of the Peak Area of the Cut Portion to the Peak Area of the Remained Portion Plotted Against the Cutting Position.

The results of these experiments show the option to precise position solvent plugs inside the separation system. The peak shapes, showed in Figure 38, as well as the progression of the peak area ratios, showed in Figure 39, prove that the plug was in fact in the calculated position and could be cut precisely.

9 Experimental Setup of the Two-Dimensional System

The main goal of this work was the setup and characterization of a 2D-CE system with MS detection. While chapter 8: “One-Dimensional Experiments” comprises the possibility to integrate the valve into a HV driven CE separation system in principle, the setup of the complete 2D system is described in the following.

9.1 Instrumental Setup of the 2D System

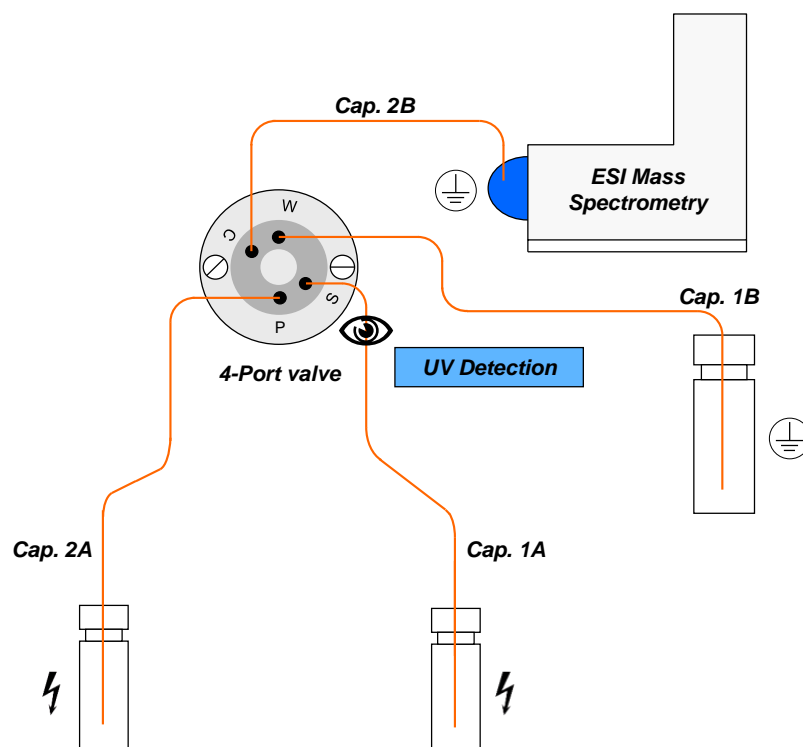


Figure 40: Schematic Setup of the Complete 2D System used during the Experimental Work.

Figure 40 shows the setup of the used 2D system. It consisted of an inlet vial for each dimension equipped with an electrode in order to enable application of separation HV. Further, a third vial was used to ground the first separation dimension. The second dimension was grounded by the ESI interface.

Thereby, the first separation capillary of the first dimension (capillary 1A) connected the inlet vial of the first dimension to port S of the valve. The second capillary of the first dimension (capillary 1B) connected port W of the valve to the grounded outlet vial.

At the capillary 1A, the additional UV/Vis detector was installed shortly in front of the valve, as described in chapter 8.4. This enabled online run-by-run determination of the switching times of the valve.

The first capillary of the second dimension (capillary 2A) connected the inlet of the second dimension to port P of the valve. The second capillary of the second dimension (capillary 2B) connected port C of the valve to the ESI interface.

Therefore, in 2D separations, the sample is injected to capillary 1A. The analytes are subsequently separated in outlet or valve direction respectively. Due to the signal of the additional detector in capillary 1A shortly in front of the valve, the time is calculated when the analyte of interest is located inside the sample loop. At this time, the valve is switched from position A to position B, introducing the sample loop into the second dimension. Application of separation HV in the second dimension leads to separation of the analytes through capillary 2B in MS direction. Therefore, the analytes only migrate through capillary 1A and 2B.

Figure 41 shows a photographic picture of the spatial arrangement of the different instruments used in the 2D system. The 2D system was mainly integrated in the Beckman PA 800 *plus* CE instrument which was placed as near as possible to the MS inlet to keep the length of capillary 2B short. The external HV source was placed on top of the PA 800 *plus* and was connected to the electrode of the inlet vial of the first dimension. Unfortunately, the external HV source was only able to deliver a positive potential.

In experiments, where a negative potential was needed in the first dimension, the HV source of the Beckman P/ACE MDQ CE instrument was used.

This instrument was placed side by side to the PA 800 *plus* because of the limited length of the HV connection cable. The three available additional detectors were placed on top of the PA 800 *plus* or besides the MS instrument respectively.

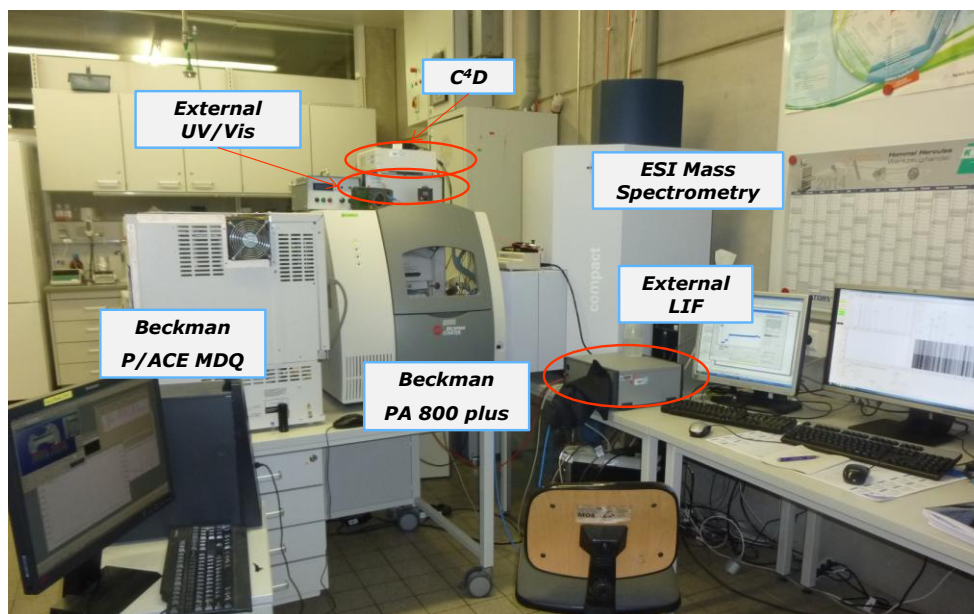


Figure 41: Photographic Picture of the 2D Setup.

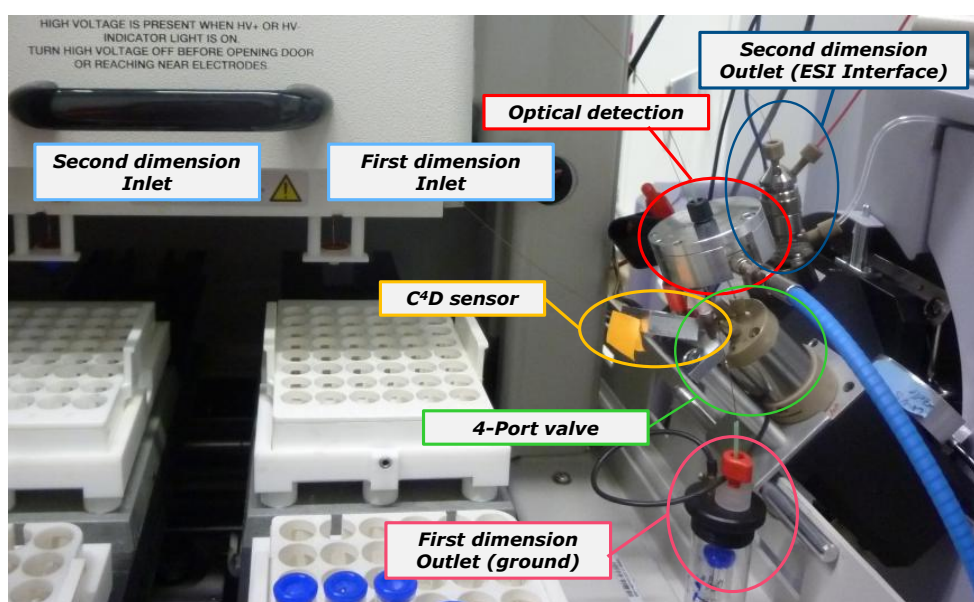


Figure 42: Detailed Photography of the Arrangement of the Different Connections and Detection Options in the 2D CE System.

Figure 42 shows in detail the arrangement of the sensor of the C⁴D in the second and the UV/LIF cell in the first dimension near the valve. Further, it shows the two inlet electrodes and the autosampler. First dimension grounding at the outlet of capillary 1B was carried out by the additional grounded outlet vial while the second dimension was grounded by the ESI interface.

During the first experiments, it turned out, that it is hardly possible to inject solvent (MeOH) plugs using the injection system of the PA 800 *plus* in the described setup (Figure 43 A). It was assumed that the operating speed of the autosampler of the PA 800 *plus* is too low and solvent is pouring off the capillary during the injection steps.

As a consequence, the second separation dimension was integrated in the Agilent G1600AX 3D CE instrument (Figure 43 B) while the first dimension was still implemented in the PA 800 *plus*. The usage of the injection system of the Agilent instrument in the second dimension enabled successful and repeatable positioning of the solvent plugs. As a further benefit of using two CE instruments, an additional inlet was available. Therefore, the outlet of the PA 800 *plus* could be used as grounded outlet of the first dimension (capillary 1B) instead of the additional grounding vial. Moreover, the current or the HV respectively could be observed and recorded by the control computer of the CE instrument which was hardly possible when the external HV source was used. Anyhow, capillary 2A needed to be comparably long in this setup to cover the distance between the G1600AX 3D CE instrument and the valve which was installed as near as possible to the ESI interface.



Figure 43 A-B: Comparison of the two 2D Setups using A: The Beckman PA 800 plus for Both Dimension in Combination with the HV Power Supply of the Beckman P/ACE MDQ Instrument, and B: using the Beckman PA 800 plus only for the First and the Agilent G1600AX 3D for the Second Dimension.

9.2 Capillary Lengths in the 2D System

The capillary lengths are depending on the spatial arrangement of the 2D system and are limited downwards. Figure 44 shows a scheme of the capillary lengths on the example of the 2D system using the Beckman PA 800 *plus* for first and second dimension in combination with the external HV power supply and the external grounding vial.

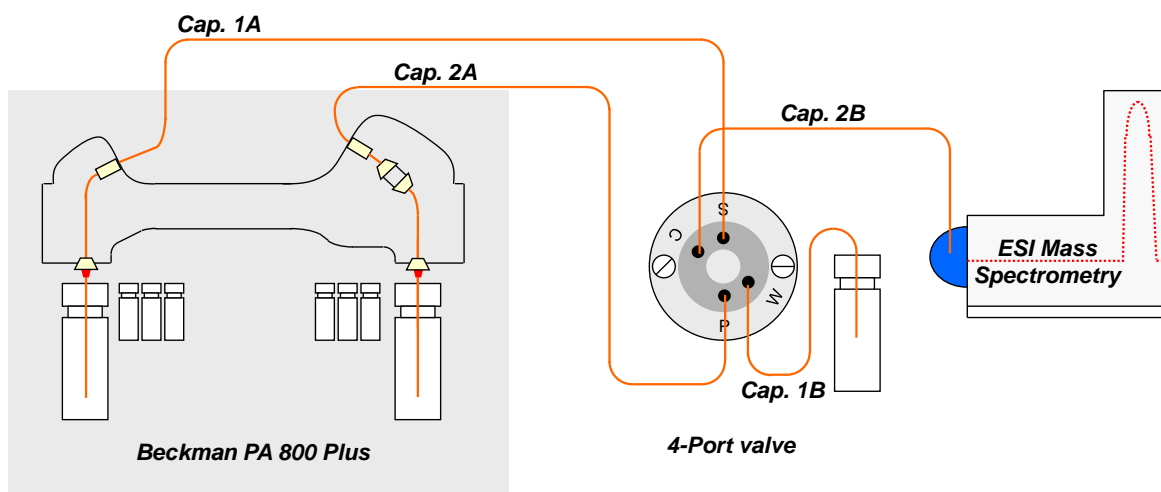


Figure 44: Scheme of the Spatial Instrument Arrangement in the 2D System with Respect to the Capillary Lengths.

Since in this project the second dimension should be used only as a cleanup stage and not as an additional separation step, capillary 2B should be comparably short to avoid peak broadening by diffusion and to minimize total analysis time. As shown, the three components CE instrument, valve, and MS instrument, were positioned in a row. This arrangement allowed the usage of a short capillary 2B (about 20 cm).

In contrast, capillary 1A needed to be long enough to provide an adequate number of theoretical plates to enable sufficient separation of the components. In Figure 44 the inlet of capillary 1A is located in the inlet of the CE instrument. This limits the capillary length to about 55 cm or longer resulting in a total separation capillary length of 75 cm (Capillary 1A and 2B). If a shorter capillary should be used for capillary 1A, the outlet of the CE instrument could be used as first dimension inlet, enabling capillary lengths down to about 40 cm.

The length of capillary 2A and 1B is uncritical because they are only used as inlet (capillary 2A) and outlet (capillary 1B). Anyway, the application of very long capillaries increases the time consumption for flushing (important especially if a high viscosity BGE like e.g. CSE matrix should be applied) and increases the electric resistance of the specific dimension.

10 Two-Dimensional Experiments

In the previous experiments, it was shown that it is possible to conduct separation through the valve and that the valve is able to cut single peaks. Further, the external UV detector was introduced, enabling switching time determination run-by-run without the need of a reference experiment. Subsequently, the second dimension was introduced to the system.

In the following the application of the two-dimensional system is described. The second dimension was introduced (as shown in chapter 9) and the possibility to transfer the cut portion from the first to the second dimension was tested. Therefore, a CZE-CZE system with UV detection in front of the valve and MS detection in the second dimension was set up. The system was again tested using a BSA tryptic digest as model analyte. Single signals were successfully cut, transferred to the second dimension, and detected by the MS. In addition, multiple switching in one run was conducted and the applicability of coated capillaries could be shown on the example of 2D CZE-CZE-MS analysis of proteins.

Subsequently, the system was then used for a CZE-CZE separation with a non-ESI-MS compatible, phosphate based, BGE in the first and a volatile, HAc based, BGE in the second dimension. It is shown, that the system was capable to separate the interfering phosphate from the analytes before MS detection.

10.1 Peptide Analysis by 2D CZE-CZE MS

First 2D experiments were conducted to evaluate the options of cutting specific peaks from the first dimension, transferring them to the second dimension, and detect by MS. A BSA tryptic digest was chosen as model analyte.

The BSA tryptic digest provides a comparable high number of signals which enables inference of the actual cutting position by comparing the adjacent peaks in a 1D reference experiment. Further, a simple BGE system without capillary coating can be applied reducing possible faults.

For evaluation of the options to transfer the cut portion from the first to the second dimension, the 2D system with UV detection in the first dimension in front of the valve and MS detection in the second dimension (outlet of capillary 2B) was set up (Figure 45). In both dimensions the same BGE was used.

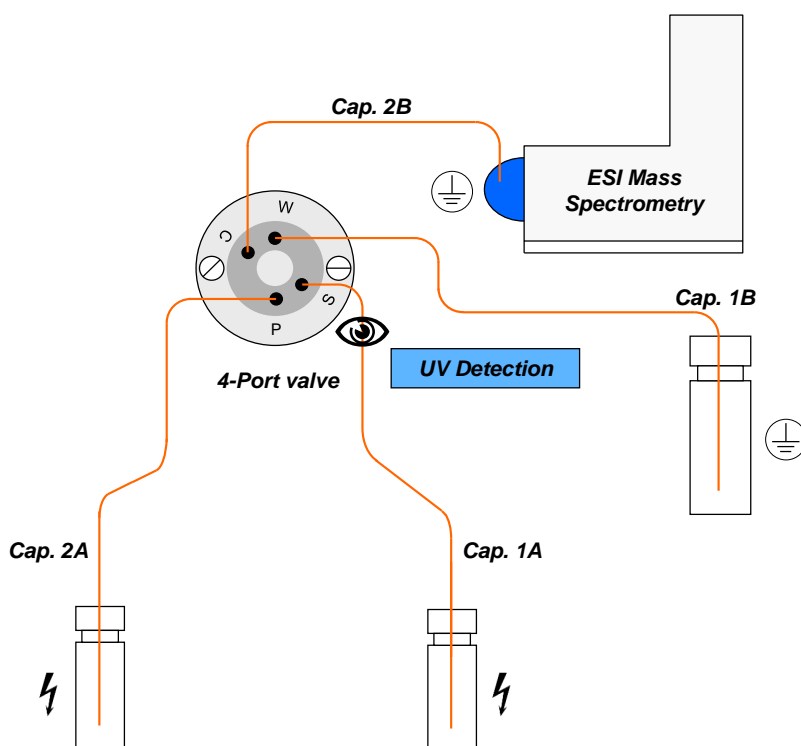


Figure 45: Schematic Setup of the 2D System with MS Detection and Additional UV Detection in front of the Valve [139].

For first, the BSA tryptic digest sample was injected into the second dimension, separated, and detected by the MS without switching the valve in order to perform a 1D reference experiment.

In two subsequent experiments, the sample was injected into the first dimension and detected by the additional UV detector in front of the valve. In the two experiments, two different signals were chosen from the UV electrochromatogram and the associated switching times were calculated.

The specific signals were cut by the valve and transferred to the second dimension. Subsequently, second dimension separation was conducted and analytes were detected by the MS at the end of capillary 2B.

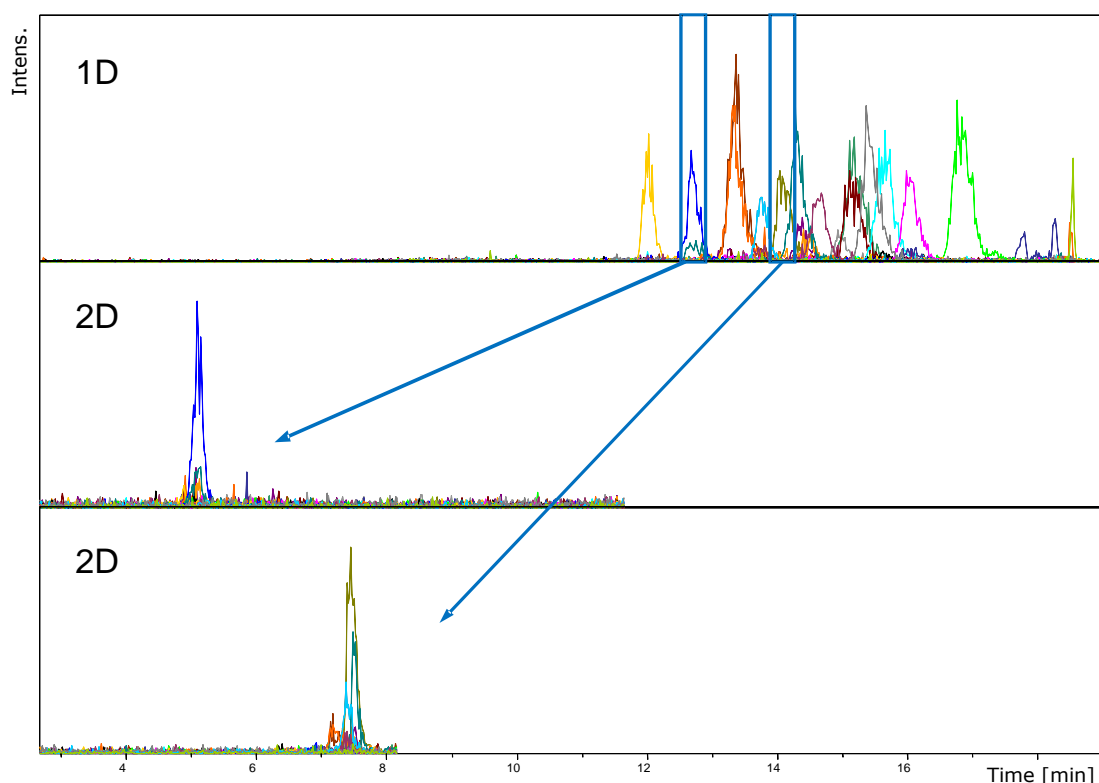


Figure 46: Transfer Experiments; EIEs, Top: Reference Experiment using only the Second Dimension; Middle: First 2D Experiment, Transfer of the Blue Signal (m/z : 480.60); Switching Time: 4.5 min; Bottom: Second 2D Experiment, Transfer of the Green (m/z : 488.52) and Turquoise (m/z : 379.71) Signal; Switching Time: 5.1 min; Sample: 5 μ M BSA Tryptic Digest; CE Instrument: PA 800 plus; Separation HV Delivery in the Second Dimension: External HV Power Supply; Capillary Lengths: Capillary 1A: 38.0 cm, Capillary 1B: 53.0 cm, Capillary 2A: 40.0 cm, Capillary 2B: 55.0 cm; Effective Length with Respect to the UV Detection in Capillary 1A: 34.0 cm; UV Detection 4.0 cm in front of the Valve in Capillary 1A; MS Detection in the Outlet of Capillary 2B: Bruker Esquire 6000 3D IT; BGE: 10 % Aqueous HAc; Hydrodynamic Injection: 10 s at 100 mbar; Separation HV in Both Dimensions: + 30 kV [139].

Figure 46 top shows the electropherogram for the reference experiment using only the second dimension. Figure 46 middle and bottom shows the electropherograms for the two 2D experiments. In these two experiments, the blue (Figure 46 middle) and the green and turquoise (Figure 46 bottom) signals were successfully cut by the valve from the first dimension, transferred to the second dimension, and detected by the MS. This shows the suitability of the valve for its use as an interface for 2D CE.

In these experiments, first dimension separation HV was stopped before switching until the separation in the second dimension was finished. Since only one transfer step was applied in one run, both dimensions were flushed after the separation in the second dimension was finished.

In further experiments the possibility to perform multiple switching in one run was evaluated. Again, the BSA tryptic digest sample was injected to the first dimension. Upcoming peptides were detected by the UV detector in front of the valve and switching times were calculated.

In contrast to the previous experiments, the first dimension separation HV was not stopped for switching and first dimension separation kept running through the short-cut of the valve after switching. Second dimension HV was applied for second dimension separation. After a delay of about 2 min, the valve was switched back to position A without stopping the separation HV in any dimension. Second dimension separation kept running through the short-cut while the loop could again be filled in the first dimension for a second cutting step. Thus, three cutting and transfer steps were performed in a single run.

Figure 47 shows the EIEs of the three cutting steps A, B, and C performed in a single experiment. The peptides were cut from the first dimension, transferred to the second, and detected by the MS. The results prove that multiple switching in a single run is possible. Nevertheless, the risk of separation current breakdowns, probably generated by air bubble formation during the six switching steps, in one of the two dimensions is comparably high and increases with every additional cutting step.

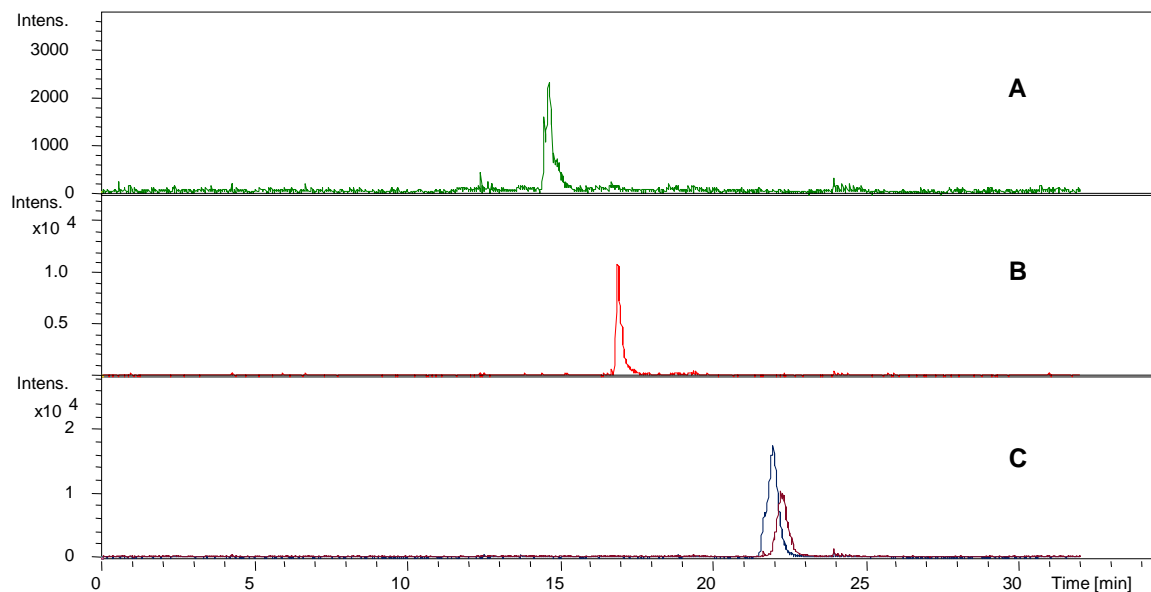


Figure 47: Multiple Switching in a Single Electrophoretic Run; Three Different Switching Positions A (16.0 min - 17.8 min) Green Signal m/z : 417.20, B (25.2 min - 28.0 min) Red Signal m/z : 473.88, C (27.5 min - 31.0 min) Blue Signal m/z : 547.32 and Purple Signal m/z : 627.91; Sample: 5 μ M BSA Tryptic Digest; CE Instrument: PA 800 plus; Separation HV Delivery in the Second Dimension: External HV Power Supply; Capillary Lengths: Capillary 1A: 38.0 cm, Capillary 1B: 53.0 cm, Capillary 2A: 40.0 cm, Capillary 2B: 55.0 cm; Effective Length with Respect to the UV Detection in Capillary 1A: 34.0 cm; UV Detection 4.0 cm in front of the Valve in Capillary 1A; MS Detection in the Outlet of Capillary 2B: Bruker Esquire 6000 3D IT; BGE: 10 % Aqueous HAc; Hydrodynamic Injection: 10 s at 100 mbar; Separation HV First Dimension: + 17 kV at 7.1 - 7.9 μ A; Separation Current Second Dimension: 7.0 μ A at + 15.4 kV.

Although multiple switching was performed, the system was still used as a heart-cut and not as a comprehensive approach. After transferring the first portion to the second dimension, the valve needed to stay in position B until the loop was completely emptied in the second dimension.

Since the first dimension separation HV was still applied during this waiting time, first dimension separation kept running. Hence, analytes passing the valve during the waiting time were lost. To conduct comprehensive separation, the first dimension HV needs to be stopped until the loop is emptied in the second dimension and the valve is switched back to position A.

10.2 Application of Coated Capillaries for the 2D CZE-CZE Analysis of Proteins

Since intact proteins tend to adsorb on the fused silica capillary surface, the capillaries need to be treated with a coating. In the following, the applicability of coated capillaries to the 2D system was tested by the separation of a mixture of the 5 proteins lysozyme, β -lactoglobulin, RNase A, myoglobin, and RNase B to test the applicability of the system for protein analysis. In this case, the capillary surface was coated with PVA.

All four capillaries were coated separately and were afterwards connected to the CE instrument and the valve. Again, a 1D reference experiment was carried out using only the second dimension with MS detection. Further, the mixture was injected into the first dimension of the 2D system. The Proteins were detected by the UV detector in front of the valve and the switching time was calculated in order to cut the first signal (lysozyme).

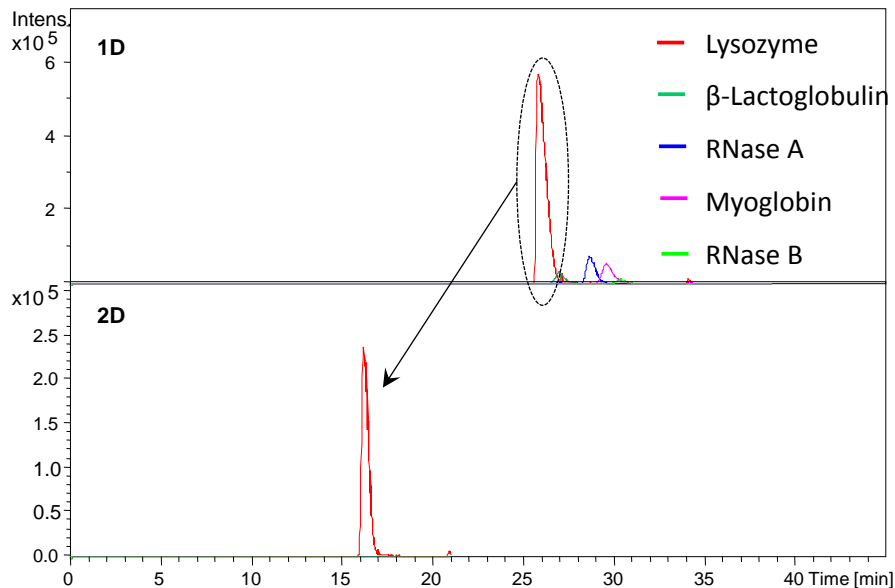


Figure 48: Separation of a Mixture of Lysozyme (200 ppm), β -Lactoglobulin (400 ppm), RNase A (400 ppm), Myoglobin (400 ppm), and RNase B (1000 ppm) using PVA Coated Capillaries; EIEs; Top: Reference Experiment using only the Second Dimension; Bottom: 2D Separation, Transfer of the Lysozyme Signal, Switching Time: 23.5 min; CE Instrument: Beckman PA 800 plus; Separation HV Delivery in the Second Dimension by the External HV Power Supply; Capillary Lengths: Capillary 1A: 40.0 cm, Capillary 1B: 72.5 cm, Capillary 2A: 69.5 cm, Capillary 2B: 40.0 cm; Effective Length of Capillary 1A with Respect to UV Detection: 36.0 cm; UV Detection in Capillary 1A 4.0 cm in Front of the Valve; MS Detection in the Outlet of Capillary 2B; MS Instrument: Bruker micro TOF-Q; Hydrodynamic Injection 20 s at 100 mbar; Separation HV First Dimension: + 19 kV at 6.6-6.8 μ A; Separation Current Second Dimension: 7.0 μ A at + 18.0 kV.

Figure 48 illustrates the results of these experiments. Figure 48 top shows the reference experiment, using only the second dimension. Because in the reference experiment, separation occurred through the valve, this experiment proves that there is no issue with protein adsorption or carry-over inside the valve. The bottom electropherogram in Figure 48 shows the successful 2D separation of lysozyme which was cut from the protein mixture. This is proving the applicability of the system for 2D protein separation using PVA coated capillaries.

The application of PVA coated capillaries is easily possible. Further, there is no indication like e.g. carry-overs for an interaction of the analyzed proteins and the non-coated plastic material of the valve. Due to the thermal immobilization of the PVA during the coating process, the capillaries are permanently coated [140].

Therefore, the coating process is not needed to be repeated after a small number of experiments, like e.g. when using the LN coating, and it is possible to conduct the coating process before the connection of the capillaries to the 2D system. This procedure might be impractical for dynamic coatings because the capillaries need to be flushed while attached to the valve. Therefore, the influence of the coating agents on the plastic material of the valve needs to be studied before the application of such coatings.

10.3 Application of a non-ESI-MS Compatible BGE in the First Dimension

In subsequent experiments, the applicability of a non-ESI-MS compatible BGE in the first dimension was tested. For this reason, a BSA tryptic digest sample was separated in the first dimension using a non-volatile, phosphate based, BGE which shows properties which are different from them of the HAc based BGE used in the previous experiments [141]. Further, emerging phosphate would quench the signals of the peptides in the MS and would lead to pollution of the ESI interface.

The peptides were detected in the first dimension in front of the valve by the external UV detector and transferred via the valve to the second dimension. Here, the previously used volatile HAc based BGE was applied. Subsequently, the phosphate was separated from the analytes and then the peptides were successfully detected by MS.

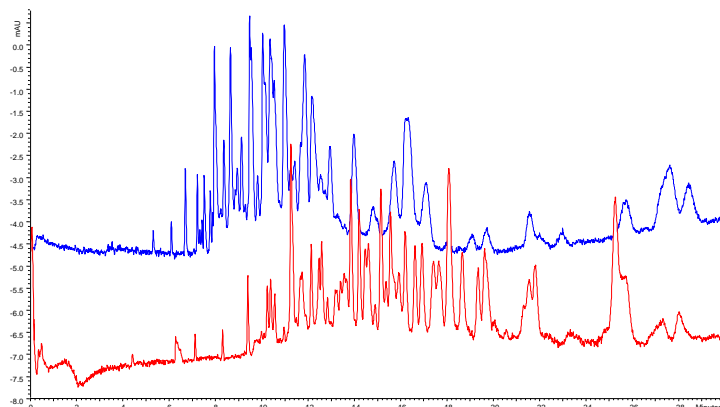


Figure 49: Comparison of the Selectivity using Different BGEs: 10 % v/v HAc (Blue Electropherogram) and 10 mM Phosphoric Acid at pH 2.5 (Red Electropherogram); Separation of a BSA Tryptic Digest Sample (5 μ M) using CE-UV; CE Instrument: Beckman PA 800 plus; Capillary Lengths: Capillary 1A: 38.2 cm, Capillary 1B: 52.8 cm, Capillary 2A: 55.1 cm; Capillary 2B: 40.2 cm; Hydrodynamic Injection: 10 s at 200 mbar; Separation HV: +20 kV.

At first, the sample was analyzed twice using the HAc and the phosphate BGE with CE-UV using the internal DAD of the Beckman PA800 *plus* instrument. Figure 49 shows the two electropherograms using the two different BGEs. Obviously, the phosphate BGE (Figure 49, red electropherogram) leads to a slightly different selectivity and different migration times of the tryptic peptides in comparison to the HAc based BGE (Figure 49, blue electropherogram).

Subsequently, a reference experiment was conducted using only the second dimension of the 2D system. Hence, the peptides were separated by the dimension with the HAc BGE applied and are detected by ESI-MS. Figure 50 A shows the obtained electropherogram. Further on, the sample was injected to the first dimension. The peptides were detected by the external UV detector in front of the valve and the signals were cut at the specific switching times. Subsequently, the analytes were transferred to the second dimension and successfully detected by ESI-MS.

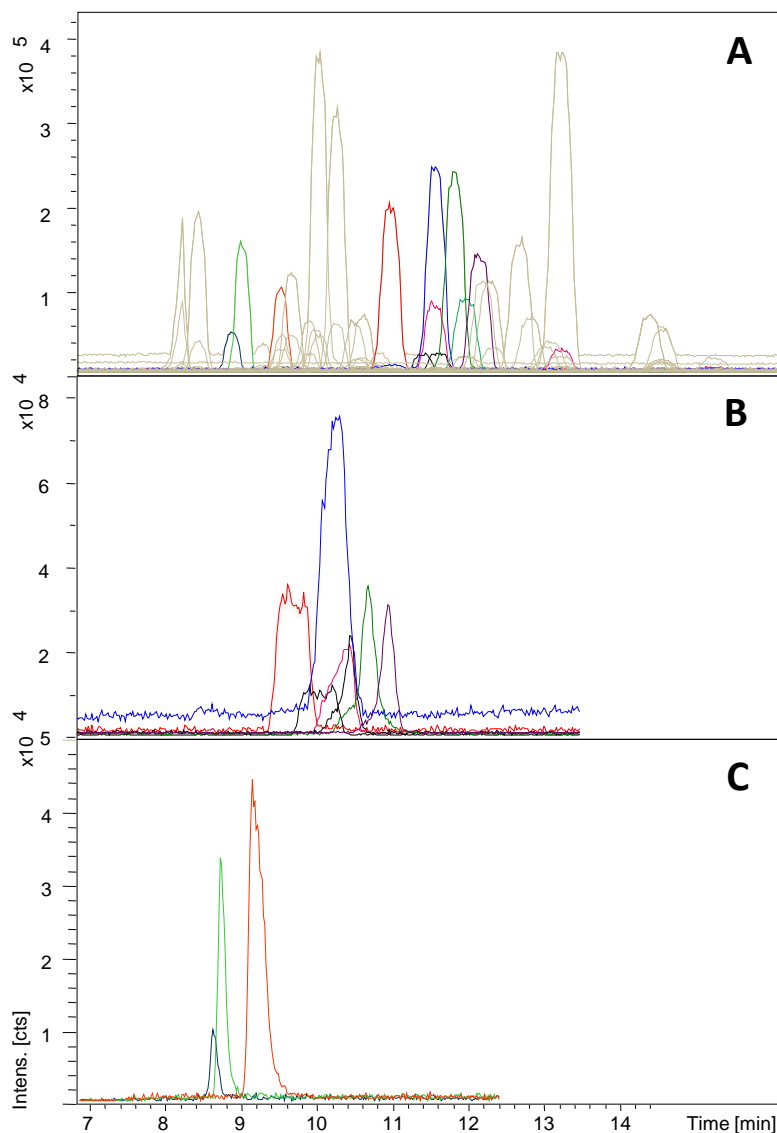


Figure 50 A-C: 2D Separation of 5 μ M Tryptic BSA Digest using Phosphate BGE in the First and HAc BGE in the Second Dimension; A: Reference Experiment using only the Second Dimension; B: 2D Experiment, Cutting at 7.2 min (m/z : 526.25, 547.32, 627.97, 464.23); C: 2D Experiment Cutting at 6.0 min (m/z : 507.80, 536.75, 571.84); the Cut Signals of the Two 2D Experiments are Highlighted in the Reference Experiment; CE Instrument: Beckman PA 800 plus; MS Detection in the Outlet of Capillary 2B: Bruker Compact Q-TOF; Capillary Lengths: Capillary 1A: 38.2 cm, Capillary 1B: 52.8 cm, Capillary 2A: 55.1 cm; Capillary 2B: 40.2 cm; External UV Detection 4.0 cm in Front of the Valve; Effective Capillary Length with Respect to the External UV Detector: 34.2 cm; BGEs: 10 mM Phosphoric Acid at pH 2.5 in the First Dimension, 10 % HAc v/v in the Second Dimension; Hydrodynamic Injection: 10 s at 200 mbar; Separation HV: +20 kV at a Corresponding Current of about 7 μ A; HV Delivery by the External HV Power Supply in the First Dimension.

Figure 50 B and C shows the electropherograms for two switching experiments.

In subsequent experiments, the blue signal in Figure 50 B was reproducible cut three times at slightly different cutting times determined by the additional UV detection in the first dimension.

In the cutting experiment in Figure 50 B, besides the blue main signal, also the dark green and purple signal was successfully cut. However, the light green signal (m/z : 517.77), which is located under the dark green and the purple signal in the reference experiment (Figure 50 A), is missing. This underlines the different selectivity achieved by the usage of a phosphate in comparison to a HAc based BGE.

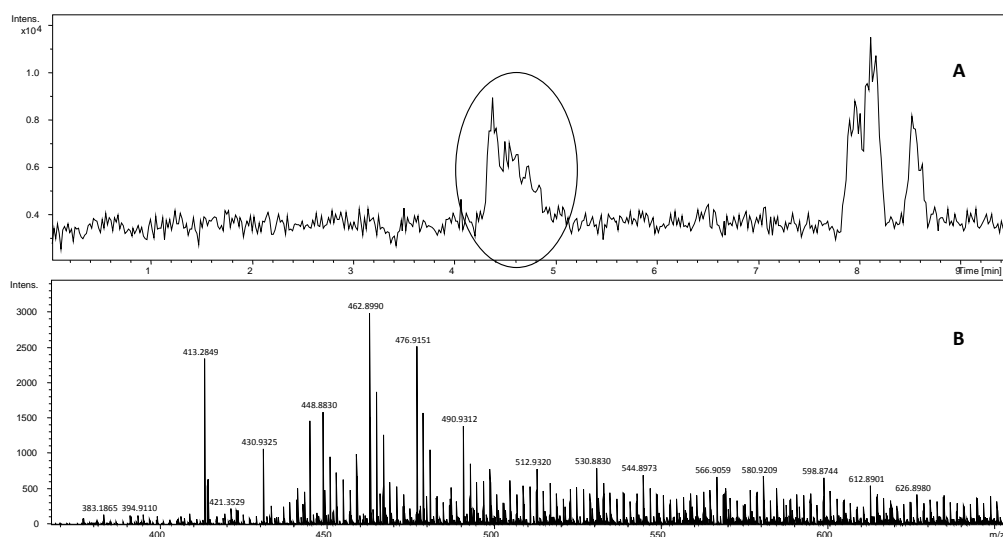


Figure 51 A-B: Separation of the BGE Matrix in the Second Dimension; A: Electropherogram of the Cutting Experiment; B: Mass Spectrum of the Highlighted Signal in A.

In all cutting experiments, an additional signal appeared with a migration time of about 4.5 min in the second dimension with MS detection (Figure 51 A). The mass spectrum (Figure 51 B) confirmed that this signal was generated by acetate and formate clusters.

These clusters were formed by the sodium, contained in the phosphate based BGE, the acetate of the HAc based BGE, and the formate used in the sheath liquid. This proves the successful removal of the non-ESI-MS compatible compounds from the phosphate based BGE in the first dimension, enabling interference-free MS detection of the analytes.

11 Pitfalls and Technical Issues

During the project work, unfortunately, many problems arose, especially regarding the instrumentation and the valve or the valve material respectively. In the following, these issues as well as the solutions or the solution approaches are described in detail.

At first, problems and possible improvements of the instrumentation are discussed like the automation of the 2D system, the spatial arrangement of the single system parts and the capillary lengths, and problems with capillary clogging, followed by a discussion of the valve geometry and the valve material. Here, the various problems which arose with the valve material and, therefore, with the robustness of the valve are shown.

11.1 Automation of the 2D System

As described, starting with the 2D experiments, an external HV power supply was applied for the delivery of the HV in the second dimension. The power supply could be controlled by one of the two relays of the PA 800 *plus* CE instrument. Therefore, the second dimension separation HV could be controlled by the PA 800 *plus* control software and could be included into the CE method list. Nevertheless, switching times often varied and were mostly determined run-by-run by the signal of the additional detection in front of the valve. Hence, separation HV in the second dimension needed to be switched on and off manually in most cases. In later experiments, where the Beckman P/ACE MDQ or the Agilent 7100 CE instrument was used to deliver the separation HV in the second dimension, the potential needed to be controlled manually by the software of the specific instrument anyway.

However, when the analyte reached the sample loop, the first dimension separation HV was stopped and the valve was switched to position B. The analyte was stored inside the loop and only diffusion could influence the second dimension separation. Therefore, short time delays between switching to position B and starting of the second dimension separation HV are uncritical and manual control of the HV power supply is easily possible.

All four detectors used in the 2D system (UV, LIF, C⁴D and MS) could also be triggered by the relays of the Beckman PA 800 *plus* CE instrument. Unfortunately, only two relays were available. For switching time determination the migration time or the migration velocity respectively needed to be precisely determined. Hence, one of the relays was used to control first dimension optical detection (LIF or UV) to enable the simultaneously starting of the data acquisition and the first dimension separation HV.

Plug positioning in the second dimension is a separate step before separation is started in the first dimension. The plugs were mobilized by pressure. Due to problems with capillary clogging (discussed in the following) positioning times varied strongly and the pressure needed to be shut off manually anyway when the calculated position was reached. Therefore, there was hardly any requirement to control the C⁴D automatically.

Because exact migration time determination in the second dimension was not necessary, MS detection was not needed to be triggered by the CE instrument and MS data acquisition was started manually after application of second dimension separation HV. Switching the valve was also carried out manually by the electric valve actuator. Automation of valve switching by a software and a control computer is not possible at present. As described, both HV power supplies were shut off and, hence, separation was stopped while performing switching. Thus, a short time delay existed in every run enabling manual control of the various instruments.

Anyway, a higher degree of automation would probably improve significantly the robustness of the 2D system. Ideally, all instruments could be controlled by only one computer. Further on, triggering of the valve by the signal of the first dimension detector and automatic switching would lead to a much lower effort for single runs.

However, since switching times and especially the time delay between the detection in front of the valve and analytes reaching the sample loop varies from run-to-run it appears to be very difficult to develop a proper control software. Especially at this point it would help a lot to enable detection inside the valve and not in front of the valve in any way which is, unfortunately, hardly possible.

11.2 Capillary Clogging

During the experiments, problems arose with capillary clogging, especially in capillary 1B and 2B. Abrasion of the valve material emerging from the valve-capillary connections, impurities inside the loop or the short-cuts, and the later described black matter which was formed inside the valve during the experiments were plugging the inlets especially of the two mentioned capillaries periodically.

In most cases, the particles inside the capillaries could easily be located by a microscope and removed by cutting the capillary tip. However, particularly in capillary 2B the capillary could not be shortened by cutting the tip for removal of the clogging because it was cut accurate to get the shortest possible capillary length. Therefore, a clogged capillary 2B needed to be exchanged completely leading to higher costs. Future work on the valve material should aim to minimize capillary clogging.

11.3 Valve Damages

During the project work, considerable problems with the valve material occurred. Apparently, the valve material did not show the required wear resistance, especially the material of the stator. Due to particle contamination of the valve, the rotor and the stator were damaged during the switching steps resulting in scratches in between the single channels (Figure 52 A and B). These scratches led to leakages and the valve became unusable.

The valve could be checked for a leakage by voltage measurement in the different dimensions. For this, high voltage was applied to the first dimension. If in the second dimension voltage or current could be detected, leakage was confirmed.

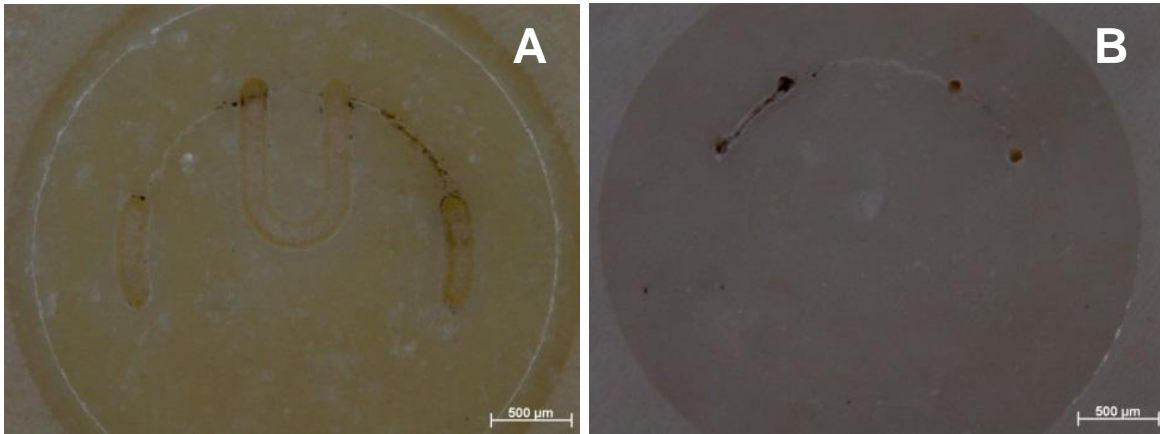


Figure 52 A-B: Damaged Valve; Microscopic Image of A: The Rotor, and B: The Stator.

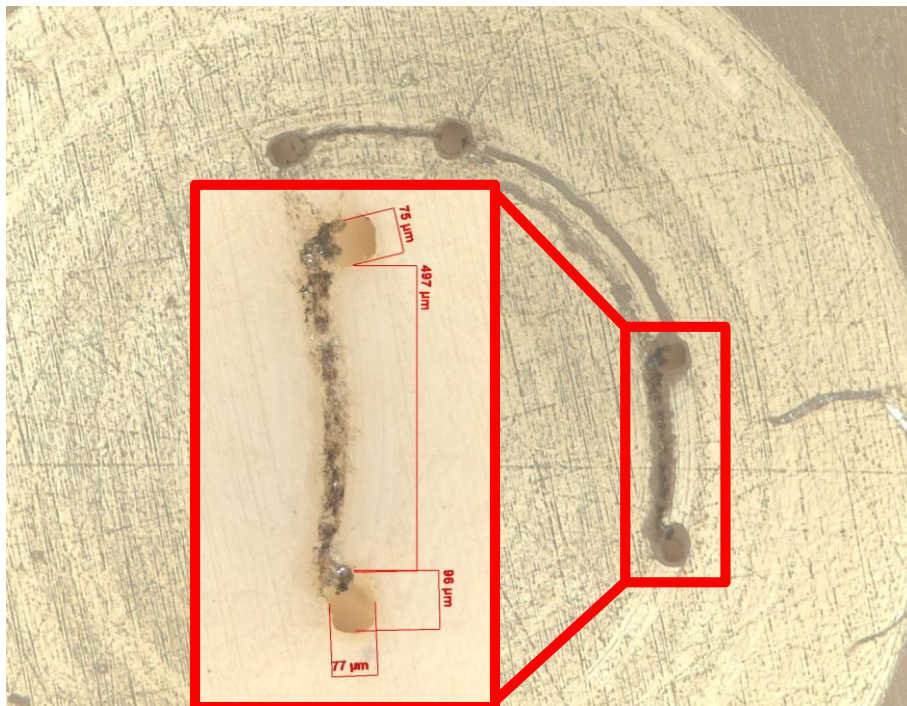


Figure 53: Detailed Microscopic Image of the Damages at the Stator of the Valve.

Figure 53 shows a detailed microscopic image of the described scratches at the stator surface. Obviously, the scratches are too deep to ensure pressure resistance and tightness of the valve. Further, analyte molecules would partly migrate through the additional channels from the one to the other dimension and, therefore, cannot be determined. In addition, these leakages led to massive peak broadening and HV/current fluctuations or even breakdowns.

To have the valve available for further experiments, the damaged stator was polished. Figure 54 A shows a microscopic image of a polished stator which was previously damaged. The polishing procedure was carried out in-house at the faculty of surface engineering.

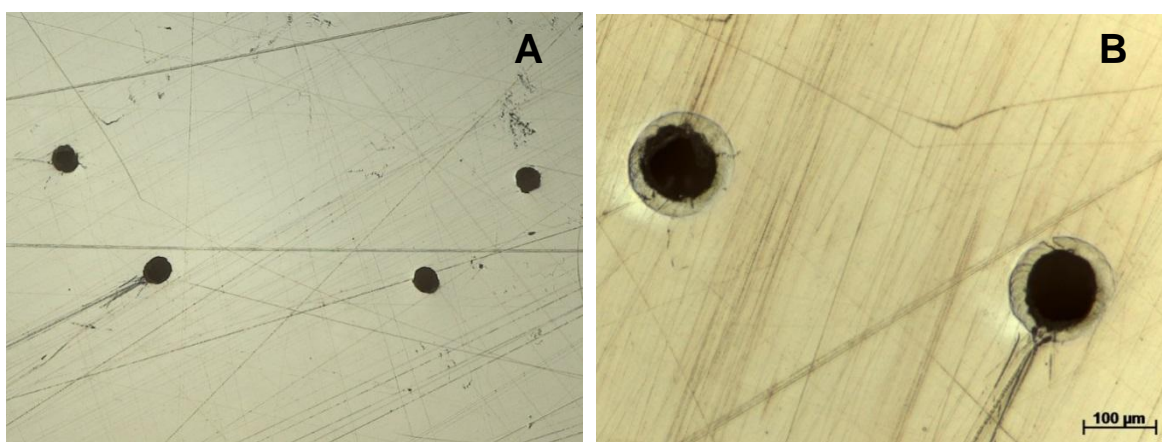


Figure 54 A-B: Processed Stator; A: Stator Polished after Damage; B: Edges of the Stator Connections Rounded by Laser Ablation.

The material removal occurring during the polishing procedure was not specified. Because the angle of the connecting bores is comparable steep, possibly the valve geometries could be changed such that the connections of the stator do no more match with the channels of the rotor. Therefore, the distances between the single connections were measured after polishing, revealing that even after three polishing steps, the valve geometries were not changed significantly. The rotors showed only little damages in comparison to the stators. Therefore, in most cases they could be further used.

Because the rotors were too small, it was not possible to polish them by the available polishing machines. Hence, those rotors that were damaged too much for further use were exchanged by new parts.

To avoid further damage of the valve, different measures were taken. First, potential external pollution of the system (e.g. pollutions of the BGEs/sample solutions, pollution of the CE instrument, and abrasion of the vial caps) was excluded. Therefore, the CE instrument was meticulously cleaned, all solutions were filtered by a syringe filter, and the vial caps were modified. Unfortunately, damages at the valve during the experiments could not be avoided by these measures.

It was further assumed, that the high fields at the edges inside the valve led to thermal degradation of the valve material. The breakdown voltage of the valve material (> 40 kV/mm for PTFE) is in fact high enough to insulate the valve body from the CE HV circuit (rotor thickness: 1.3 mm) but at the edges and in between the channels, flashovers can possibly occur. Degradation of the valve material thereby is due to heat exposure inside the valve and not due to electrochemical modification of the valve material.

In order to minimize degradation of the valve material or formation of particles inside the valve respectively, in further experiments, separation HV was limited to a corresponding current of max. 7 μ A. In addition, the edges at the connection bores of the stator were rounded. First, this was carried out by laser ablation at the Institut für Mikrotechnik Mainz (IMM) (Figure 54 B). In further experimental work, this rounding of the edges was carried out in-house by a fine syringe needle with the help of a microscope.

Limited currents and rounding of the edges minimized significantly the formation of particles but did not prevent it completely. Hence, the stator still needed to be polished periodically. Further on, because the valve parts are very expensive, systematic evaluation of the conditions causing formation of the black matter was not possible. Improving the valve material should be a main objective in future works in order to increase the overall robustness of the system and enabling the application in routine analysis.

12 Concluding Remarks

The presented work describes the complete setup of a novel 2D system for the hyphenation of CE modes and techniques to MS detection which are in principle not accessible for ESI and, therefore, MS detection. The key point of this setup is the usage of a completely electric insulated valve as the interface. The 2D system was set up and characterized in several steps.

For first the valve properties, required for its implementation into the CE HV circuit and for its use as 2D CE interface were discussed. Possessing the required properties, a particular modified 4-port valve was chosen. This valve was completely electrically insulated and had a 20 nL sample loop which was ideally suited for the complete transfer of a defined volume from the first to the second dimension. The design of the valve further enabled the complete spatial separation of the two dimensions which led to almost unlimited selection possibilities for separation method, mode, and technique in the two dimensions.

For conducting 2D separations, an additional detection option in front of or at the interface respectively is very important to enable precise cutting of specific signals. Hence, different available detection options, UV, LIF, and C⁴D were successfully tested on their applicability for additional detection in the 2D system. Throughout the experimental work, mostly UV was applied.

Subsequently, the valve was integrated into the CE HV circuit using a simplified 1D setup. It could be shown that implementation and separation through the valve is possible. Thereby it was revealed, that the implementation of the valve to the CE system leads to a slight peak broadening. Anyhow, this slight peak broadening seemed to be acceptable for most applications.

Still using a 1D system, it was demonstrated, that the valve is capable of cutting, storing, and reintroducing single signals. Thereby, the additional detection option was integrated and used for the determination of precise switching times.

A complete 2D system was set up and 2D CZE-CZE separations were successfully performed. It was shown, that the valve enabled cutting of specific signals from the first and transferring them to the second dimension. Therefore, the 2D system is applicable for its use for the hyphenation of non-ESI compatible CE modes and techniques with MS detection. This was demonstrated on the 2D separation of a BSA tryptic digest sample using a phosphate based, non-ESI compatible, BGE in the first dimension with successful, interference-free MS detection in the second dimension.

Anyhow, issues with the robustness of the valve material arose during the experimental work. Increasing the robustness of the valve and the overall system will be a key topic of future works. Further, a higher degree of automation, e.g. automated switching of the valve based on the detection in the first dimension, of the system would enable even more systematic characterization of the system.

The innovative 2D CE system introduces various new possibilities in CE-MS coupling. Peak identification via MS detection is now possible, using this system, even in (validated) methods and modes which are not MS accessible in principle. The used special 4-port valve enabled the complete transfer of a defined volume without any dilution. The first hyphenation of two CZE modes in a 2D approach using a mechanical valve as interface could be shown. Besides that, due to the complete spatial separation of the two dimensions, the selection of technique, mode, and method for the two separation dimensions is nearly unlimited. Even the application of pressure driven techniques like e.g. CEC or HPLC is possible. This enables further application of the 2D system for the combination of two orthogonal separation techniques in order to reach a very high peak capacity for the separation of complex samples in a classical 2D approach.

Appendix

List of Figures

Figure 1: Schematic Illustration of the Three Different Strategies (A-C) in 2D CE in a Single Capillary [42].	37
Figure 2: Setup of a 2D CIEF-CGE Approach using a Dialysis Interface which is Constructed of: 1) Methacrylate Plate, 2) Separation Capillaries, 3) Teflon Tubes, 4) Hollow Fiber, and 5) Buffer Reservoir [59].	39
Figure 3: Schematic Setup of the Clear Flow Gating Interface [68].	41
Figure 4: Frame-Grabbed Video Images of the Injection Process using the Transparent Flow Gating Interface [68].	42
Figure 5: Schematic Diagram of a CIEF-pCEC 2D System using a Six-Port Valve as the Interface. The Two HV Driven Separation Dimension are Grounded in Front of the Valve or Behind the Valve Respectively [92]. ..	44
Figure 6: Schematic Setup of a CE Instrument.	50
Figure 7: Typical Setup of a DAD.	54
Figure 8 A-B: Comparison of Two-Dimensional Data achieved by an UV Detector with Variable Wavelength at 190 nm (A) and Three-Dimensional Spectral Data achieved by a DAD (B).	54
Figure 9: Schematic Setup of a C ⁴ D.	55
Figure 10: Schematic Illustration of the ESI Process.	58
Figure 11: Illustration of the Agilent Coaxial Triple Tube CE-MS Sheath Liquid Sprayer.	60
Figure 12 A-B: A: Schematic Setup of a 3D-IT consisting of Two Endcaps (blue) and the Ring Electrode (red); B: Saddle Field of a PAUL Trap.	61
Figure 13: Typical Setup of a Reflectron Q-TOF Instrument.	64

- Figure 14: Mass Spectra Obtained by the Usage of Capillaries Filled with four Different CSE Matrix Compounds Dextran, HPC, HPMC, and PEG, each 1 wt % dissolved in 1.5 M FAc. Capillary length: 60 cm; Separation HV: +20 kV; CE Instrument: Agilent 7100; MS Instrument: Bruker micro TOF-Q; Mass Spectra averaged over 1 min.....67
- Figure 15: Separation of a RNase B Sample using a 50 % CSE BGE Filled Capillary, UV Detection at 200 nm, CSE BGE: 1.5 % w/w HPC MW 100,000 in 1.5 M FAc, Volatile BGE: 1.5 M FAc; Sample: 1 µg/L RNase B; CE Instrument: Agilent G7100A; Capillary Length: 60 cm Total Length, 52 cm Effective Length.68
- Figure 16: Valve, Equipped with Detection Cell, Cell Housing, and Cell Mount.75
- Figure 17: Individual Parts of the used 4-Port Microinjector Valve.87
- Figure 18 A-C: Different Valves which were used During the Experiments. ...88
- Figure 19 A-C: Connections of the Stator; A: Photography of the Stator Connections; B: Schematic Cross Section of the Stator Connection Geometry; C: Microscopic Picture of the Stator Connection Through Hole.89
- Figure 20: Rotor; Left: Photographic Picture of the Rotor; Right: Schematic Geometrys of the Sample Loop and the Two Short-Cuts.....90
- Figure 21: Profile of the Sample Loop Channel; Depth: Left: 180 µm, Right: 80 µm.90
- Figure 22: Switching Scheme of the Valve; Position A: Load Position; Position B: Inject Position [139].....91
- Figure 23: Electropherograms and Illustration of the Noise Level of Three Separations of Lysozyme and Myoglobin at a Concentration of 0.30 µg/µL (Blue), 0.06 µg/µL (Green), and 0.03 µg/µL (Gray) Detected with the CCD Detector at 200 nm. CE Instrument: Agilent 7100; Capillary Total Length: 60.0 cm, Effective Length with Respect to the External Detector: 24.0 cm.95
- Figure 24: CE-LIF Electropherograms of Analysis of Phenylalanine (Grey), Tyrosine (Green), and Tryptophan (Blue) at a Concentration of 0.5 µg/µL

- Each; Excitation Wavelength: 266 nm; CE Instrument: Agilent 7100; Capillary Total Length: 60.0 cm, Effective Length with Respect to the External Detector: 24.0 cm..... 95
- Figure 25: CE-LIF Electropherograms of Analysis of Cytochrome C (Green), and Myoglobine (Blue) at a Concentration of 0.5 $\mu\text{g}/\mu\text{L}$ Each; Excitation Wavelength: 266 nm; CE Instrument: Agilent 7100; LN Coated Capillary; Capillary Total Length 80.5 cm, Effective Length 44.0 cm; Electrokinetic Injection: 10 s at 7 kV. 96
- Figure 26: Schematic Setup of the 1D System with UV Detection.....100
- Figure 27: Comparison of the Separation of Glu-Fib and Leu-Enk at a Concentration of 0.05 $\mu\text{g}/\mu\text{L}$ each, using the System with the Integrated Valve (Green Electropherogram) and a System Equipped with a Continuous Capillary (Blue Electropherogram); UV Detection at 210 nm; CE Instrument: Agilent 7100; Capillary lengths: Capillary 1A: 23.5 cm; Capillary 1B: 37.5 cm; Continuous Capillary: 61.0 cm; BGE: 0.2 M FAC; Hydrodynamic Injection 6 s at 100 mbar; Separation HV: +25 kV.101
- Figure 28: Schematic Setup of the 1D System with ESI-MS Detection.102
- Figure 29 A-B: Comparison of the Separation of a BSA Tryptic Digest Sample (5 μM) using the System with the Integrated Valve (A) and a System Equipped with a Continuous Capillary (B) with ESI-MS Detection. EIEs of the Single Tryptic Peptides (m/z Ratios are Listed in Table 5); CE Instrument: Beckman PA 800 plus; ESI-MS Instrument: Bruker Compact Q-TOF; Capillary lengths: Capillary 1A: 23.5 cm, Capillary 1B 37.5 cm, Continuous Capillary: 62.0 cm; BGE: 10 % v/v Aqueous HAC; Hydrodynamic Injection 10 s at 100 mbar; Separation Current: 7 μA ; Resulting HV: ~ 15 kV [138].....103
- Figure 30: Schematic Setup of the 1D System with UV Detection.....104
- Figure 31: Switching Scheme for Cutting and Reintroducing of the Glu-Fib Signal from a Glu-Fib / Leu-Enk Sample (0.05 $\mu\text{g}/\mu\text{L}$ each); CE Instrument: Agilent 7100; UV Detection at 210 nm; Capillary Lengths: Capillary 1A: 23.5 cm, Capillary 1B: 37.5 cm; BGE: 0.2 M FAC; Hydrodynamic Injection 6 s at 100 mbar; Separation HV: +25 kV.105

Figure 32: Schematic Setup of the 1D System with UV Detection and Additional UV Detection in Front of the Valve.	107
Figure 33: Agilent 7100 CE Instrument Equipped with the Modified Cover Enabling the Installation of the Valve and the Additional UV Detection Inside the CE Instrument.	108
Figure 34: UV Detection in Front of the Valve; Separation of Glu-Fib and Leu-Enk (0.05 $\mu\text{g}/\mu\text{L}$ each); CE Instrument: Agilent 7100; UV Detection at 200 nm; Capillary length: Capillary 1A: 23.5 cm, Capillary 1B: 37.5 cm; Effective Length: 20.9 cm; Detection Cell 2.6 cm in Front of the Valve; BGE: 0.2 M FAc; Hydrodynamic Injection 6 s at 100 mbar; Separation HV: +25 kV.	109
Figure 35: Cutting and Reintroducing of the Single Signals of a Glu-Fib and Leu-Enk Sample (0.05 $\mu\text{g}/\mu\text{L}$ each) after Switching Time Determination by Additional UV Detection; Red: Reference Analysis without Switching the Valve; Blue: Cutting of the Glu-Fib Signal and Reintroducing after 4 min; Green: Cutting of the Leu-Enk Signal and Reintroducing after 4 min; CE Instrument: Agilent 7100; UV Detection at 200 nm; Capillary length: Capillary 1A: 23.5 cm, Capillary 1B: 37.5cm; BGE: 0.2 M FAc; Hydrodynamic Injection 6 s at 100 mbar; Separation HV: +25 kV.	110
Figure 36: Schematic Setup of the 1D System with MS Detection and Additional C^4D in front of the Valve.	111
Figure 37: Calculated Cutting Positions in the Negative C^4D Signal for the 7 Positioning Experiments.	112
Figure 38: EIE (m/z: 159.111) of the 7 Positioning Experiments; Separation of 1000 ppm Caffeine in MeOH; CE Instrument: Beckman PA 800 plus; Capillary Lengths: Capillary 1A: 47.0 cm; Capillary 1B: 41.0 cm; Effective Length with Respect to the C^4D : 43.0; Detection in Capillary 1A, 4 cm in Front of the Valve: C^4D ; MS Detection in the End of Capillary 1B; MS Instrument: Bruker Compact Q-TOF.	112
Figure 39: Positioning Experiment, Ratio of the Peak Area of the Cut Portion to the Peak Area of the Remained Portion Plotted Against the Cutting Position.	113

- Figure 40: Schematic Setup of the Complete 2D System used during the Experimental Work.115
- Figure 41: Photographic Picture of the 2D Setup.....117
- Figure 42: Detailed Photography of the Arrangement of the Different Connections and Detection Options in the 2D CE System.....117
- Figure 43 A-B: Comparison of the two 2D Setups using A: The Beckman PA 800 plus for Both Dimension in Combination with the HV Power Supply of the Beckman P/ACE MDQ Instrument, and B: using the Beckman PA 800 plus only for the First and the Agilent G1600AX 3D for the Second Dimension.118
- Figure 44: Scheme of the Spatial Instrument Arrangement in the 2D System with Respect to the Capillary Lengths.....119
- Figure 45: Schematic Setup of the 2D System with MS Detection and Additional UV Detection in front of the Valve [139].122
- Figure 46: Transfer Experiments; EIEs, Top: Reference Experiment using only the Second Dimension; Middle: First 2D Experiment, Transfer of the Blue Signal (m/z : 480.60); Switching Time: 4.5 min; Bottom: Second 2D Experiment, Transfer of the Green (m/z : 488.52) and Turquoise (m/z : 379.71) Signal; Switching Time: 5.1 min; Sample: 5 μ M BSA Tryptic Digest; CE Instrument: PA 800 plus; Separation HV Delivery in the Second Dimension: External HV Power Supply; Capillary Lengths: Capillary 1A: 38.0 cm, Capillary 1B: 53.0 cm, Capillary 2A: 40.0 cm, Capillary 2B: 55.0 cm; Effective Length with Respect to the UV Detection in Capillary 1A: 34.0 cm; UV Detection 4.0 cm in front of the Valve in Capillary 1A; MS Detection in the Outlet of Capillary 2B: Bruker Esquire 6000 3D IT; BGE: 10 % Aqueous HAc; Hydrodynamic Injection: 10 s at 100 mbar; Separation HV in Both Dimensions: + 30 kV [139].....123
- Figure 47: Multiple Switching in a Single Electrophoretic Run; Three Different Switching Positions A (16.0 min - 17.8 min) Green Signal m/z : 417.20, B (25.2 min - 28.0 min) Red Signal m/z : 473.88, C (27.5 min - 31.0 min) Blue Signal m/z : 547.32 and Purple Signal m/z : 627.91; Sample: 5 μ M BSA Tryptic Digest; CE Instrument: PA 800 plus; Separation HV Delivery in the Second Dimension: External HV Power Supply; Capillary Lengths:

Capillary 1A: 38.0 cm, Capillary 1B: 53.0 cm, Capillary 2A: 40.0 cm, Capillary 2B: 55.0 cm; Effective Length with Respect to the UV Detection in Capillary 1A: 34.0 cm; UV Detection 4.0 cm in front of the Valve in Capillary 1A; MS Detection in the Outlet of Capillary 2B: Bruker Esquire 6000 3D IT; BGE: 10 % Aqueous HAc; Hydrodynamic Injection: 10 s at 100 mbar; Separation HV First Dimension: + 17 kV at 7.1 – 7.9 μ A; Separation Current Second Dimension: 7.0 μ A at + 15.4 kV..... 125

Figure 48: Separation of a Mixture of Lysozyme (200 ppm), β -Lactoglobulin (400 ppm), RNase A (400 ppm), Myoglobin (400 ppm), and RNase B (1000 ppm) using PVA Coated Capillaries; EIEs; Top: Reference Experiment using only the Second Dimension; Bottom: 2D Separation, Transfer of the Lysozyme Signal, Switching Time: 23.5 min; CE Instrument: Beckman PA 800 plus; Separation HV Delivery in the Second Dimension by the External HV Power Supply; Capillary Lengths: Capillary 1A: 40.0 cm, Capillary 1B: 72.5 cm, Capillary 2A: 69.5 cm, Capillary 2B: 40.0 cm; Effective Length of Capillary 1A with Respect to UV Detection: 36.0 cm; UV Detection in Capillary 1A 4.0 cm in Front of the Valve; MS Detection in the Outlet of Capillary 2B; MS Instrument: Bruker micro TOF-Q; Hydrodynamic Injection 20 s at 100 mbar; Separation HV First Dimension: + 19 kV at 6.6-6.8 μ A; Separation Current Second Dimension: 7.0 μ A at + 18.0 kV..... 126

Figure 49: Comparison of the Selectivity using Different BGEs: 10 % v/v HAc (Blue Electropherogram) and 10 mM Phosphoric Acid at pH 2.5 (Red Electropherogram); Separation of a BSA Tryptic Digest Sample (5 μ M) using CE-UV; CE Instrument: Beckman PA 800 plus; Capillary Lengths: Capillary 1A: 38.2 cm, Capillary 1B: 52.8 cm, Capillary 2A: 55.1 cm; Capillary 2B: 40.2 cm; Hydrodynamic Injection: 10 s at 200 mbar; Separation HV: +20 kV..... 128

Figure 50 A-C: 2D Separation of 5 μ M Tryptic BSA Digest using Phosphate BGE in the First and HAc BGE in the Second Dimension; A: Reference Experiment using only the Second Dimension; B: 2D Experiment, Cutting at 7.2 min (m/z: 526.25, 547.32, 627.97, 464.23); C: 2D Experiment Cutting at 6.0 min (m/z: 507.80, 536.75, 571.84); the Cut Signals of the Two 2D Experiments are Highlighted in the Reference Experiment; CE

Instrument: Beckman PA 800 plus; MS Detection in the Outlet of Capillary 2B: Bruker Compact Q-TOF; Capillary Lengths: Capillary 1A: 38.2 cm, Capillary 1B: 52.8 cm, Capillary 2A: 55.1 cm; Capillary 2B: 40.2 cm; External UV Detection 4.0 cm in Front of the Valve; Effective Capillary Length with Respect to the External UV Detector: 34.2 cm; BGEs: 10 mM Phosphoric Acid at pH 2.5 in the First Dimension, 10 % HAc v/v in the Second Dimension; Hydrodynamic Injection: 10 s at 200 mbar; Separation HV: +20 kV at a Corresponding Current of about 7 μ A; HV Delivery by the External HV Power Supply in the First Dimension.129

Figure 51 A-B: Separation of the BGE Matrix in the Second Dimension; A: Electropherogram of the Cutting Experiment; B: Mass Spectrum of the Highlighted Signal in A.130

Figure 52 A-B: Damaged Valve; Microscopic Image of A: The Rotor, and B: The Stator.134

Figure 53: Detailed Microscopic Image of the Damages at the Stator of the Valve.134

Figure 54 A-B: Processed Stator; A: Stator Polished after Damage; B: Edges of the Stator Connections Rounded by Laser Ablation.135

List of Tables

Table 1: Different Interfaces, Advantages and Disadvantages.	39
Table 2: Detection Techniques in CE.	53
Table 3: Comparison of the Electrophoretic Resolution Achieved by the Separation of a RNase B Sample with a System using a Completely and a Partially Filled Capillary. BGE: 1.5% w/w HPC MW 100.000 in 1.5 M FAc, Sample: 1 $\mu\text{g}/\mu\text{L}$ RNase B; CE Instrument: Agilent 7100; Capillary Length: 60 cm Total Length, 52 cm Effective Length.	69
Table 4: Different BGEs which were used During the Experiments.....	78
Table 5: m/z Ratios used for the Creation of EIEs in the Peptide Analysis Experiments.	80
Table 6: m/z Ratios used for the Creation of EIEs in the Protein Analysis Experiments.	80
Table 7: Comparison Signal Height [mAU] and S/N Achieved by the Internal DAD of the Agilent 7100 CE Instrument and the J&M CCD Detector; Detection at 200 nm; Samples: Lysozyme and Myoglobin at Three Different Concentration Levels (0.03, 0.06, and 0.03 $\mu\text{g}/\mu\text{L}$ Each); CE Instrument: Agilent 7100; Capillary Total Length: 60.0 cm, Effective Length with Respect to the External Detector: 24.0 cm; Effective Length with Respect to the Internal Detector: 51.5 cm.	94
Table 8: Comparison of the Peak Area and the Area-to-Noise Ratio Obtained by the Internal DAD and the Additional C ⁴ D Analyzing Cytochrome C, Myoglobine, Tryptophan, Tyrosine, and Phenylalanine at a Concentration of 0.5 $\mu\text{g}/\mu\text{L}$ Each; CE Instrument: Agilent 7100; LN Coated Capillary; Total Length: 80.0 cm, Effective Length with Respect to the C ⁴ D: 70.0	

cm, Effective Length with Respect to the UV Detector: 72.0 cm;
Electrokinetic injection: 10 s at 7 kV; Separation HV: +30 kV.....97

Bibliography

- [1] Kohl, F. J., Sánchez-Hernández, L., Neusüß, C., *Electrophoresis* 2015, *36*, 144-158.
- [2] Stoll, D. R., Li, X., Wang, X., Carr, P. W., Porter, S. E. G., Rutan, S. C., *J. Chromatogr., A* 2007, *1168*, 3-43.
- [3] Jandera, P., *cent.eur.j.chem.* 2012, *10*, 844-875.
- [4] Wang, Y., Chen, Q., Norwood, D. L., McCaffrey, J., *Journal of Liquid Chromatography and Related Technologies* 2010, *33*, 1082-1115.
- [5] Tscherch, K., Biller, J., Lehmann, M., Trusch, M., Rohn, S., *Phytochem. Anal.* 2013, *24*, 436-445.
- [6] Giddings, J. C., *Anal. Chem.* 1984, *56*, 1258A-1270A.
- [7] Gao, D., Liu, H., Jiang, Y., Lin, J.-M., *Lab Chip* 2013, *13*, 3309-3322.
- [8] Tia, S., Herr, A. E., *Lab Chip* 2009, *9*, 2524-2536.
- [9] Kašička, V., *Electrophoresis* 2014, *35*, 69-95.
- [10] Guihen, E., *Electrophoresis* 2014, *35*, 138-146.
- [11] Evans, C. R., Jorgenson, J. W., *Anal. Bioanal. Chem.* 2004, *378*, 1952-1961.
- [12] Stroink, T., Ortiz, M. C., Bult, A., Lingeman, H., de Jong, G. J., Underberg, W. J. M., *Journal of Chromatography B* 2005, *817*, 49-66.
- [13] Xu, X., Liu, K., Fan, Z. H., *Expert Review of Proteomics* 2012, *9*, 135-147.
- [14] Kler, P., Sydes, D., Huhn, C., *Anal. Bioanal. Chem.* 2015, *407*, 119-138.

- [15] Valcárcel, M., Arce, L., Ríos, A., *Journal of Chromatography A* 2001, 924, 3-30.
- [16] Mikuš, P., Marákova, K. n., in: Fazel, P. R. (Ed.), *Biomedical Engineering - From Theory to Applications*, InTech, Rijeka, Croatia 2011.
- [17] Issaq, H. J., Chan, K. C., Janini, G. M., Muschik, G. M., *Electrophoresis* 1999, 20, 1533-1537.
- [18] He, Y., Yeung, E. S., Chan, K. C., Issaq, H. J., *Journal of Chromatography A* 2002, 979, 81-89.
- [19] Issaq, H. J., Chan, K. C., Liu, C., Li, Q., *Electrophoresis* 2001, 22, 1133-1135.
- [20] Garcia-Villalba, R., Carrasco-Pancorbo, A., Vazquez-Martin, A., Oliveras-Ferraros, C., Menendez, J. A., Seguera-Carretero, A., Fernandez-Gutierrez, A., *Electrophoresis* 2009, 30, 2688-2701.
- [21] Janini, G. M., Chan, K. C., Conrads, T. P., Isaaq, H. J., Veenstra, T. D., *Electrophoresis* 2004, 25, 1973-1980.
- [22] Cesla, P., Fischer, J., Jandera, P., *Electrophoresis* 2010, 31, 2200-2210.
- [23] Eckhardt, A., Mikšík, I., Charvátová, J., Deyl, Z., Forgács, E., Cserhádi, T., *J. Liq. Chromatogr. Relat. Technol.* 2005, 28, 1437-1451.
- [24] Mikulíková, K., Eckhardt, A., Mikšík, I., *J. Sep. Sci.* 2006, 29, 1126-1131.
- [25] Strausbauch, M. A., Madden, B. J., Wettstein, P. J., Landers, J. P., *Electrophoresis* 1995, 16, 541-548.
- [26] Jaworska, M., Klaczkow, G., Wilk, M. A., E., *Acta Poloniae Pharmaceutica* 2012, 69, 799-808.
- [27] Voelter, W., Schütz, J., Tsitsiloni, O. E., Weiler, A., Grübler, G., Paulus, G., Stoeva, S., Lehmann, R., *Journal of Chromatography A* 1998, 807, 135-149.
- [28] Zhu, K., Kim, J., Yoo, C., Miller, F. R., Lubman, D. M., *Anal. Chem.* 2003, 75, 6209-6217.

- [29] Sanz-Nebot, V., Benavente, F., Barbosa, J., *Journal of Chromatography A* 2002, 950, 99-111.
- [30] Udiavar, S., Apffel, A., Chakel, J., Swedberg, S., Hancock, W. S., Pungor, E., *Anal. Chem.* 1998, 70, 3572-3578.
- [31] Escoubas, P., Whiteley, B. J., Kristensen, C. P., Célérier, M.-L., Corzo, G., Nakajima, T., *Rapid Commun. Mass Spectrom.* 1998, 12, 1075-1084.
- [32] Jia, L., Liu, B.-F., Terabe, S., Nishioka, T., *Anal. Chem.* 2004, 76, 1419-1428.
- [33] Jia, L., Tanaka, N., Terabe, S., *Electrophoresis* 2005, 26, 3468-3478.
- [34] Mao, Y., Zhang, X., *Electrophoresis* 2003, 24, 3289-3295.
- [35] Yu, W., Li, Y., Deng, C., Zhang, X., *Electrophoresis* 2006, 27, 2100-2110.
- [36] Mao, Y., Li, Y., Zhang, X., *Proteomics* 2006, 6, 420-426.
- [37] Shen, Y., Berger, S. J., Smith, R. D., *Journal of Chromatography A* 2001, 914, 257-264.
- [38] Wall, D. B., Kachman, M. T., Gong, S., Hinderer, R., Parus, S., Misek, D. E., Hanash, S. M., Lubman, D. M., *Anal. Chem.* 2000, 72, 1099-1111.
- [39] Gao, H., Shen, Y., Veenstra, T. D., Harkewicz, R., Anderson, G. A., Bruce, J. E., Pasa-Tolic, L., Smith, R. D., *J. Microcolumn Separations* 2000, 12, 383-390.
- [40] Fang, X., Yang, L., Wang, W., Song, T., Lee, C. S., DeVoe, D. L., Balgley, B. M., *Anal. Chem.* 2007, 79, 5785-5792.
- [41] Santos, B., Simonet, B. M., Rios, A., Valcarcel, M., *Electrophoresis* 2007, 28, 1345-1351.
- [42] Cottet, H., Biron, J. P., Taillades, J., *Journal of Chromatography A* 2004, 1051, 25-32.
- [43] Cottet, H., Biron, J. P., *Macromol. Chem. Phys.* 2005, 206, 628-634.
- [44] Anouti, S., Vandenabeele-Trambouze, O., Koval, D., Cottet, H., *Anal. Chem.* 2008, 80, 1730-1736.

- [45] Kukusamude, C., Srijaranai, S., Quirino, J. P., *Anal. Chem.* 2014, 86, 3159-3166.
- [46] Anouti, S., Vandenabeele-Trambouze, O., Koval, D., Cottet, H., *Electrophoresis* 2009, 30, 2-10.
- [47] Anouti, S., Vandenabeele-Trambouze, O., Cottet, H., *Electrophoresis* 2010, 31, 1029-1035.
- [48] Zhang, X., Zhang, Z., *Journal of Chromatography B* 2011, 879, 1641-1646.
- [49] Zhang, Z., Du, X., Li, X., *Anal. Chem.* 2011, 83, 1291-1299.
- [50] Tong, W., Link, A., Eng, J. K., Yates, J. R., *Anal. Chem.* 1999, 71, 2270-2278.
- [51] Lee, W.-H., Wang, C.-W., Her, G.-R., *Rapid Commun. Mass Spectrom.* 2011, 25, 2124-2130.
- [52] Ramautar, R., de Jong, G. J., Somsen, G. W., *Electrophoresis* 2012, 33, 243-250.
- [53] Ramautar, R., Somsen, G. W., de Jong, G. J., *Electrophoresis* 2010, 31, 44-54.
- [54] Puig, P., Borrull, F., Calull, M., Aguilar, C., *TrAC Trends in Analytical Chemistry* 2007, 26, 664-678.
- [55] Mohan, D., Pasa-Tolic, L., Masselon, C. D., Tolic, N., Bogdanov, B., Hixson, K. K., Smith, R. D., Lee, C. S., *Anal. Chem.* 2003, 75, 4432-4440.
- [56] Zhou, F., Johnston, M. V., *Anal. Chem.* 2004, 76, 2734-2740.
- [57] Yang, C., Liu, H., Yang, Q., Zhang, L., Zhang, W., Zhang, Y., *Anal. Chem.* 2003, 215-218.
- [58] Mohan, D., Lee, C. S., *Electrophoresis* 2002, 23, 3160-3167.
- [59] Liu, H., Yang, C., Yang, Q., Zhang, W., Zhang, Y., *Journal of Chromatography B* 2005, 817, 119-126.
- [60] Liu, H., Zhang, L., Zhu, G., Zhang, W., Zhang, Y., *Anal. Chem.* 2004, 76, 6506-6512.

- [61] Wang, T., Ma, J., Wu, S., Sun, L., Yuan, H., Zhang, L., Liang, Z., Zhang, Y., *Journal of Chromatography B* 2011, 879, 804-810.
- [62] Zhang, Z.-X., Zhang, M.-Z., Zhang, S.-S., *Electrophoresis* 2009, 30, 1958-1966.
- [63] Kler, P. A., Posch, T. N., Pattky, M., Tiggelaar, R. M., Huhn, C., *Journal of Chromatography A* 2013, 1297, 204-212.
- [64] Zhang, Z. X., Zhang, X. W., Li, F., *Science China* 2010, 53, 1183-1189.
- [65] Zhang, J., Hu, H., Gao, M., Yang, P., Zhang, X., *Electrophoresis* 2004, 25, 2374-2383.
- [66] Lemmo, A. V., Jorgenson, J. W., *Anal. Chem.* 1993, 65, 1576-1581.
- [67] Moore, A. W., Jorgenson, J. W., *Anal. Chem.* 1995, 67, 3448-3455.
- [68] Hooker, T. F., Jorgenson, J. W., *Anal. Chem.* 1997, 69, 4134-4142.
- [69] Bergström, S. K., Dahlin, A. P., Ramström, M., Andersson, M., Markides, K. E., Bergquist, J., *Analyst* 2006, 131, 791-798.
- [70] Cabaleiro, O., Lores, M., Cela, R., *Analisis* 1999, 27, 468-471.
- [71] Zhang, X., Hu, H.-l., Xu, S., Yang, X., Zhang, J., *Journal Separation Science* 2001, 24, 385-391.
- [72] Michels, D. A., Hu, S., Dambrowitz, K. A., Eggertson, M. J., Lauterbach, K., Dovichi, N. J., *Electrophoresis* 2004, 25, 3098-3105.
- [73] Hu, S., Michels, D. A., Fazal, M. A., Ratisoontorn, C., Cunningham, M. L., Dovichi, N. J., *Anal. Chem.* 2004, 76, 4044-4049.
- [74] Kraly, J. R., Jones, M. R., Gomez, D. G., Dickerson, J. A., Harwood, M. M., Eggertson, M., Paulson, T. G., Sanchez, C. A., Odze, R., Feng, Z., Reid, B. J., Dovichi, N. J., *Anal. Chem.* 2006, 78, 5977-5986.
- [75] Gonzalez-Gomez, D., Cohen, D., Dickerson, J. A., Chen, X., Cañada-Cañada, F., Dovichi, N. J., *Talanta* 2009, 78, 193-198.
- [76] Chen, X., Fazal, M. A., Dovichi, N. J., *Talanta* 2007, 71, 1981-1985.

- [77] Fazal, M. A., Palmer, V. R., Dovichi, N. J., *Journal of Chromatography A* 2006, *1130*, 182-189.
- [78] Harwood, M. M., Christians, E. S., Fazal, M. A., Dovichi, N. J., *Journal of Chromatography A* 2006, *1130*, 190-194.
- [79] Harwood, M. M., Bleecker, J. V., Rabinovitch, P. S., Dovichi, N. J., *Electrophoresis* 2007, *28*, 932-937.
- [80] Michels, D. A., Hu, S., Schoenherr, R. M., Eggertson, M. J., Dovichi, N. J., *Mol. Cell. Proteomics* 2002, *1*, 69-74.
- [81] Dickerson, J. A., Ramsay, L. M., Dada, O. O., Cermak, N., Dovichi, N. J., *Electrophoresis* 2010, *31*, 2650-2654.
- [82] Bergström, S. K., Samskog, J., Markides, K. E., *Anal. Chem.* 2003, *75*, 5461-5467.
- [83] Lewis, K., Opiteck, G., Jorgenson, J., Sheeley, D., *J. Am. Soc. Mass Spectrom.* 1997, *8*, 495-500.
- [84] Schoenherr, R. M., Ye, M., Vannatta, M., Dovichi, N. J., *Anal. Chem.* 2007, *79*, 2230-2238.
- [85] Li, Y., Wojcik, R., Dovichi, N. J., *Journal of Chromatography A* 2011, *1218*, 2007-2011.
- [86] Flaherty, R. J., Hugel, B. J., Bruce, S. M., Dada, O. O., Dovichi, N. J., *Analyst* 2013, *138*, 3621-3625.
- [87] Bushey, M. M., Jorgenson, J. W., *Anal. Chem.* 1990, *62*, 978-984.
- [88] Li, Y., Fang, X., Zhao, S., Zhai, T., Sun, X., Bao, J. J., *Chem. Lett.* 2010, *39*, 983-985.
- [89] Lemmo, A. V., Jorgenson, J. W., *J. Chromatogr.* 1993, *633*, 213-220.
- [90] Chen, J., Balgley, B. M., DeVoe, D. L., Lee, C. S., *Anal. Chem.* 2003, *75*, 3145-3152.
- [91] Wang, Y., Rudnick, P. A., Evans, E. L., Li, J., Zhuang, Z., DeVoe, D. L., Lee, C. S., Balgley, B. M., *Anal. Chem.* 2005, *77*, 6549-6556.

- [92] Wei, J., Gu, X., Wang, Y., Wu, Y., Yan, C., *Electrophoresis* 2011, 230-237.
- [93] Zhang, M., El Rassi, Z., *J. Proteome Res.* 2006, 5, 2001-2008.
- [94] Wu, Y., Wang, Y., Gu, X., Zhang, L., Yan, C., *Journal Separation Science* 2011, 34, 1027-1034.
- [95] Stroink, T., Schravendijk, P., Wiese, G., Teeuwsen, J., Lingeman, H., Waterval, J. C. M., Bult, A., de Jong, G. J., Underberg, W. J. M., *Electrophoresis* 2003, 24, 1126-1134.
- [96] Stroink, T., Wiese, G., Teeuwsen, J., Lingeman, H., Waterval, J. C. M., Bult, A., de Jong, G. J., Underberg, W. J. M., *Electrophoresis* 2003, 24, 897-903.
- [97] Kuhn, R., Hoffstetter-Kuhn, S., *Capillary Electrophoresis: Principles and Practice*, Springer Verlag 1993.
- [98] Altria, K. D. (Ed.), *Capillary Electrophoresis Guidebook: Principles, Operation, and Applications*, Humana Press Inc., Totowa, New Jersey 1996.
- [99] Jorgenson, J. W., Lukacs, K. D., *Anal. Chem.* 1981, 53, 1298-1302.
- [100] Escuder-Gilabert, L., Martín-Biosca, Y., Medina-Hernández, M. J., Sagrado, S., *Journal of Chromatography A* 2014, 1357, 2-23.
- [101] Gübitz, G., Schmid, M. G., *Journal of Chromatography A* 1997, 792, 179-225.
- [102] Huang, Y.-F., Huang, C.-C., Hu, C.-C., Chang, H.-T., *Electrophoresis* 2006, 27, 3503-3522.
- [103] Dolník, V., Gurske, W. A., *Electrophoresis* 1999, 20, 3373-3380.
- [104] Karim, M. R., Janson, J.-C., Takagi, T., *Electrophoresis* 1994, 15, 1531-1534.
- [105] Gomis, D. B., Junco, S., Expósito, Y., Gutiérrez, D., *Electrophoresis* 2003, 24, 1391-1396.
- [106] Hu, S., Zhang, L., Cook, L. M., Dovichi, N. J., *Electrophoresis* 2001, 22, 3677-3682.

- [107] Gennes, P.-G. d., *Scaling Concepts in Polymer Physics*, Cornell University Press 1979.
- [108] Simpson Jr, S. L., Quirino, J. P., Terabe, S., *Journal of Chromatography A* 2008, *1184*, 504-541.
- [109] Zemann, A. J., *Electrophoresis* 2003, *24*, 2125-2137.
- [110] Zemann, A. J., Schnell, E., Volgger, D., Bonn, G. K., *Anal. Chem.* 1998, *70*, 563-567.
- [111] Sparkmann, D. O., Watson, T. J., *Introduction to Mass Spectrometry*, Wiley & Sons 2007.
- [112] Schmitt-Kopplin, P., Frommberger, M., *Electrophoresis* 2003, *24*, 3837-3867.
- [113] Wilm, M., *Mol. Cell. Proteomics* 2011, *10*.
- [114] Iribarne, J. V., Thomson, B. A., *The Journal of Chemical Physics* 1976, *64*, 2287-2294.
- [115] Fenn, J., Mann, M., Meng, C., Wong, S., Whitehouse, C., *Science* 1989, *246*, 64-71.
- [116] Zamfir, A. D., *Journal of Chromatography A* 2007, *1159*, 2-13.
- [117] Whitt, J. T., Moini, M., *Anal. Chem.* 2003, *75*, 2188-2191.
- [118] Tomer, K. B., *Chem. Rev. (Washington, DC, U. S.)* 2001, *101*, 297-328.
- [119] Schmitt-Kopplin, P., Englmann, M., *Electrophoresis* 2005, *26*, 1209-1220.
- [120] Smith, R. D., Olivares, J. A., Nguyen, N. T., Udseth, H. R., *Anal. Chem.* 1988, *60*, 436-441.
- [121] Pioch, M., Bunz, S.-C., Neusüß, C., *Electrophoresis* 2012, *33*, 1517-1530.
- [122] Zhao, S. S., Zhong, X., Tie, C., Chen, D. D. Y., *Proteomics* 2012, *12*, 2991-3012.

- [123] Hopfgartner, G., Varesio, E., Tschäppät, V., Grivet, C., Bourgoigne, E., Leuthold, L. A., *J. Mass Spectrom.* 2004, 39, 845-855.
- [124] Paul, W., *Reviews of Modern Physics* 1990, 62, 531-540.
- [125] de Hoffmann, E., Stroobant, V., *Mass Spectrometry - Principles and Applications*, John Wiley & Sons Ltd 2007.
- [126] Guilhaus, M., *J. Mass Spectrom.* 1995, 30, 1519-1532.
- [127] Russell, D. H., Edmondson, R. D., *J. Mass Spectrom.* 1997, 32, 263-276.
- [128] Landers, J. P., *Handbook of Capillary Electrophoresis, Second Edition*, CRC Press 1996.
- [129] Haselberg, R., Ratnayake, C. K., de Jong, G. J., Somsen, G. W., *Journal of Chromatography A* 2010, 1217, 7605-7611.
- [130] Eriksson, J. H. C., Mol, R., Somsen, G. W., Hinrichs, W. L. J., Frijlink, H. W., de Jong, G. J., *Electrophoresis* 2004, 25, 43-49.
- [131] Rundlett, K. L., Armstrong, D. W., *Anal. Chem.* 1996, 68, 3493-3497.
- [132] Nelson, W. M., Tang, Q., Harrata, A. K., Lee, C. S., *Journal of Chromatography A* 1996, 749, 219-226.
- [133] Rudaz, S., Cherkaoui, S., Gauthier, J.-Y., Lantéri, P., Veuthey, J.-L., *Electrophoresis* 2001, 22, 3316-3326.
- [134] Tanaka, Y., Otsuka, K., Terabe, S., *Journal of Chromatography A* 2000, 875, 323-330.
- [135] Xia, S., Zhang, L., Lu, M., Qiu, B., Chi, Y., Chen, G., *Electrophoresis* 2009, 30, 2837-2844.
- [136] Wiedmer, S. K., Jussila, M., Riekkola, M.-L., *Electrophoresis* 1998, 19, 1711-1718.
- [137] Sánchez-Hernández, L., Montealegre, C., Kiessig, S., Moritz, B., Neusüß, C., 2015.
- [138] Kohl, F. J., Montealegre, C., Neusüß, C., *Electrophoresis* 2016, 37, 954-958.

[139] Kohl, F. J., Neusüß, C., in: Schmitt-Kopplin, P. (Ed.), Humana Press 2016.

[140] Horvath, J., Dolník, V., *Electrophoresis* 2001, 22, 644-655.

[141] Atamna, I. Z., Metral, C. J., Muschik, G. M., Issaq, H. J., *J. Liq. Chromatogr.* 1990, 13, 3201-3210.

Curriculum Vitae

Felix Jonas Kohl

Döhler GmbH

Riedstraße

D-64295 Darmstadt

Telefon: +49 6151-306-2467

Fax: +49 6151-306-82467

Email: felix.kohl@doehler.com



Personal Details:

Date of birth:	10.06.1985
Place of birth:	Landshut, Germany
Nationality:	german
Marital status:	married

Academic grade:

Diplom-Ingenieur (FH)

Final Grade:	2.0 (good)
Diploma thesis title:	Low flow coupling techniques in capillary electrophoresis-electrospray ionization-mass spectrometry
Diploma thesis grade:	1.0 (very good)

Education and professional experience

- Since 09/2015 Analytics Specialist HPLC at Döhler GmbH, Darmstadt. Food analytics, control of incoming goods, internal production, and customer complaints.
- 06/2010 – 10/2014 Research associate at the working group of Prof. Dr. Christian Neusüß, Aalen University, Faculty of Chemistry for the Project "Kapillargelelektrophorese/Massenspektrometrie – neuer Ansatz zur Kopp- lung zweier bedeutender Techniken zur Proteincha- rakterisierung" supported by the Bundesministerium für Bildung und Forschung (BMBF), Förderlinie "Inge- nieurNachwuchs" der Förderrunde 2010 (FKZ 17N1110).
- 08/2009 – 02/2010 Diploma thesis at the working group of Prof. Dr. Christian Neusüß, Aalen University.
- 03/2008 – 08/2008 Internship at Zweckverband Landeswasserversor- gung, Langenau.
Drink water monitoring, organic trace analysis, non- target analysis, nano-HPLC/TOF-MS, solid phase ex- traction.
- 03/2007 – 07/2007 Internship at Siltronic AG, Freiberg.
Inorganic analysis, ICP-OES, TXRF, ultra trace analy- sis under clean-room conditions.
- 02/2005 – 08/2005 Internship at VARTA Microbattery, Ellwangen.
Inorganic analysis, incoming-goods inspection, inter- nal production control.
- 03/2004 – 02/2010 Studies of chemistry and analytical chemistry at the Aalen University, graduation as Dipl. Ing. (FH).
- 03/2001 – 07/2003 Staatliche Fachoberschule Neu-Ulm, entrance qualifi- cation for university of applied sciences.

